University of Nevada, Reno

Understanding the role of the intestine in the molecular hypotriglyceridemic actions of a grape seed procyanidin extract

A thesis submitted in partial fulfillment of the
requirements for the degree of Master of Science in
Nutrition

by

Gianella C Caiozzi

Dr. Marie-Louise Ricketts/Thesis Advisor

May, 2013

University of Nevada, Reno
Statewide • Worldwide

THE GRADUATE SCHOOL

We recommend that the thesis
prepared under our supervision by

GIANELLA CATERINA CAIOZZI APABLAZA

entitled

Understanding the role of the intestine in the molecular hypotriglyceridemic actions of a grape seed procyanidin extract

be accepted in partial fulfillment of the
requirements for the degree of

MASTER OF SCIENCE

Marie-Louise Ricketts, Ph.D., Advisor

Stanley Omaye, Ph.D., Committee Member

Mike Teglas, Ph.D., Committee Member

David Shintani, Ph.D., Graduate School Representative

Marsha H. Read, Ph. D., Dean, Graduate School

May, 2013

Abstract

Hypertriglyceridemia is a prevalent condition that is associated with cardiovascular disease. Grape seed procyanidin extract (GSPE), a natural compound rich in procyanidins, has recently been shown to reduce serum triglyceride (TG) levels *in vivo* in normolipidemic animals. This effect was shown to be mediated via farnesoid X receptor (FXR), a member of the nuclear hormone receptor (NHR) superfamily. NHRs are ligand-inducible, and in some cases ligand-independent, transcription factors that interact with DNA to regulate gene expression. Activation of FXR by its endogenous ligand, bile acids (BA), modulates TG and BA homeostasis via regulation of hepatic and intestinal gene expression. Activation of FXR in the liver by BAs increases the expression of small heterodimer partner (SHP), which then acts as a repressor to decrease hepatic expression of sterol response element binding protein 1c (SREBP1c), a key transcription factor regulating lipogenic gene expression, thereby lowering serum TG levels. Studies have shown that in the liver, GSPE acts as a co-agonist ligand for FXR resulting in enhancement of BA-bound FXR activation *in vitro*, and that the TG-lowering ability of GSPE is lost *in vivo* in both, FXR and SHP knockout mouse models. Recently, utilizing a FXRE-luciferase reporter mouse model, it was shown that the intestine has the highest bile acid-induced FXR signaling under physiological conditions. FXR activation in the intestine induces the expression of several FXR target-genes including intestinal bile acid-binding protein (IBABP), organic solute transporters (OST) α/β, and fibroblast growth factor (FGF) 15/19, while repressing the expression of the apical sodium dependent bile acid transporter (ASBT), which contributes to bile acid enterohepatic recirculation and bile acid homeostasis.

The overall aim of this research was to further investigate the effects of GSPE to aid in the understanding of its molecular hypotriglyceridemic mode of action. Based on the fact that FXR is a bridge between the liver and the intestine to control bile acid levels and to regulate bile acid synthesis and enterohepatic flow, the first aim was to discern whether or not GSPE exerts any effects on intestinal FXR which could then contribute to the TG-lowering effect of GSPE. Therefore, the effects of GSPE on the regulation of known

FXR target-genes in the intestine was investigated, to provide further insight into the inter-relationship between the intestine and the liver in the regulation of lipid homeostasis by GSPE.

Studies have previously established the ability of GSPE to lower serum TG levels in a normolipidemic state, therefore, the second aim was to determine the potential of GSPE to lower serum TG levels in a hypertriglyceridemic state, and to identify the underlying molecular events.

Our results indicate that in the intestine, GSPE may act as a gene-selective bile acid receptor modulator (BARM), rather than a bile acid-dependent co-agonist of FXR, as previously reported to occur in the liver. In the course of the studies conducted herein, GSPE treatment resulted in alterations in the expression of ileal FXR-target genes in different ways, i.e., GSPE acted as a FXR co-agonist thereby suppressing ASBT gene expression, while in contrast it acted a FXR modulator by decreasing CDCA-induced IBABP and OSTα/β mRNA expression. Therefore, these results indicate that GSPE may impair bile acid enterohepatic recirculation, which is achieved by decreasing the intestinal up-take of bile acids, as well as by decreasing the amount of BA that return to the liver via the portal circulation. Furthermore, GSPE also induced a rapid and transit increase in FGF19 expression *in vitro* in Caco2 cells. We hypothesize that the above-mentioned effects induced by GSPE on intestinal FXR-target gene expression may therefore be contributing to changes in overall body BA homeostasis and also its serum TG lowering ability.

Additionally, our results show that GSPE treatment effectively reduces serum TG levels by 27% when assessed in a fructose-fed rat model representing a hypertriglyceridemic state. Consequently, GSPE may represent a promising natural compound for the treatment of hypertriglyceridemia and its' related conditions.

Dedication

To the pillars of my life:

My husband Cristian

My parents Juany and Patricio

My siblings Antonella, Francesca and Patricio

And now my loved son Tomás, who is on his way and has been accompanying me during the last 7 months.

Thank you all for your support these 2 years and half I have been studying in the US. Either here with me or far away in distance, I can feel your love and care.

Without all of you in my life, this would not have been possible. We made it!

Acknowledgments

Foremost, I would like to express my deep gratitude to my master thesis advisor, Dr. Marie-Louise Ricketts. I have learned too many things from her since I started to work in her Laboratory and I really appreciate all her support, guidance, dedication, and immense knowledge. Without her help, this thesis would have not been possible.

I am also indebted to the members of my Thesis Committee, Dr Stan Omaye, Dr Mike Teglas, and Dr David Shintani, with whom I have interacted during the course of my research study, and they have always been very helpful when I have needed assistance.

I am grateful to all the people that have worked with me in the Lab: Brian Wong, Tim Thompson, and, more recently, Erin Lyons and Dianna Pope. Their company and help were essential to keep going and finish the work.

I would also like to thank several people that helped this research project be successful: John Hasenau, Lana Manzanares and Jarred Smith, from Lab Animal Medicine; Dr Sanford Barsky from Pathology and Laboratory Medicine; and Dr Liwei Gu from the Food Science and Human Nutrition Department at the University of Florida, for the HPLC analysis of GSPE.

Finally, I am very grateful to my husband Cristian Diaz, who has always been helping me with technological assistance, and more importantly, supporting and loving me.

I am sure this Master's Thesis would have not been possible without all the help of the people mentioned above. Thank you.

Table of Contents

List of Tables

List of Figures

Chapter 1

Introduction

1 Introduction

1.1 Nuclear Hormone Receptors

Nuclear hormone receptors (NHRs) are a family of ligand inducible or in certain cases, ligand independent transcription factors (1). They act as intracellular receptors for numerous hormones and small lipophilic molecules such as steroid and thyroid hormones, vitamin D, fatty acids, pregnanes and bile acids (2). NHRs have been identified to play important roles in the regulation of growth, differentiation, metabolism, reproduction, as well as immunity (1, 3-7).

In contrast to receptors found in the plasma membrane, NHRs are located in the cytosol or inside the nucleus and directly regulate the expression of target genes by binding to specific DNA sequences, called response elements (REs), which are frequently located within the promoter regions of target genes (1, 3-7). However, for certain NHRs such as the estrogen, androgen, glucocorticoid receptors and peroxisome proliferator receptor γ, the RE can be located distally from the promoter, specifically in intergenic and intronic regions (8). The response element directly reflects the mode of receptor binding, which can be as either monomers, homodimers or heterodimers (9). Steroid receptors almost exclusively bind as homodimers to the RE, i.e. two steroid receptor monomers bind cooperatively to their response elements organized as two palindromic hexanucleotide repeats (usually 5`-AGAACA-3`) separated by 3 base pairs (bp) (3, 7). In contrast, certain NHRs function as heterodimers with the retinoid X receptor (RXR). A vitamin A derivative, 9-*cis* retinoic acid, is the physiological ligand of RXR (10). Additionally, RXR functions as an obligate heterodimer partner for other NHRs and consequently serves as a master regulator of several crucial regulatory pathways (10). Heterodimeric receptors usually bind to response elements that are organized as two direct repeats of the 5`-AGGTCA-3`consensus half-site sequence separated by 1-5 bp (3, 7). A considerable subset of NHRs function as monomeric DNA-binding receptors, and therefore the response element contains only a single half-site where the monomeric NHR binds. Most of these NHRs constitute part of the orphan receptor family, for which a physiological ligand is still unknown (for further detail see section 1.1.3) (3, 7).

NHRs require the presence of co-regulator proteins, namely co-activators and co-repressors, for efficient transcriptional regulation (11, 12). Consequently, co-regulators are proteins that control NHR induced transcriptional activity of target genes at several functional levels, such as direct interaction with the basal transcription machinery and enzymatic modification of histones linked to gene regulation, namely histone acetyl transferase (HAT) or histone deacetylase (HDAC) activity (11, 12). Histone acetyl transferases can acetylate conserved lysine amino acids on histones, activating transcription (11, 12). Otherwise, histone deacetylases catalyze the removal of acetyl groups on the amino-terminal lysine residues of core nucleosomal histones, an activity which is associated generally with transcriptional repression (11, 12). Co-activators are defined as molecules that interact with NHRs and enhance their transactivation; while co-repressors are proteins that interact with NHRs and lower the transcription rate of their corresponding target genes (11, 12). Generally, ligand binding to a NHRs results in the release of HDAC-containing co-repressor complexes and the concomitant recruitment of coactivator complexes, which possess HAT activity, which facilitates transcriptional activation (11, 12).

The knowledge of the existence of this superfamily of receptors was demonstrated in the mid-1980s (13). By that time, several biochemical studies had provided evidence for the existence of the classical model of steroid hormone action, and in addition the glucocorticoid, estrogen and progesterone receptors had been cloned (2, 14). These receptors are structurally related and were found to share sequence homology with the avian erythroblastosis virus *v-erbA* oncogene, leading to the discovery of its' mammalian cellular counterpart, namely the thyroid hormone receptor (15, 16). The identification in 1987 of the receptor for vitamin A (retinoic acid), namely retinoic acid receptor (RAR), solidified the view of the existence of a NHR superfamily (14, 17), since chemically distinct ligands were able to interact with structurally related receptors. Promptly after that, came the identification of the receptors for all nuclear hormones, as well as the cloning of several new orphan nuclear receptors, for which a ligand was unknown at the time (2). In 1990, Mangelsdorf and colleagues cloned the retinoid X receptor (RXR) (10), which represented another important advance in identifying the mediator of NHR heterodimerization.

In humans, 48 members of nuclear receptor superfamily have been identified (1, 18), while mouse contains 49 and rat 47 NHRs (19). All of the NHRs have common structural features due to the fact they are comprised of 5 distinct regions (as shown below in Figure 1): a variable amino (NH_2)- terminal region (A/B), a conserved DNA binding domain (DBD) also called region C, a hinge region (D), a conserved ligand binding domain (LBD) or region E, and a carboxyl (COOH) terminal region (1, 6).

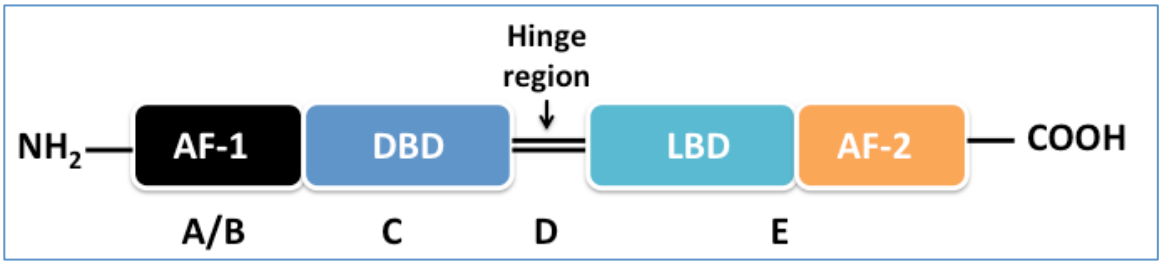

Figure 1: Representation of the functional domains of a nuclear hormone receptor (NHR)
A typical NHR is composed of a NH_2- terminal region, also known as A/B, which contains the ligand-independent transactivation domain AF-1, a conserved DNA binding domain (DBD) also called region C, a linker region called the hinge region (D) that connects the DBD with the ligand binding domain (LBD) or region E, and a COOH terminal region where the ligand-dependent activation function 2 (AF-2) is found.

The DBD and LBD are highly conserved structures, while the DBD is the most conserved domain present in the NHRs (3). It is involved not only in DNA binding, but also in receptor dimerization (3, 7) and it consists of 66 residues where two zinc-finger motifs are contained (as shown in Figure 2). Each of the zinc fingers have a zinc ion that is tetrahedrally co-ordinated by four highly conserved cysteine residues (3, 7). The DBD folds into two perpendicular alpha helices: the first alpha helix forms between the two zinc finger motifs and interacts directly with the major groove of the response element through an amino acid region in the alpha helix, called the proximal or *P box* (20). The second alpha helix, formed at the end of the second zinc finger, is responsible for additional although less specific interactions with the DNA backbone (21). The second zinc-finger contains the distal or *D box*, which is involved in dimerization (3). In addition to the core DBD, sequences located immediately C-terminal to the second

zinc finger, known as the C-terminal extension (CTE), also participate in DNA binding via interactions with the minor grooves of DNA (22). It has been shown that the CTE region is highly variable between the different NHRs (3, 7).

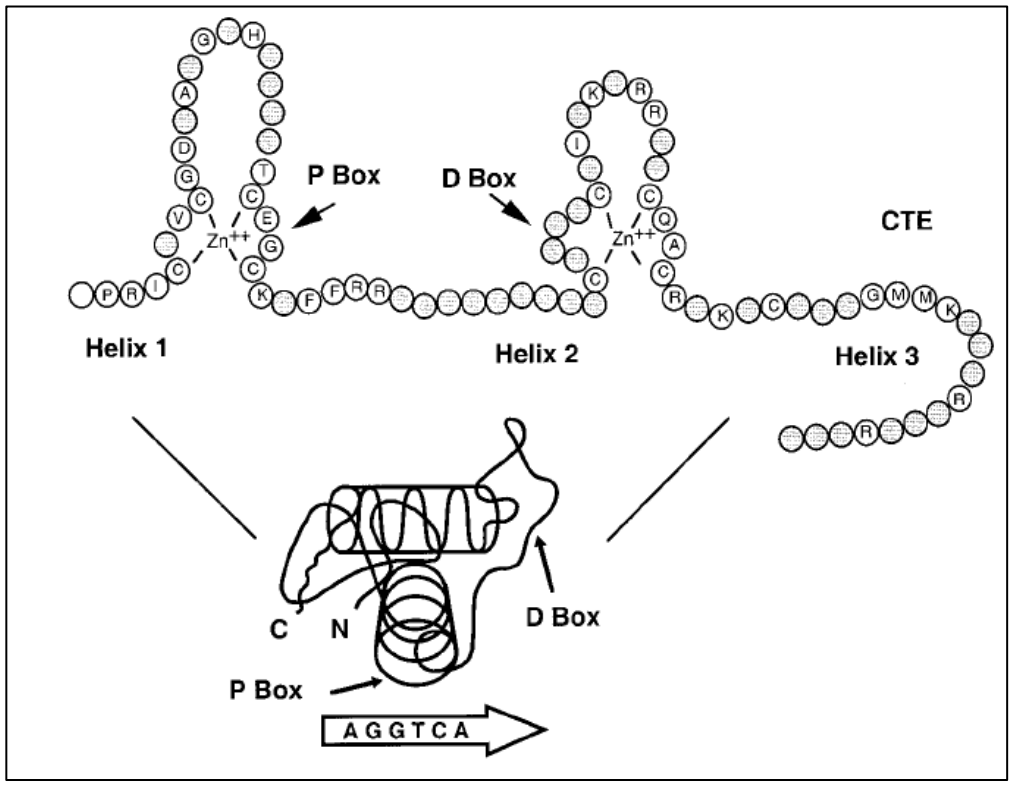

Figure 2: Structure of the DNA binding domain (DBD) of nuclear hormone receptors
The DBD contains: (1) two zinc fingers where four cysteine residues coordinate a zinc ion, (2) the P box, involved in the discrimination of the response element, (3) the D box that forms a dimerization interface, and (4) the CTE that participates in DNA binding. The 66 residues forming the DBD fold into two perpendicular alpha helices. Reproduced from Aranda et al, 2001 (1).

The LBD has a key role in ligand binding, nuclear localization, receptor dimerization, and interaction with co-regulators, namely co-activators and co-repressors (3). LBDs consist of 11 to 13 α-helices and 2 to 4 β-sheets (3). The COOH-terminal helix (usually helix 12) contains the activation function 2 (AF-2) which is ligand-dependent (3). A central core layer of three helices creates a cavity where the ligand can

bind. The binding of a ligand to the NHR induces a conformational change in the LBD of the receptor, specifically in the AF-2 domain, thereby switching the NHR from an "off" to an "on" state (3). The new AF-2 position forms a hydrophobic pocket that favors binding of coactivators containing the peptide motif LXXLL in their structure (where L is leucine and X is any other amino acid) (3).

The remainder of the regions are generally poorly conserved in their structure (3). The N terminal domain (A/B) is highly variable in size and sequence between the NHR's, and it usually contains the ligand-independent transactivation function (AF-1). This AF-1 domain provides protein interaction surfaces for co-regulatory proteins such as certain co-activators, for example, the vitamin D receptor-interacting protein 150 (DRIP150) (23). The hinge region is a flexible linker that allows rotation between the DBD and the LBD, to facilitate binding to the RE and dimerization of NHRs (3). In addition, it has been proposed that the hinge region contributes markedly to receptor function (24). For example, in the peroxisome-proliferator-activated receptor α (PPARα), the hinge region provides interaction surfaces for corepressors and contains a sequence of positively charged basic amino acids, termed the nuclear localization signal (NLS) (24). The NLS located in the hinge region contributes to the nuclear import of, for example, PPARα (24).

NHRs are typically subdivided into three classes according to their mechanism of action and their DNA binding characteristics (1, 3, 6, 7, 25):

1.1.1 Class I nuclear hormone receptors

Also known as the steroid receptor family, these receptors bind as homodimers to the RE in a specific target gene (3, 7). In the absence of ligand, the receptor is located in the cytoplasm in a complex with heat shock proteins (3, 7). Ligand binding induces a conformational change in the receptor, which results in dissociation from the heat shock protein, homodimerization with another receptor and nuclear translocation, where the receptor binds as a homodimer to the RE and activates transcription of the respective target gene (3, 7). The RE of class I NHRs are organized as palindromic hexanucleotide repeats

(usually 5`-AGAACA-3`) separated by 3 base pairs (bp) (3, 7). This class of NHRs consists of the steroid receptors that are activated by high affinity hormones, namely, the estrogen receptor (ER), androgen receptor (AR), progesterone receptor (PR), mineralocorticoid receptor (MR), and the glucocorticoid receptor (GR) (3, 7).

1.1.2 Class II nuclear hormone receptors

This class of NHRs is also known as the thyroid/retinoid family class of receptors. These NHRs are located in the nucleus and are constitutively bound to their RE, even in the absence of ligand, as a heterodimer with the retinoid X receptor (RXR) (3, 7). In the absence of ligand, they are bound with corepressors that inhibit the formation of transcriptionally active complexes (3, 7). Ligand binding induces a conformational change in the NHR that displaces the corepressors and recruits coactivator proteins (3, 7). These bind to the complex, resulting in the ligand-dependent induction of transcription, mediated by the recruitment of several transcription factors and RNA polymerase II. The most common RE for class II NHRs consists of a direct repeat organization of a core recognition motif, compared to the palindromic RE found in the class I receptors (9). The RE is organized as two direct repeats (DR) of the 5`-AGGTCA-3`consensus half-site sequence separated by 1-5 bp (termed a DR1, DR2, DR3, DR4 or DR5). Additionally, the RE can be composed of everted repeats (ERs) or inverted repeats (IRs) of the core 5`-AGGTCA-3` (9), as shown in Table 1.

Table 1: Consensus sequences present in the response element for class II nuclear hormone receptors

Response element	Sequence
Direct Repeat (DR)	5' AGGTCA (n) AGGTCA 3'
Inverted Repeat (IR)	5' AGGTCA (n) TGACCT 3'
Everted Repeat (ER)	5' TGACCT (n) AGGTCA 3'

The response elements are organized as two repeats of the 5`-AGGTCA-3`consensus half-site sequences, either as a direct repeat, inverted repeat or everted repeat. The consensus sequences are separated by a certain number of base pairs (n) in each response element.

As an example, one member of this NHR class, the farnesoid X receptor (FXR), usually binds to an IR1 and less frequently to a DR4 or an ER8 (9). This class of NHR includes endocrine receptors such as the thyroid hormone receptor and retinoic acid receptor as well as the group of "*adopted*" or former orphan receptors (9).

Classical NHRs, i.e. steroid receptors, were cloned subsequent to the knowledge of the existence of their respective hormones, e.g. estrogen. However, there were a group of proteins with structural features resembling those of the other NHRs that were originally cloned without any prior knowledge as to their respective ligand (1), and were originally termed "orphan" receptors. Subsequent studies identified naturally occurring ligands and determined their physiological roles, and the receptors were subsequently called "adopted" or former orphan receptors. This group of receptors includes the peroxisome-proliferator-activated receptors (PPARs), liver X receptors (LXRs), pregnane X receptor (PXR), constitutive androstane receptor (CAR) and farnesoid X receptor (FXR) (1). Their ligands are a multitude of different small lipophilic metabolites ranging from abundant low-affinity ligands to less abundant high-affinity ligands (5). Accordingly, this class of receptors functions as metabolic sensors that regulate the metabolic status of the cell (5).

1.1.3 Class III nuclear hormone receptors

This class of NHRs is also known as the orphan receptor family, and includes all those proteins that have been identified by comparative sequence analysis as belonging to the NHR superfamily, but for which the cognate ligand is still unknown (2). Orphan receptors can either bind as heterodimers with RXR or as monomers to their respective response element (2). Receptors in this class include the nuclear receptor related 1 protein (NURR1) (26), NUR77 (27), steroidogenic factor 1 (SF1) (28), dosage-sensitive sex reversal, adrenal hypoplasia critical region, on chromosome X, gene 1 (DAX1) (29), the Rev-Erb receptor (30), and small heterodimer partner (SHP) (31).

SHP is a unique NHR in that it lacks a conserved DBD (32), and consequently executes its' regulatory function via protein-protein interactions with other NHR's and transcription factors. SHP functions as a transcriptional repressor of gene expression (31, 33), and binds to the AF-2 domain of a NHR via two LXXLL-related motifs (33). Many NHRs have been reported to target the SHP promoter and regulate SHP gene expression, for example FXR ligands, both endogenous and synthetic, have been shown to be potent inducers of SHP mRNA expression (34, 35). In humans, SHP is expressed in the liver, heart, pancreas, kidney, spleen, small intestine, adrenal gland and stomach (31). Numerous studies have shown that SHP plays important roles in the regulation of bile acid, lipid and glucose metabolism, as well as apoptosis (33, 35-37).

1.2 "Adopted"/Former Orphan Nuclear Receptors

In the following pages, a brief description of the main "adopted" orphan NHRs will be discussed, with a particular emphasis on FXR.

1.2.1 Constitutive androstane receptor (CAR)

This receptor was initially designated as *constitutive activated receptor* because it was found to activate target gene transcription even in the absence of ligand stimulation (38). It has subsequently been referred to as "*constitutive androstane receptor*", due to the fact that androstanol and androstenol were identified to act as inverse agonist ligands that work by repressing the constitutive activity of CAR *in vitro* by promoting the release of coactivators from the LBD (39). CAR (nuclear receptor subfamily 1, group I, member 3, NR1I3) is important for both xenobiotic and endobiotic metabolism and is expressed primarily in the liver and intestine (40, 41). CAR and PXR are closely related since both are involved in xenobiotic metabolism and share many target genes, including certain cytochrome P450 (CYPs) enzymes involved in phase I metabolism, and also uridine diphosphate glucuronosyltransferases (UGTs) and sulfotransferases (SULTs) contributing to phase II metabolism and the multidrug-resistance drug transporters (40, 41). Additionally, recent studies have linked CAR to lipid metabolism and energy homeostasis (41). It has been shown that CAR inhibits lipogenesis by reducing the levels of sterol regulatory element-binding protein 1c (SREBP1c), a master regulator of lipogenesis (41). Additionally, CAR has been shown to inhibit fatty acid β-oxidation by competing with PPARα for its binding site in certain target gene promoters involved in β-oxidation of fatty acids, as well as by decreasing the expression of carnitine palmitoyltransferase 1 (CPT1), a rate-limiting enzyme in β-oxidation (41). Recent reports suggest that CAR is also involved in the regulation of gluconeogenesis. The hepatic gluconeogenic enzymes phosphoenolpyruvate carboxykinase (PEPCK) and glucose 6-phosphatase were reported to be repressed in a CAR dependent-manner (42). Based upon these observations, CAR is now being investigated as to whether or not CAR agonist ligands may be beneficial in the treatment of patients with hyperglycemia and hyperlipidemia (41). Synthetic agonists of CAR include 1,4-bis[2-[3,5 dichloropyridyloxyl]] benzene (abbreviated to TCPOBOP) and 6-(4-Chlorophenyl) imidazo[2,1-b][1,3] thiazole-5-carbaldehyde O-3,4-dichlorobenzyl) oxime (abbreviated to CITCO) (40). The activation of CAR by these synthetic agonists is species-specific: TCPOBOP induces mouse CAR but not rat or human CAR (40), while CITCO has been

identified as an activator of human CAR (40). TCPOBOP and CITCO have been used in humanized rodent toxicological models in which mouse PXR or CAR is genetically knocked out and replaced by its human counterpart to make a humanized receptor animal model, in order to determine receptor-induced drug response *in vivo* in an animal model (43). CAR is not the only NHR involved in xenobiotic detoxification. Together with the pregnane x receptor (PXR), which will be described in section 1.2.4, they act as sensors of toxic byproducts derived from endogenous metabolites and of exogenous chemicals. In order to enhance their elimination, CAR and PXR exhibit promiscuous xenobiotic activation capability. It appears that CAR agonist ligands are less promiscuous than those of PXR, possibly due to the smaller size of the ligand-binding pocket found in CAR, whereas PXR possesses a bulky and flexible ligand-binding cavity, which enables it to accommodate a more structurally promiscuous library of ligands (40). Other interesting distinctions between these two xenobiotic receptors is that CAR can be activated by either direct ligand binding or ligand-independent (indirect) pathways, while PXR activation is dependent exclusively on ligand binding (40).

1.2.2 Liver X receptors (LXRs)

Liver X receptors (LXRs) are crucial regulators of cholesterol metabolism: they stimulate cholesterol efflux in macrophages, promote bile acid synthesis in the liver and inhibit cholesterol absorption (44). LXRα (nuclear receptor subfamily 1, group H, member 3, NR1H3) and LXRβ (nuclear receptor subfamily 1, group H, member 2, NR1H2) are the two isoforms, which differ significantly in their tissue distribution: with LXRα expression predominating in metabolic tissues such as the liver, adipose tissue, intestine, kidney and tissue macrophages, while LXRβ is ubiquitously expressed (45, 46). Oxysterol ligands, which are oxidized cholesterol metabolites, are the main natural ligands of LXR (47, 48). In mice, the CYP7A1 gene is a direct target gene for LXR activation (49), based upon the fact that it contains a LXR response element (LXRE) in the promoter region (49). CYP7A1 is a member of the

cytochrome P450 family encoding cholesterol 7α-hydroxylase, which is the rate limiting enzyme in the synthesis of bile acid from cholesterol (45, 46). However, no LXRE has been found in the human CYP7A1 promoter. Therefore, there appears to be diverse molecular mechanisms for the regulation of cholesterol metabolism between humans and mice (50). LXR also controls the expression of certain ABC transporters, namely, the ATP-binding cassette sub-family G member 5 (ABCG5) and ABCG8, which both promote cholesterol elimination via the bile, as well as decreasing the absorption of cholesterol by enterocytes (51). In addition, LXRs are also involved in the promotion of reverse cholesterol transport in peripheral cells, which is mediated via two additional members of the ABC transporter family, namely ABCA1 and ABCG1 (45, 46). Several synthetic agonists have been developed, including GW3965 (by Glaxo Wellcome) and T0901317 (by Taconic) (52, 53). GW3965 has been shown to be a much more selective agonist for both LXRs, since T0901317 has been shown to also activate other NHRs, namely PXR and FXR at higher concentrations (52, 53).

1.2.3 Peroxisome-proliferator-activated receptors (PPARs)

The PPAR subfamily of NHRs consists of three members: PPARα (nuclear receptor subfamily 1, group C, member 1, NR1C1), PPARγ (nuclear receptor subfamily 1, group C, member 3, NR1C3), and PPARδ (nuclear receptor subfamily 1, group C, member 2, NR1C2) (54-57). These receptors bind as heterodimers with RXR to their respective REs, namely a direct repeat of two 5' AGGTCA 3' hexamers separated by one base pair, i.e. a DR1 (54). All three subtypes are highly expressed in tissues relevant to energy homeostasis and are activated by certain dietary fatty acids and their metabolic derivatives; therefore, they have been identified as essential regulators of energy homeostasis and metabolism (54-57).

PPARα was the first member of this family to be cloned in 1990 (54). PPARα was identified based on the observation that a diverse group of chemical compounds including fibrates (a triglyceride lowering

medication), herbicides and industrial plasticizers were able to trigger an increase, in size and number, of peroxisomes in cells, while also increasing fatty acid β-oxidation (54). PPARα is expressed predominantly in the liver, but is also expressed in cardiac myocytes, kidney tubular epithelial cells, skeletal muscle, large intestine epithelium, endothelial and smooth muscle cells, as well as in immune cells, including macrophages, lymphocytes and granulocytes (54-56). The major function of PPARα is to promote fatty acid β-oxidation, which is achieved via increased transcription of many genes involved in the hepatic clearance of very low density lipoprotein (VLDL), fatty acid uptake, fatty acid activation and transport into the mitochondria, as well as peroxisomal and mitochondrial β-oxidation, and certain enzymes involved in mitochondrial respiration, e.g. NADH cytochrome c reductase (54-56). PPARα is induced by fasting and is required for ketogenesis. Physiological ligands of PPARα include saturated and unsaturated fatty acids and the arachidonic acid-derived eicosanoids (54-56), additionally fibrate drugs which are commonly used in the treatment of hypertriglyceridemia, are synthetic ligands of this NHR (56).

PPARγ plays a central role in fat cell differentiation and lipid storage (56) and is consequently commonly referred to as the "*master regulator of adipogenesis*". It is most abundantly expressed in white and brown adipose tissue, but is also present in pancreatic β-cells, the spleen, and intestine (56). PPARγ is necessary for the differentiation and survival of white and brown fat adipocytes (56). While the main function of white adipose tissue is to serve as an energy store; brown adipose tissue increases energy expenditure by dissipating energy as heat through uncoupling proteins (UCPs) (56). UCPs are proton transporters located in the inner mitochondrial membrane, where they uncouple the mitochondrial proton gradient from ATP production, leading to energy being lost as heat, thereby mediating an increase in energy expenditure (58). The activation of PPARγ also impacts glucose homeostasis since it increases insulin sensitivity, which is mediated via the reduction of circulating free fatty acids, by decreasing lipid accumulation in non-adipose tissue, as well as via the regulation of adipocyte-secreted hormones, such as adiponectin, resistin, and

tumor necrosis factor alpha (TNFα) (54-56). Of these, adiponectin increases insulin sensitivity, while resistin and TNFα induce insulin resistance. Fatty acids such as omega-3 and omega-6 fatty acids have been identified as natural ligands of PPARγ (54). The thiazolidinediones, a class of anti-diabetic pharmaceutical drugs, are the most commonly recognized synthetic ligands of PPARγ (54), and work by increasing hepatic and adipose tissue insulin sensitivity via activation of PPARγ (54), which subsequently results in increased expression of certain genes including insulin receptor substrate-1 (IRS-1), UCP-2 and adiponectin (59, 60).

PPARδ, also known as PPARβ, is ubiquitously expressed in many tissues and is a powerful regulator of fatty acid catabolism, as well as energy homeostasis (56). Activation of PPARδ in adipose tissue increases adipocyte differentiation and oxidation (55). Furthermore, it increases energy expenditure via induction of UCPs in brown adipose tissue (55). In skeletal muscle, PPARδ activation also increases β-oxidation of fatty acids, improves insulin sensitivity and augments the number of oxidative muscle fibers (55). Transgenic mice overexpressing PPARδ in skeletal muscle were shown to be protected against high fat diet-induced obesity, muscular lipid accumulation, hyperinsulinemia, and insulin resistance (55). Physiological ligands for PPARδ are saturated and unsaturated fatty acids and certain eicosanoids (54, 55). Synthetic agonists, namely GW501516, GW0742, GW2433 and GW9578, have also been developed by Glaxo Smith Kline, however, these are not currently used clinically (54, 55).

1.2.4 Pregnane X receptor (PXR)

Pregnane X receptor (PXR), (nuclear receptor subfamily 1, group I, member 2, NR1I2), is highly expressed in the liver and intestine (40, 61) and plays an integral role in xenobiotic and endobiotic metabolism by regulating the expression of drug-metabolizing enzymes and transporters, as well as genes related to endobiotic metabolism (40, 41, 61). In xenobiotic metabolism, PXR is involved in the

regulation of phase I and phase II enzymes, as well as in the regulation of drug transporters, such as the multidrug resistance transporters e.g. multidrug resistance protein 1 (MDR1) and multidrug resistance-associated protein 2 (MRP2) (40, 61). PXR induces the major phase I cytochrome P450 enzymes (CYPs) that catalyze the first step in the detoxification of lipophilic compounds (40, 61). Human CYP3A4, and the murine homolog Cyp3A11, are the major CYPs regulated by PXR. In humans, CYP3A4 is critical for drug metabolism and it has been reported to metabolize approximately 50% of all prescription drugs (62, 63). PXR also regulates the expression of phase II enzymes, namely UGT, SULT and glutathione S-transferase (GST) (40, 61). These enzymes add polar molecules to xenobiotics, producing water-soluble metabolites that can reach the biliary or urinary systems in order to be excreted (40, 61). Another recently identified action of PXR, although studied to a much lesser degree, is its' role as a regulator of endobiotics and its' role in metabolism (41). For example, it has been shown that PXR promotes lipogenesis while suppressing fatty acid β-oxidation and gluconeogenesis (41). Compared with other NHRs, there is a large spectrum of compounds that can act as ligands for PXR, including dietary supplements and herbal remedies, prescription drugs, endogenously produced metabolites and environmental pollutants. (40, 61). The sequence divergence in the LBD of PXR among species is believed to be responsible for the observed species-specific activation and target gene induction by this receptor (40, 61, 64). For example, pregnenolone 16α-carbonitrile (PCN) is a specific mouse PXR agonist ligand, while rifampicin (RIF) potently activates human PXR with no effect observed on mouse PXR (40, 61). Therefore, understanding how the xenobiotic response differs among species is essential to developing high-quality models and characterization of potential risk from chemical exposure. The most common clinical implication for the activation of human PXR is the occurrence of drug-drug interactions, mediated by up-regulation of CYP3A isoenzymes. Typically, rodent models do not predict drug-drug interactions mediated by human PXR due to the species differences in response to ligand, as mentioned above. Consequently, a humanized PXR mouse model, lacking the expression of mouse PXR, was developed that can be used to assess any effects on human PXR and to aid in determining drug-drug

interactions (64, 65). Displaying a human drug-response profile, this mouse represents a unique tool to dissect the drug-induced xenobiotic response and should aid in the development of safer drugs (64, 66)

1.2.5 Farnesoid X receptor (FXR)

FXR (nuclear receptor subfamily 1, group H, member 4, NR1H4) has been shown to be important for the maintenance of bile acid, lipid and glucose homeostasis (45, 67-69). Two FXR genes have been identified: FXRα and FXRβ. FXRα is conserved from human to fish (70), while FXRβ encodes a functional NHR only in rodents, rabbits and dogs (70). The conserved FXRα amino acid sequence in different species suggests the critical role of this NHR (69). FXR is highly expressed in the liver, intestine, kidney, and adrenal gland (69). The human and mouse FXRα gene each encode four different isoforms (FXRα1, FXRα2, FXRα3 and FXRα4) (69), which results from alternative splicing of exon 5 and the use of two different promoters that initiate transcription from either exon 1 or exon 3. Many FXR target genes are regulated in an isoform independent-manner (69). However, certain genes including intestinal bile acid binding protein (IBABP), fibroblast growth factor 19 (FGF19), syndecan-I, and αA-crystallin appear to be more responsive to the FXRα2 and FXRα4 isoforms (71). Interestingly, these two isoforms both lack a four amino acid sequence (MYTG) in the hinge region, as compared to the FXRα1 and FXRα3 isoforms (as depicted in Figure 3). However, a more detailed explanation regarding the physiological importance of gene regulation by each specific FXR isoform still remains to be established (69)

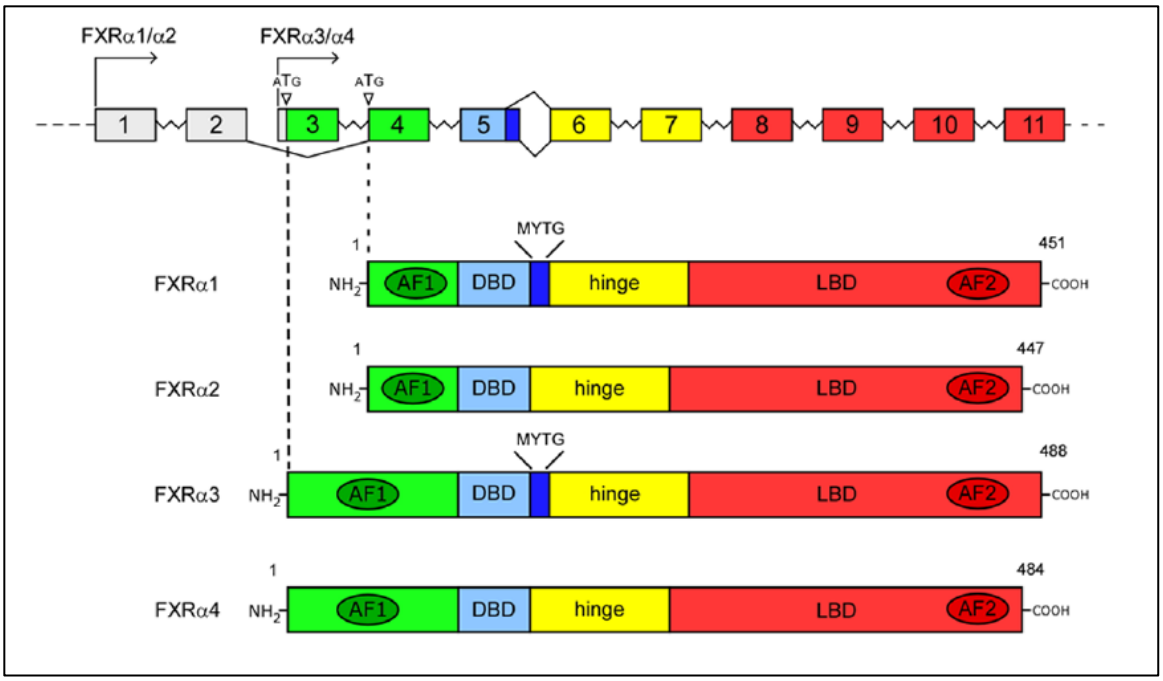

Figure 3: Structure and transcripts of the FXRα gene
The human and mouse FXRα gene are characterized by 11 exons and two different promoters. Transcription initiated from either exon 1 or exon 3, and alternative slicing of the region of exon 5 that encodes the amino acids MYTG, determines the generation of four different transcripts (FXRα1, FXRα2, FXRα3 and FXRα4). Reproduced from Modica S. et al, 2010. (69)

As previously mentioned, the FXR response element (FXRE) usually contains 2 copies of the consensus sequence *5' AGGTCA 3'*, arranged as inverted repeats (IR) separated by 1 bp, termed an IR1. Less frequently, the FXRE is comprised of everted repeats (ER) separated by 8 bp (ER8), e.g. in the multidrug resistance-associated protein 2 (MRP2) gene. MRP2 mediates the efflux of conjugated bile acids from the hepatocyte into the bile canaliculi (72). It has also been shown that FXR can bind to direct repeats separated by 4 bp (DR4), e.g. in the gene encoding cholesteryl ester transfer protein (CETP), resulting in the down-regulation of CETP expression (67, 68, 73). FXR was originally cloned in 1995 as a receptor that was weakly activated by farnesol metabolites (74). In 1999, bile acids were identified as the endogenous ligands of FXR (75, 76). BAs are amphipathic molecules derived from cholesterol catabolism (77) and can be classified as either primary bile acids (chenodeoxycholic acid and cholic acid), which are

synthesized from cholesterol in the liver, or as secondary bile acids (deoxycholic acid and lithocholic acid), which are produced by intestinal bacteria from primary BAs. In contrast to primary BAs, secondary BAs are poorly absorbed in the distal ileum via enterohepatic circulation (77). As mentioned above, primary BAs are the main physiological ligands of FXR: with chenodeoxycholic acid (CDCA) being identified as the most potent FXR activator in humans, while cholic acid (CA) is a more potent activator of mouse FXR (67-69). Bile acids not only activate FXR, but they have also been shown to activate other NHR's, including PXR, CAR and the vitamin D receptor (VDR) (67-69). Interestingly, secondary BAs such as lithocholic acid (LCA) have predominantly been demonstrated to activate both PXR and VDR (78). High concentrations of LCA have been shown to promote colon cancer via inducing DNA strand breaks, the formation of DNA adducts and inhibition of DNA repair enzymes (79). Detoxification of LCA is mediated by CYP3A4, the expression of which is induced by PXR and VDR (78, 80). Therefore, PXR and VDR activation by LCA and their physiological ligands, helps to eliminate high levels of LCA from the body, preventing otherwise potentially toxic effects (78, 80).

When FXR is bound to a ligand, it has two docking sites for interaction with LXXLL motifs, which results in an increased binding affinity for coactivators with more than one LXXLL NHR interaction domain (67). Examples of the coactivators that are recruited to the FXR/RXR heterodimer bound to the FXRE on a target gene include the peroxisome proliferator-activated receptor gamma coactivator 1-alpha (PGC1α), steroid receptor coactivator-1 (SRC-1), sirtuin-1 (SIRT1), brahma-related gene 1 (Brg-1), p300, coactivator-associated arginine methyltransferase 1 (CARM1), protein arginine N-methyltransferase 1 (PRMT1), and activating signal cointegrator-2 -containing complex (ASCOM) (67). Co-activators determine an increased transcriptional rate of target genes via direct interaction with the basal transcription machinery or enzymatic modification of histones, as mentioned earlier.

During the last few years, there has been increased interest in finding new agonists of FXR that could be used as therapeutic pharmacological agents (81), since FXR target genes have crucial functions in the

regulation of bile acid and lipoprotein metabolism. Consequently, GW4064, fexaramine, AGN34 and 6α-ethyl-chenodeoxycholic acid (6-ECDCA) have been developed as synthetic ligands for FXR (67-69), while a new oral and selective agonist, XL335 (WAY-362450) was described in 2009 (82). Moreover, agonist ligands for FXR have been proposed as treatments for dyslipidemia, cholestasis, non-alcoholic steatohepatitis (NASH) and type 2 diabetes (81).

The importance of FXR in the regulation of metabolism with respect to bile acid and lipid homeostasis will be reviewed in more detail below. The role of FXR in the regulation of glucose metabolism will be discussed briefly, since the focus of the present study is the role of FXR in triglyceride regulation.

1.2.5.1 FXR and glucose metabolism

Activation of FXR by bile acids decreases gluconeogenesis, increases glycogen synthesis and induces insulin sensitivity (68, 69). It has been shown that FXR knockout mice develop an age-dependent hyperglycemia and insulin resistance, with significant higher glycemic levels in 12-week-old mice (83). The observed insulin resistance may result from elevated free fatty acids, which was noted in the plasma of FXR knockout mice (83). It has been demonstrated that FXR agonists induce GLUT-4 transcription through a FXRE in the GLUT4 promoter, in both adipocyte and hepatocyte cell lines (84). Furthermore, activation of hepatic FXR has been shown to repress phosphoenoylpyruvate carboxykinase (PEPCK) and glucose-6-phosphatase, as well as increasing levels of dephosphorylated/active glycogen synthase (68, 69). Overall, these combined effects result in decreased hepatic gluconeogenesis and increased hepatic glycogen synthesis (68, 69).

1.2.5.2 FXR and bile acid metabolism

FXR plays a key role in every aspect of bile acid metabolism, including synthesis, conjugation, secretion, absorption, as well as refilling of the gall bladder (67-69).

Bile acids are synthesized in the liver from cholesterol. Therefore, BAs represent the primary pathway for cholesterol catabolism and account for about 50% of the daily turnover of cholesterol (77). In the distal ileum, 95% of the BAs are actively absorbed and returned back to the liver to be recycled and re-secreted into the bile (85). This process is called "*enterohepatic circulation"*. Only 5% of the BAs are lost in the feces on a daily basis, which is compensated for by *de novo* hepatic synthesis (85). Additionally, BAs are involved in the absorption of lipids in the small intestine, determining the amount of cholesterol lost in the feces (77). These two main routes therefore explain the essential function of BAs in removing excess cholesterol from the body (77).

Cholesterol 7α-hydroxylase, which is encoded by the CYP7A1 gene, is the rate-limiting enzyme in the classical hepatic BA synthesis pathway (86). LXR and the liver receptor homolog-1 (LRH-1), are two important inducers of CYP7A1 in rodents (48, 49, 87). In addition to CYP7A1, the enzyme 12α-hydroxylase, encoded by the CYP8B1 gene, is also involved in BA synthesis, through the production of CA and in the regulation of the ratio of the CA:CDCA (85). Newly synthesized BAs are conjugated with two amino acids, namely taurine and glycine, and are then actively secreted into the gall bladder by two transporters belonging to the ABC transporter family, namely bile salt export pump (BSEP) and MRP2, which are both induced via FXR activation (85). During the postprandial state, BAs are secreted from the gall bladder into the small intestine to aid in the absorption of lipophilic nutrients (85). At the apical membrane of the enterocyte, the apical sodium-dependent bile acid transporter (ASBT), also known as ileal bile acid transporter (IBAT), determines the uptake of BAs (88). Inside the enterocyte, BAs are bound and transported by IBABP to the basolateral membrane, where BAs are then secreted in the portal blood circulation, via the organic solute transporters (OST)α/β (89). The hepatocellular uptake of BAs

from the portal circulation is achieved by 2 transporters located on the basolateral membrane of hepatocytes: namely the sodium-dependent sodium taurocholate cotransporting polypeptide (NTCP) and the sodium-independent organic anion transporting polypeptides (OATP) (90). NTCP activity accounts for more than 80% of conjugated BA uptake, but less than 50% of unconjugated BA reabsorption (90). Following reabsorption of the BAs by the liver, bile formation occurs (90). This complex pathway of BA metabolism is entirely regulated by FXR and is shown in Figure 4.

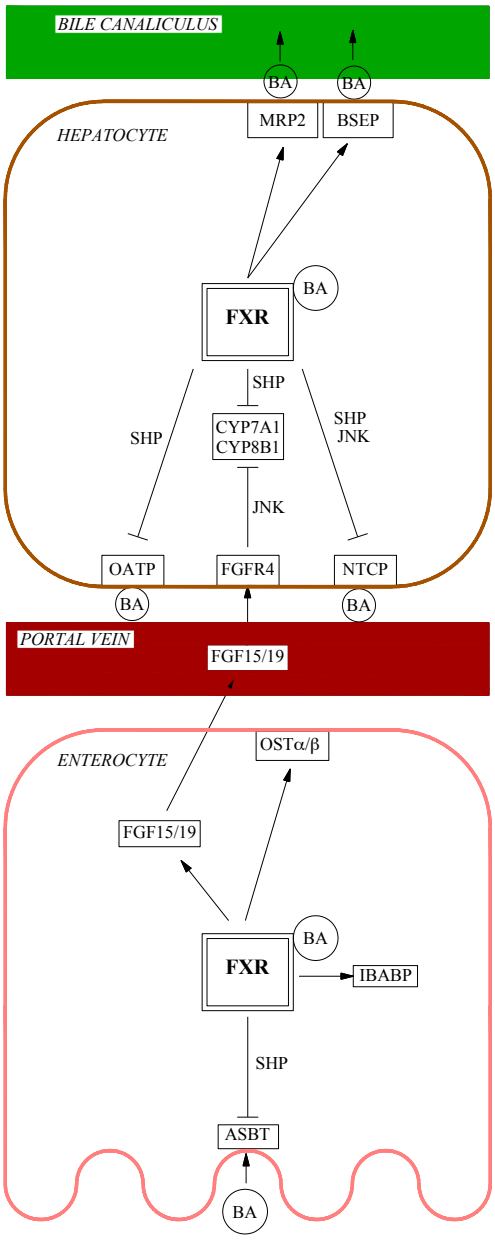

Figure 4: FXR regulation of bile acid metabolism

Bile acids (BAs) activate hepatic and intestinal FXR to regulate genes important for BA metabolism and enterohepatic circulation. In the liver, FXR activation (1) represses BA synthesis by reducing the expression of CYP7A1 and CYP8B1, via SHP, (2) increases BA secretion into the bile canaliculi by increasing MRP2 and BSEP, and (3) decreases uptake of BAs from the portal circulation by reducing the expression of the transporters NTCP and OATP. In the intestine, FXR activation (1) decreases luminal reabsorption of BAs by reducing ASBT expression, (2) facilitates transport of BA through the enterocyte and into the portal circulation via induction of IBABP and OSTα/β respectively, and (3) it also induces secretion of FGF15/19 from the enterocyte into the portal circulation, which then signals to the liver through FGFR4 to repress CYP7A1 and CYP8B1, and ultimately bile acid synthesis. MRP2: Multidrug resistance-associated protein 2, BSEP: bile salt export pump, OATP: organic anion-transporting polypeptide, FGFR4: Fibroblast growth factor receptor 4, NTCP: Na-Taurocholate cotransporting polypeptide, OSTα/β: organic solute transporter alpha-beta, FGF15/19: Fibroblast growth factor 19, IBABP: Intestinal Bile Acid-Binding Protein, ASBT: Apical sodium dependent bile acid transporter.

BAs induce a negative feedback mechanism in order to repress their own synthesis via activation of FXR, both in the liver and in the intestine (67-69). When BAs bind to FXR, this increases the expression of SHP (67-69). SHP is another NHR that represses gene transcription by inhibiting other transcription factors, e.g. SHP interacts with LRH-1 repressing its' activity (91). This SHP-LRH-1 interaction then results in reduced expression of both CYP7A1 and CYP8B1, ultimately inhibiting BA synthesis (67-69). Additionally, a second mechanism has been shown to mediate the CYP7A1 repression induced by FXR, which involves fibroblast growth factor (FGF) 15 in mice or FGF19, the human homologue (92-94). FXR activation in the ileum in mice has been shown to induce the expression of FGF15, a hormone secreted into the portal circulation that after reaching the liver, binds to the fibroblast growth factor receptor 4 (FGFR4) in hepatocytes, leading to repression of CYP7A1 (93). SHP was shown to contribute to FGF15-mediated repression of CYP7A1 in a SHP knockout mouse model (93). However, SHP-independent mechanisms may also be involved, including the c-jun N-terminal kinase-dependent (JNK) pathway which was demonstrated to mediate the inhibition of CYP7A1 in rats (92). It has also been demonstrated that the induction in the expression of FGF15 by the activation of FXR in the enterocytes, promotes refilling of the gall bladder by inducing relaxation of smooth muscle (95).

FXR activation in the liver also induces the expression of BSEP (96) and MRP2 (72), thereby increasing the secretion of BAs into the gall bladder, and consequently avoiding BA accumulation in the liver and subsequent hepatic injury (72, 96). The activation of FXR in the distal ileum down-regulates the expression of ASBT via the induction of SHP (88), while concomitantly inducing IBABP (97) and OSTα/β expression (89). These FXR-mediated effects lead to a reduced uptake of BAs at the luminal membrane of the enterocyte, as well as increased transport of BAs from the enterocyte into the portal circulation (88, 89). The induction of IBABP may limit the free concentration of bile acids intracellularly, therefore avoiding BA toxicity within the enterocyte (97). Finally, FXR also negatively regulates the expression of the transporters NTCP and OATP, which are both involved in hepatocyte uptake of BAs

from the portal circulation (90). These genes are both regulated via a SHP-mediated processes (36), however other SHP-independent pathways leading to the repression of NTCP may also exist, and it has been suggested that this may involve JNK signaling and phosphorylation-mediated decreased binding of RXR to the NTCP promoter (98).

1.2.5.3 FXR and lipid metabolism

As previously mentioned, bile acids are the end product of hepatic cholesterol catabolism, and they are important for lipid absorption from the intestinal lumen and represent the major way for eliminating cholesterol from the body (68). Consequently, the bile acid pool size has an important effect on lipid metabolism (68). The administration of bile acids to humans or animals results in reduced plasma triglyceride (TG) and high-density lipoprotein (HDL) levels, as well as increased levels of low-density lipoprotein (LDL) (45, 68). As mentioned earlier, the effects of bile acids are in part due to their activation of FXR (67, 68, 99).

FXR activation decreases plasma TG levels via reduced TG synthesis, increased TG clearance and increased fatty acid catabolism (as shown in Figure 5) (68, 69). Treatment of mice with FXR agonists induces the expression of SHP, which ultimately results in the repression of sterol regulatory element-binding protein 1c (SREBP1c) mRNA levels (68, 69). SREBP1c is a key transcription factor regulating lipogenic genes, including fatty-acid synthase (FAS), acetyl-coA synthase (AceCS), acetyl-coA carboxylase (ACC) and glycerol-3-phosphate acyltransferase (GPAT) (100). Therefore, hepatic TG synthesis is reduced following the repression of SREBP1c by the FXR-mediated induction of SHP (68, 69). Activation of FXR also decreases blood TG levels by promoting TG clearance, which is achieved by increasing the hepatic expression of syndecan-1 and the VLDL receptor, as well as by increasing the expression of lipoprotein lipase (LPL). The observed increase in LPL expression is mediated by inhibition

in the expression of apolipoprotein CIII (ApoCIII) and an increase in ApoCII expression (68, 69). Finally, FXR induces fatty acid β-oxidation via activation of PPARα (68, 69), as discussed earlier (section 1.2.3).

In order to facilitate the fundamental physiological importance of FXR, a whole body FXR knockout mouse model was generated in 2000 (101). This mouse produces a transcript from the disrupted gene that lacks the sequence encoding a critical portion of the receptor ligand binding/dimerization domain, and therefore does not express a functional FXR (101). FXR knockout mice have increased plasma LDL and HDL levels (68, 69). FXR was also shown to mediate a down-regulation in the proprotein convertase subtilisin/kexin 9 (PCSK9), which promotes intracellular degradation of the LDL receptor by interfering with its recycling to the plasma membrane (68, 69). Therefore, it has been proposed that FXR may reduce plasma LDL levels via enhanced activity of the LDL receptor (68, 69). FXR can also cause a reduction in blood HDL levels by inducing the expression of hepatic scavenger receptor B1 (SR-B1), which regulates HDL uptake by the liver and peripheral tissues, thereby increasing the rate of HDL clearance from the blood. In addition, FXR represses the synthesis of the primary protein constituent of HDL, apolipoprotein AI (ApoAI) (68, 69).

Moreover, liver-specific and intestine-specific FXR knockout mice were developed and used to demonstrate differential but complementary roles for FXR in liver and intestine in regulating bile acid homeostasis (102). FXR in the intestine was demonstrated to control bile acid synthesis in the liver therefore supporting the role of intestinally-produced FGF15 to regulate liver CYP7A1 expression (102). The tissue-specific FXR knockout mouse-models may represent powerful tools allowing for further investigation into the tissue-specific roles of FXR in bile acid metabolism and lipid homeostasis.

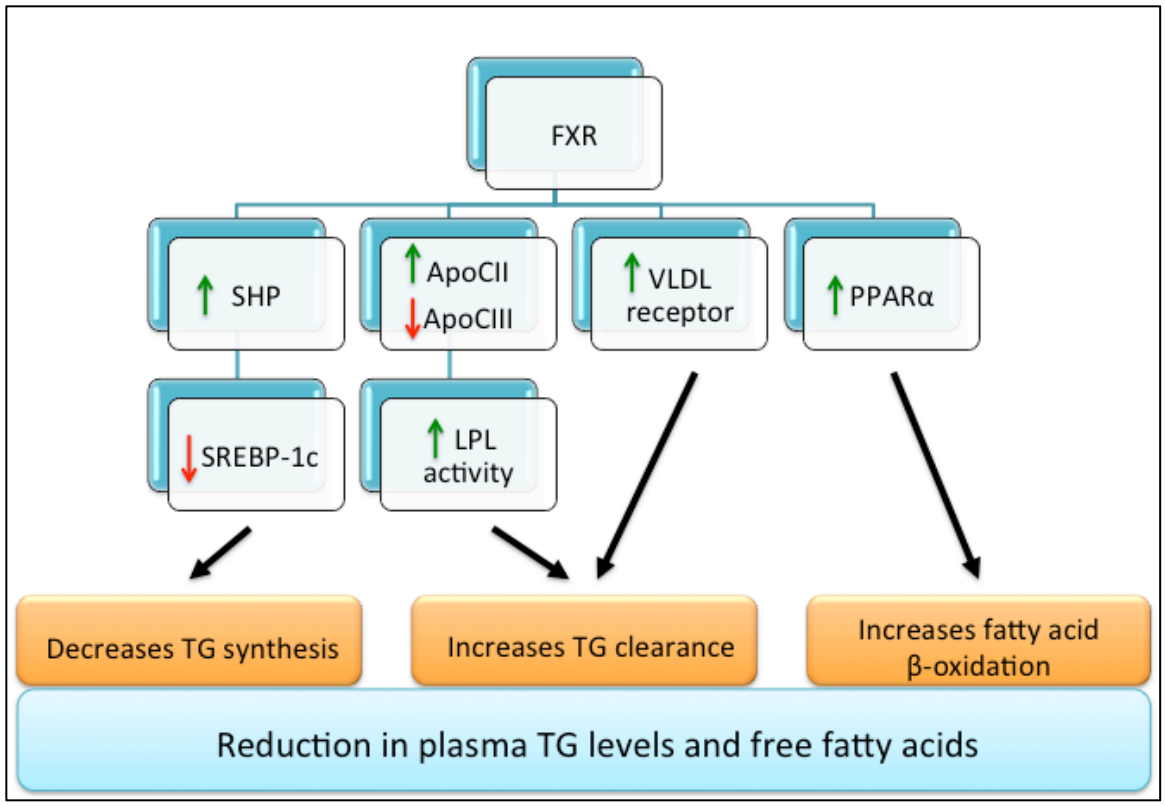

Figure 5: Effect of FXR on triglyceride metabolism
The activation of FXR reduces plasma TG levels by decreasing TG synthesis, increasing TG clearance and increasing fatty acid catabolism. These result from: (a) repression of hepatic TG synthesis mediated via a SHP-dependent inhibition of SREBP-1c; (b) induction of ApoCII and repression of ApoCIII leading to enhanced LPL activity; (c) induction in the expression of the VLDL receptor; and (d) induction in PPARα expression. FXR: Farnesoid x receptor, SHP: Small heterodimer partner, ApoC: Apolipoprotein C, VLDL: very low density lipoprotein, PPARα: Peroxisome-proliferator-activated receptor alpha, SREBP1-c: Sterol regulatory element binding protein 1-c, LPL: lipoprotein lipase, TG: triglyceride.

1.3 Grape Seed Procyanidin Extract (GSPE)

Procyanidins (or proanthocyanidins) are members of a specific group of polyphenolic compounds called flavonoids (103-106). Flavonoids are secondary plant metabolites characterized by a phenylbenzopyran chemical structure. They are ubiquitously found in plants and are the second most abundant natural phenolic compound after lignin (103). Flavonoids are further divided into subgroups, with tannins being one subgroup (103). Procyanidins are one of the two main categories of plant tannins known as condensed tannins (103). Procyanidins can be found in cereals, legumes, fruits, vegetables and beverages

such as red wine and tea, however, the major source in the American diet includes apples, chocolate and grapes (107). Procyanidins are oligomers and polymers of the monomeric unit flavan-3-ol, namely (+) cathechin and (-) epicatechin (103). These flavan-3-ol units can be linked through C4-C8 and C4-C6 bonds (called B-type), but they can also be doubly linked by an additional ether bond between C2-C7 (called A-type) (103, 105). The most common dimers are the Procyanidins B1 to B4 that have the C4-C8 linkage, as well as the procyanidins B5 to B8 (linked by C4-C6 bonds) (103, 105). GPSE is essentially composed of oligomers of (+)-catechin and (-)-epicatechin (dimers, trimers, tetramers and pentamers), as shown in Figure 6 and Figure 7, which have been shown to be highly bioavailable, when compared to polymers (103).

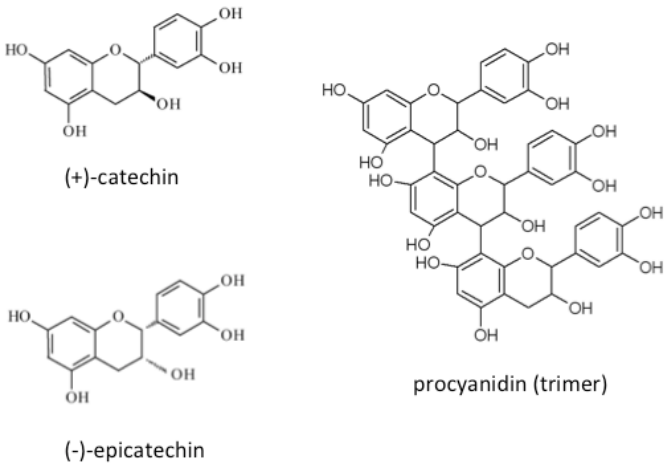

Figure 6: Structure of procyanidins
Procyanidins are essentially composed of oligomers of the monomers catechin and epicatechin. Reproduced from Fine et al, 2000 (105).

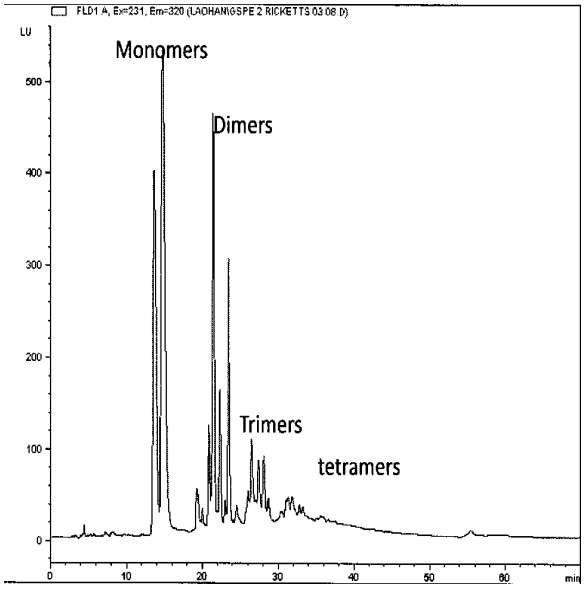

Figure 7: High Performance Liquid Chromatography (HPLC) profile showing the procyanidin composition of GSPE
GSPE is composed of monomers and oligomers of the procyanidins (+)-catechin and (-)-epicatechin. Courtesy of Dr Liwei Gu, FSHN, University of Florida.

Procyanidins have been reported to exhibit several beneficial health effects by acting as antioxidants (103, 105). They also possess anti-atherogenic, anti-carcinogenic, anti-bacterial, anti-viral properties, and can also act as neuroprotective agents (103, 105). Procyanidins may interfere in the pathogenesis of cardiovascular disease via several mechanisms including: increasing plasma HDL, decreasing LDL-derived atherosclerotic lesions, attenuating the formation of free radicals and increasing endothelium-dependent vasodilation (103, 104, 108). GSPE has also been proposed as a beneficial agent for cardiovascular disease in relation to its' positive effects on parameters of the "*metabolic syndrome*". The "*metabolic syndrome*" is defined as a combination of metabolic risk factors such as hypertriglyceridemia, hypertension and hyperglycemia that commonly cluster together and confer an increased risk for cardiovascular disease (109). Therefore, since GSPE modulates glucose homeostasis (110) and decreases plasma TG levels (34, 35, 99, 108), it may exert beneficial effects in patients with the metabolic syndrome, consequently decreasing associated cardiovascular risk factors.

Several studies have assessed the safety of grape seed procyanidin extracts indicating that they lack any associated toxicity (111, 112). Acute, subchronic and chronic toxicity have been evaluated using rodent models with no evidence of acute oral toxicity at dosages of 2 and 4 g/kg being found (112). The no-observed-adverse-effect level (NOAEL) of grape seed extracts in the subchronic toxicity study was 2% in the diet (equal to 1410 mg/kg body weight/day in males and 1501 mg/kg body weight/day in females) (112). Chronic administration of GSPE at 100 mg/kg/day for twelve months or 500 mg/kg/day for six months was demonstrated to be safe when tested in a B6C3F1 mouse model (111).

It has been shown that GSPE decreases blood TG levels in rodents (34, 35, 99) via hepatic induction of FXR. The effect following administration of a single dose of GSPE on plasma lipid levels and lipoprotein profile was demonstrated using healthy male Wistar rats fed a normal chow diet (35). Administration of a single dose of GSPE (250 mg/kg body weight) via oral gavage to the rats resulted in a 50% reduction in serum TG levels ($p<0.05$) after 5 hours post-administration, as well as an improved atherosclerotic risk index, compared to the control group. Although significant effects were observed in regards to TG levels, serum total cholesterol (TC) levels were not altered at this time point (35). These findings were associated with a 50% decrease in total plasma ApoB48 lipoprotein levels and a significant reduction in plasma free fatty acid levels (35). Additionally, changes in the expression of genes related to lipid metabolism in the liver were identified using a microarray followed by qPCR confirmation, and demonstrated an increase in mRNA levels for SHP, CYP7A1, and cholesterol biosynthetic enzymes including 3-hydroxy-3-methylglutaryl CoA reductase (HMG-CoAR), while reducing ApoAII, ApoCI and ApoCIII (35). Since SHP and CYP7A1 are under the control of FXR/RXR and ERα, it was suggested that GSPE may act as a ligand for FXR, RXR, or ERα (35).

Subsequently, a second study was undertaken to elucidate whether or not SHP was the mediator of the GSPE-induced reduction in TG-rich ApoB-containing lipoproteins (34). In this study, GSPE reduced ApoB and TG secretion in *vitro* (in HepG2 cells, a human hepatocarcinoma cell line), while inducing

SHP mRNA and protein expression (34). GSPE has also been shown to transiently stabilize the rapidly degraded SHP mRNA in HepG2 cells, and to maintain significantly elevated SHP mRNA levels after 60 minutes of GSPE treatment (113). When SHP was silenced, via transfection of HepG2 cells with a SHP-siRNA, the effect of GSPE on TG secretion was abolished (34). Utilizing SHP knockout mice, SHP was also demonstrated to be a key mediator in the hypotriglyceridemic effect exerted by GSPE *in vivo* (34), since the 50% reduction in plasma TG levels following GSPE treatment seen in C57BL/6 wild type mice was abolished in the SHP knockout mice (34). Moreover, several genes related to lipid metabolism showed a SHP-dependent response (34), including SREBP1c, the master regulator of lipid and lipoprotein metabolism. Several of the SHP-dependent genes identified have previously been described as targets of SREBP1c, indicating SHP as a major mediator in the observed effects induced by GSPE treatment (34).

It is well known that the activation of FXR by bile acids enhances the expression of SHP, which subsequently reduces the expression of SREBP1c, resulting in decreased serum TG levels (114). Since known FXR agonists and GSPE appear to induce similar genes, it was hypothesized that grape procyanidins reduce TG levels via a FXR-dependent mechanism (99). Administration of GSPE to FXR knockout mice did not cause any reduction in plasma TG levels (Figure 8) analogous to the observations in SHP knockout mice, while neither repressing the expression of SREBP1c and its' target genes (99). Therefore, it was clearly demonstrated that FXR is a key mediator in the hypotriglyceridemic effect of procyanidins in mice (99). Moreover, the expression of SREBP1c arises as a mediator of the hypotriglyceridemic response, dependent on both FXR and SHP (99). In addition, an *in vitro* model using transiently transfected CV-1 cells with FXR plasmid constructs was used to better assess the effect of GSPE on the transactivation of FXR (99). As shown in Figure 9, GSPE alone did not cause transactivation of FXR/RXR in the transfected cells (99). Conversely, when GSPE was added together with 100 μM CDCA, the endogenous ligand for human FXR, it augmented the transactivation of FXR-bound CDCA in a dose-dependent manner (99). Accordingly, it was concluded that the grape seed

procyanidin extract acts as a ligand-dependent co-agonist, enhancing the activity of CDCA bound FXR. This was the first description of a natural product that can act as a co-agonist ligand for FXR (99).

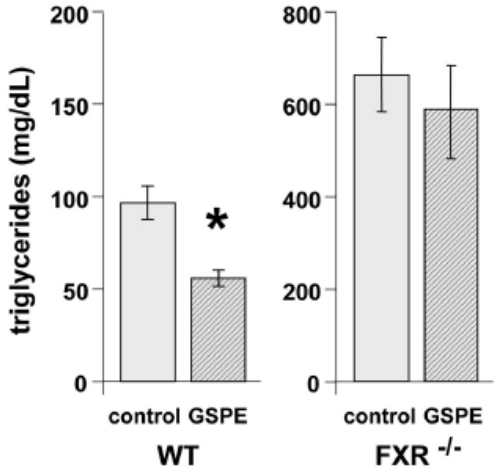

Figure 8: Effect of GSPE administration on plasma triglyceride levels in wild type and FXR knockout mice
GSPE gavage reduces serum TG levels by 50% in wild type mice, while its effect is lost in FXR knockout mice. * Denotes significant difference versus control ($p<0.05$). Reproduced from Del Bas JM et al, 2009 (99).

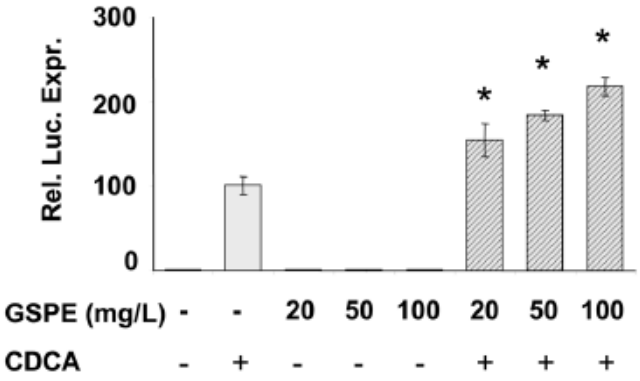

Figure 9: Effect of GSPE on the transactivation of FXR/RXR
The Gal4 DBD-FXR LBD expression vector and Gal4 luciferase reporter plasmid were cotransfected in CV-1 cells, which were treated with vehicle, GSPE and/or 100 μM CDCA. GSPE alone did not activate FXR/RXR, but it enhanced the activation of FXR mediated by CDCA in a dose dependent manner. Del Bas JM et al, 2009 (99).

In summary, GSPE has been demonstrated to enhance the activity of CDCA-bound FXR, resulting in a lowering of plasma TG levels via inhibition of hepatic SREBP1c expression and SREBP1c downstream target genes involved in lipogenesis, in a FXR/SHP dependent manner (34, 35, 99).

As previously shown, bile acid and cholesterol metabolism is also regulated by FXR expression in the intestine. Importantly, studies using an FXRE-luciferase reporter mouse model demonstrated that under physiological conditions, the terminal ileum has the highest level of FXRα signaling (115). Consequently, this raises the question as to whether GSPE exerts any effects on intestinal FXR. We hypothesize that GSPE exerts effects on intestinal FXR target genes, which then contributes to the TG lowering ability.

As already described, GSPE has been shown to lower serum TG levels in a normolipidemic state (34, 35, 99), however the ability of GSPE to lower serum TG levels in a hyperlipidemic state have not yet been determined. We hypothesize that GSPE lowers serum TG levels in a hypertriglyceridemic state.

Therefore, the aims of this thesis are as follows:

Aim 1: Investigate the effects of GSPE on the regulation of FXR target-genes in the intestine

As mentioned above the effects of GSPE on the liver have been characterized and have determined that the regulation of TG metabolism by GSPE is mediated via modulation of a bile acid-dependent pathway mediated via FXR/SHP/SREBP1c (34, 35, 99). As outlined above, FXR not only plays an important role in the liver for the regulation of bile acid, and therefore cholesterol homeostasis, but it also plays an important role in the intestine, where it is a mediator of the enterohepatic recycling of bile acids back to the liver. For several years it was thought that the liver was the main bile acid signaling tissue, however, following the recent development of a FXRE-luciferase reporter mouse model it was established that the main bile acid signaling tissue under normal physiological circumstances is in fact the intestine (115). In this study, it was clearly shown that the activation of FXR in the liver occurs primarily

under conditions of excess bile acids, such as that found in cholestasis (115). Consequently, experiments were conducted to investigate whether or not GSPE exerts the same effects on FXR target genes in the intestine, as is observed on hepatic FXR target genes, i.e. does GSPE enhance the expression of FXR target genes in the intestine compared to CDCA? It is known that CDCA, via activation of FXR, regulates IBABP, ASBT and FGF15/19, therefore, initially using a human colonic cell line, namely Caco2 cells, the potential of GSPE to increase the expression of the above mentioned FXR-target genes in this cell model, as compared to the effects seen with CDCA alone, was assessed. Once it was established whether or not GSPE exerts similar effects on FXR target genes in this cell line, the effects of GSPE treatment *in vivo* in the intestine using C57BL/6 wild type mice was investigated to confirm whether or not these observations also occur *in vivo*.

Aim 2: Investigate the ability of GSPE to lower serum triglyceride levels in a hyperlipidemic state.

As previously mentioned, GSPE was found to lower serum triglyceride levels in both male Wistar rats as well as C57BL/6 wild type mice in a normolipidemic state (34, 35, 99). Consequently, in order to assess whether or not GSPE would one day be suitable as a treatment to ameliorate triglyceridemia in patients suffering from hypertriglyceridemia or the metabolic syndrome, it is important to establish whether or not GSPE is effective in lowering serum TG levels in a hyperlipidemic state. Therefore, in order to answer this aim, a rat model of hypertriglyceridemia was used to determine the efficacy of GSPE to lower serum TG levels. Male Wistar rats were fed a 60% fructose diet for 8 weeks to induce hypertriglyceridemia. It is well established that the first metabolic perturbation of fructose consumption is hypertriglyceridemia and this strain of rat has been shown to respond to a high fructose diet and develop hypertriglyceridemia relatively quickly (116-118). Following treatment for 8 weeks with fructose, the TG lowering ability of GSPE in this rat model was then assessed.

Chapter 2

Materials and Methods

2 Materials and Methods

The methods described within this chapter are common to the whole thesis. Procedures specific to individual chapters are described within those respective chapters. The protocols for preparation of buffers and reagents can be found in Appendix 2.

Chemicals and solutions were obtained from Fisher Scientific (Pittsburgh, PA, USA), and Sigma-Aldrich Chemical Company (St. Louis, MO, USA). Enzymes and associated reagents were obtained from Life Technologies (Grand Island, NY, USA), Roche Applied Science (Indianapolis, IN, USA), or New England Biolabs (Ipswich, MA, USA), unless otherwise stated.

2.1 Grape Seed Procyanidin Extract (GSPE)

GSPE was obtained from Dolcas-Biotech LLC (Chester, NJ, USA). According to the supplier, this extract contains monomeric catechins (polyhydroxyflavan-3-ol) (16.55%), dimeric (18.77%), trimeric (16%), tetrameric (9.3%), and oligomeric (5–13 units) (35.7%) procyanidins, as well as phenolic acids (4.22%). In order to confirm the content of the extract we used in these studies, high performance liquid chromatography (HPLC) analysis was performed (courtesy of Dr Liwei Gu) at the University of Florida Food Science and Human Nutrition Department, the results of which are shown in Figure 7 (section 1.3).

2.2 Cell culture

Dulbecco's modified eagle medium (DMEM), phosphate buffered saline (PBS) and fetal bovine serum (FBS) were obtained from Fisher Scientific (Pittsburgh, PA, USA). FBS was stored in 50 ml aliquots at -20˚C, and L-Glutamine was obtained from Cellgro (Manassas, VA, USA) and was stored in 10 ml aliquots at -20˚C. All solutions were pre-warmed to 37˚C in a water bath prior to use

2.2.1 Caco2 cells

Human epithelial colorectal adenocarcinoma cells (Caco2) were obtained from the American Type Culture Collection (ATCC, Manassas, VA, USA). Caco2 cells have been shown to possess the same morphological and biochemical characteristics as a mature enterocyte when cultured, which starts at 7 days and is completed within 20 days (119). Caco2 cells were routinely maintained in 10 cm Corning cell culture dishes in 10 ml of DMEM supplemented with 20% FBS and 1% L-glutamine, and were cultured at 37˚C and 5% CO_2. Cells were passaged at a ratio of 1:3 twice a week when they reached confluence.

2.2.1.1 Sub-culture

Media was removed from the cell layer and discarded. The cells were then covered in 5 ml of PBS, which was left for 5 seconds, and then removed and discarded. 2 ml of 0.25% trypsin-ethylenediaminetetraacetic acid (EDTA) (Fisher) was added and the cells were incubated at 37˚C for 3 minutes. The trypsin-EDTA solution was inactivated by the addition of 10.5 ml of serum containing media. The cells were removed from the plate by continual flushing with media and then thoroughly re-suspended in the media and then dispersed and 4 ml placed into 3 new 10 cm plates, already containing 6 ml of fresh serum-containing media.

2.2.1.2 Serum free culture

The cells were replenished with fresh media every 48 hours and after ten days the cells reached confluence, and were then sub-cultured into 6 well plates for subsequent experiments. Cells were grown as described above for 24 hours, after which the media was completely removed and replaced with DMEM supplemented with 1% L-glutamine and 0.5% charcoal-stripped FBS (see section 3.2). A lower concentration of FBS was used to minimize the effect of bile salts commonly found in FBS (120).

The cells were cultured for a further 24 hours prior to beginning the experiments.

2.2.1.3 Preparation of charcoal-stripped serum

Activated charcoal (previously washed with autoclaved milliQ water) was used to strip FBS in a ratio of 1g charcoal per 10 ml serum. FBS was added to the charcoal and it was left on a roller for at least 2 hours. It was then centrifuged at 10,000 rpm for 30 minutes, the serum was removed and filtered using a 0.22 μ filter. 50 ml aliquots of charcoal-stripped FBS (CSS) were stored at -20°C.

2.2.1.4 Trypan blue exclusion and cell viability determination

Prior to sub-culturing cells into 6 well plates, the cells were counted and cell viability was evaluated using trypan blue exclusion. After the cells were trypsinized as described above, they were mixed in a 1:1 ratio with trypan blue solution, and counted under the microscope using a hemocytometer. Blue-stained cells were considered non-viable and were therefore not counted.

2.2.1.5 MTT (3-(4,5-Dimethylthiazol-2-yl)-2,5-diphenyltetrazolium bromide) cell proliferation assay

Caco2 cell viability and proliferation after treatment with GSPE was measured using the Vybrant® MTT Cell Proliferation Assay Kit (V-13154) from Life Technologies (Grand Island, NY, USA). This method was developed by Mosmann (121), and is based on the reduction of the yellow tetrazolium salt MTT (3-(4,5-Dimethylthiazol-2-yl)-2,5-diphenyltetrazolium bromide) by metabolically active cells to generate NADH, NADPH and formazan, an insoluble intracellular purple pigment. The generated formazan can then be solubilized and quantitated by spectroscopic means. The Vybrant® MTT Cell Proliferation Assay Kit (V-13154) was utilized according to the manufacturers' instructions, briefly described below. Caco2 cells were cultured in 100 μL of serum-containing media at a concentration of 200 cells/μL in a flat-bottomed 96-well plate. After incubation for at least 24 hours, cells were treated with either water or

GSPE at different concentrations (20-100 mg/L) using serum free culture media as described in section 2.2.1.2. After 4 to 48 hours of GSPE administration, the media was removed and replaced with 100 μL of fresh phenol red-free media not supplemented with serum or glutamine. The MTT reagent was then added (10 μL per well) and the plate was incubated at 37ºC for 4 hours to allow formazan dye formation. 100 μL of the detergent reagent sodium dodecyl sulfate (SDS) was then added to each well and cells were incubated at 37ºC for an additional 4 hours to allow the solubilization of the formazan dye. The absorbance in each well was measured at 560 nm using a Finstruments™ Microplate Reader from MTX Lab Systems (Vienna, VA, USA).

2.3 RNA isolation

Total RNA was extracted from cells and tissues using either Trizol (Life Technologies, Grand Island, NY, USA) or TRI Reagent® RT (Molecular Research Center, Cincinnati, OH, USA), according to the manufacturer's instructions, briefly described below. This technique is based on the one-step acid guanidinium isothiocyanate method developed by Chomczynski and Sacchi (122). To inactivate ribonucleases, all solutions used in the process were treated with 0.1% (v/v) diethylpyrocarbonate (DEPC), incubated over-night at room temperature and then autoclaved twice to inactivate the DEPC. Surfaces of the materials used in the RNA extraction process were treated with RNAse Away solution (Fisher Scientific, Pittsburgh, PA).

2.3.1 RNA isolation from cells

In order to isolate RNA from cells, media was removed from the Caco2 culture plates and 3 ml or 4 ml of TRI Reagent® RT was added to each well in the 6 well plate or to a 10 cm Corning plate, respectively. Chloroform was then added to each sample to separate the aqueous and organic phases (200 μL per 1 mL

of TRI Reagent® RT used). The samples were vortexed thoroughly to mix and then centrifuged for 20 minutes at 10,000 rpm. 80% of the volume of the resulting aqueous upper phase was collected and transferred to a fresh tube, and RNA was precipitated by adding isopropanol (500 µl per 1 mL of TRI Reagent® RT used). The samples were then centrifuged for 20 minutes at 10,000 rpm, and the resulting supernatant was removed from each sample leaving the RNA pellet, which was then washed with 1 mL of 70% DEPC-ethanol. Samples were then centrifuged again for 10 minutes at 10,000 rpm, and the supernatant was removed and the resulting pellet was dried and then re-dissolved in 200 µl of DEPC-treated water. RNA samples were stored at -70˚C until needed. RNA was quantified by measuring the absorbance at 260/280 nm using a Biophotometer Plus from Eppendorf (Hauppauge, NY, USA) and integrity was assessed as described in section 2.3.3.

2.3.2 RNA isolation from tissue

After harvesting, livers and intestines were immediately placed in liquid nitrogen and stored at -70˚C until required. Before the beginning of the RNA extraction, the tissue samples were maintained on dry ice, in order to minimize potential RNA degradation. Approximately 1 g of tissue was immediately homogenized with 4 mL of Trizol, using a tissue homogenizer. 800 µL of chloroform was then added to each sample to separate the aqueous and organic phases. The samples were vortexed to mix thoroughly and then centrifuged for 20 minutes at 10,000 rpm. 80% of the volume of the resulting aqueous upper phase was collected and transferred to a fresh tube, and RNA was precipitated by adding 2 ml of isopropanol. The samples were then centrifuged for 20 minutes at 10,000 rpm, and the resulting supernatant was removed from each sample and the RNA pellet was re-dissolved in 400 µl of precipitation buffer (prepared by the addition of 50 µl of β-mercaptoethanol to 5 mL of guanidinium thiocyanate (GITC). 400 µl of isopropanol was then again added to each sample, and the samples were centrifuged for 20 minutes at 10,000 rpm and the supernatant was removed. The RNA pellet was washed

with 4 mL of ice-cold 70% DEPC-ethanol and then centrifuged for 10 minutes at 10,000 rpm. The supernatant was removed and the pellet was dried and re-dissolved in 250 µl of DEPC-treated water. RNA samples were stored at -70°C. RNA was quantified by measuring the absorbance at 260/280 nm using a Biophotometer Plus from Eppendorf (Hauppauge, NY, USA), and integrity was assessed as described in section 2.3.3.

2.3.3 Assessment of RNA integrity

In order to confirm the presence of intact RNA, each sample was analyzed on a 1% agarose gel via electrophoresis and visualized using ethidium bromide staining. The gel was load with 2 µL of total RNA from each sample combined with 8 µL of DEPC water and 2 µL of loading dye (10X Blue Juice, Life Technologies). Following electrophoresis, the ribosomal bands were visualized under UV light. Two distinct bands corresponding to the 18S and 28S ribosomal sub-units indicated intact RNA.

2.4 Reverse transcription

RNA isolated from cells or tissues was reverse transcribed to obtain complementary DNA (cDNA) using a Superscript III Reverse Transcriptase kit from Life Technologies, and was performed according to the manufacturer's instructions. All other reagents were also obtained from Life Technologies.

Reverse transcription was performed by mixing 1 µL of 250 ng random primers, 1 µL of 10 mM deoxyribonucleotide triphosphate (dNTP) mix, 1-4 µg of total RNA, and sterile autoclaved milli-Q water up to a total volume of 14 µL. The mixture was heated at 65°C for 5 min and then quickly chilled on ice. 4 µL of 5X First-Strand Buffer, 1 µL of 0.1M dithiothreitol (DTT), and 1 µL of 200 U/µL SuperScript™ III RT were then added to each microcentrifuge tube and mixed by gently pipetting up and down. The tubes

were then incubated at 25ºC for 5 min, followed by 60 minutes at 50˚C and finally 15 minutes at 70ºC in order to inactivate the reaction. The resultant cDNA was then stored at -20˚C until required for polymerase chain reaction (PCR).

2.5 Polymerase chain reaction (PCR)

Polymerase chain reaction (PCR) was conducted using a C1000 ^{TM} Thermal Cycler (Bio Rad, Hercules, CA, USA). Taq DNA polymerase (5U/μL) was obtained from Life Technologies. Forward and reverse primers were obtained from Sigma-Aldrich chemical company (St. Louis, MO, USA), and are shown in Table 2.

Table 2: Sequences for the human primers used in the polymerase chain reaction (PCR)

Gene	Forward Primer (5´-3´)	Reverse Primer (3´-5´)	Product size
β–actin	CGGGAAATCGTGCGTGACATTA	CTGTGTGCACTTGGGAGAGGACTGG	866
FXR	TTATTTGGTGTTTTAACAGAACAA	TCCCATCTCTTTGCATTTCCTTAG	478
LXR	TCAGAAGAACAGATCCGCCTGAAGA	AATGAGCAAGGCAAACTCGGCATCA	573
PXR	AGAGCGGCATGAAGAAGGAGATGAT	CGGCCACACTCCCAGGTTCCAGTCT	598
SHP	CGGCCCGTCCAGCTATGTG	CCCAAGAAGGCCAGCGATGTCAA	621

5 μL of 10X PCR buffer (minus Mg^{2+}), 1.5 μL of 50 mM $MgCl_2$, 1 μL of 10 mM dNTP mixture, 1 μL of 10 μM Forward primer, 1 μL of 10 μM Reverse primer, 0.4 μL of 5 U/μL Taq DNA polymerase, 1 μg of template cDNA, and autoclaved milliQ water up to a total volume 50 μL were added to a microcentrifuge tube. The content in each tube was then mixed, centrifuged and incubated in a thermal cycler using the reaction profiles shown in Table 3. The annealing temperatures performed for each transcript of interest

were previously determined via an optimization PCR reaction, in which different annealing temperatures were tested. Each PCR was preceded by one denaturation cycle at 95˚C for 3 minutes. At the end of the total number of PCR cycles, one extension cycle was performed at 72˚C for 10 min and then the reaction tubes were cooled to 4˚C.

Table 3: PCR profiles for the analysis of each transcript of interest

	Denaturation		Annealing		Extension		
Transcript	**Temp (˚C)**	**Time (sec)**	**Temp (˚C)**	**Time (sec)**	**Temp (˚C)**	**Time (sec)**	**Total number of cycles**
β-actin	95	45	65	60	72	45	35
Human FXR	95	45	59.6	60	72	45	45
Human LXR	95	45	65	60	72	45	35
Human PXR	95	45	65	60	72	45	35
Human SHP	95	45	67.5	60	72	45	45

The amplification products were analyzed on a 1% agarose gel via electrophoresis and visualized using ethidium bromide staining. An appropriate molecular weight standard (1Kb ladder) was used in each gel.

2.6 Real time polymerase chain reaction and gene expression analysis

Real time quantitative polymerase chain reaction (qPCR) was performed using a CFX96 Real-Time System (Bio Rad, Hercules, CA, USA). Taq DNA polymerase (5U/μL) was obtained from Life Technologies. Forward primers, reverse primers, and probes were designed using the Oligo Architect Software (Sigma-Aldrich) and were obtained from Sigma-Aldrich chemical company (St. Louis, MO, USA), and are shown in Table 4, Table 5, and Table 6**.**

Table 4: Sequences of the human primers and probes used in quantitative polymerase chain reaction (qPCR) to assess gene expression in Caco2 cells

Human Genes	Forward Primer (5′-3′)	Reverse Primer (3′-5′)	Probe (5′-3′)
ABST	GACATGGACCTGAGCGTCAG	TTGGTATAGATAAGGAGGCACAGC	ATGCTCCACACTGCTTGCCCTCGG
FGF19	CCGCCCAGATGGCTACAATG	GGAAATGAGAGAGTGGAAGAAAGC	ACCGATCCGAGAAGCACCGCCTCC
FXR	GACTGAATTACGGACATTC	CCCAGATTTCACAGAGAA	CACCACGCTGAGATGCTGATG
IBABP	AAGTTCACTGTTGGCAAGGAAAG	GTCTGGTGATAGTTGGGGAAATTC	AGCTTCCCGCCCTCCATCTGCACA
OSTα	CCTCACTAGCATCCTGAC	GATCCAGAGACCAAAGCA	CACAGCACAGACACCACCGT
OSTβ	GTGGTGGTCATTATAAGC	GAGCAAAGTTTCTCTTAGG	AAGAAGCATCCAGGCAAGCA
SHP	GCCCAGCATACTCAAGAAGATTC	GCTAAGCTCCAGGCTCCAG	AGGACTCCAGACAGCATTGAAGCCA

Table 5: Sequences of the mouse primers and probes used in quantitative polymerase chain reaction (qPCR) to assess gene expression in mouse tissues

Mouse genes	Forward Primer (5′-3′)	Reverse Primer (3′-5′)	Probe (5′-3′)
ABST	TCCCTATGATAGCATTGG	GGTACAGTATTCCTCCAA	TCTCTGGTTGCTCTTGTTATTCCTGT
ApoA5	CCACAAACTCACACGTAA	CAGGGAATCTCCATCTTC	CACACCAGCATCCAACGCAA
FDPS	TCTGCTGGTATCAGAAGC	CAGGTTCAGGTAGTAGGG	CATCAACGACGCTCTGCTTCTG
FGF15	GATTGCCATCAAGGACGTCAG	TCAGCCCGTATATCTTGCCG	TGCGGTACCTCTGCATGAGCGC
FXR	TCCAGGGTTTCAGACACTGG	GCCGAACGAAGAAACATGG	CCACGAAGATCAGATTGCTTTGCTCAA
HMGCS1	GCTTGTGTCTAATCAGAATG	GTGTGACTTTAAGGGAGTA	AAGCCAGAACCGTAAGAGAACACT
IBABP	CAGGAGACGTGATTGAAAGGG	GCCCCCAGAGTAAGACTGGG	CCAGCAGGACGGACAGGACTTCACC
PGC1β	CTCTCGGGAACTAAAGAA	TGGCCTCTTTTACTTCTC	CTGGCACTCTACAATCTCACCGA
OSTα	GACCAATTACAGCATCTCCCCT	CTGAGCCAGTGGTAAGAAAGGT	TTCTCTCACCCTCCCACCGCAGCC
OSTβ	AACTGCTGGAAGAAATGCTTTGG	CTTCTCAGGAGGAACATGCTTGT	TGACCACCAGGACTGCCAGGACCA
SHP	GTACCTGAAGGGCACGATCC	ACACCTGCAACAGGAGGCT	ATGTGCCAGGCCTCCGTGCC
SREBP1c	GGAGCCATGGATTGCACATT	TATGCTGGGGGTGAGACAGG	CAGCTCATCAACAACCAAGACAGTGACTTCC

Table 6: Sequences of the rat primers and probes used in quantitative polymerase chain reaction (qPCR) to assess gene expression in rat tissues

Rat genes	Forward Primer (5′-3′)	Reverse Primer (3′-5′)	Probe (5′-3′)
ApoA5	CCACAAACTCACACGTAA	ACGGATGAAGGTACTGAG	CACACCAGCATCCAACGCAA
HMGCS1	TGAGCTATTCAACCAGAA	GTGACTTTAAGGGAGTAGA	AAGCCAGAACCGTAAGAGAACACT
IL-6	GACTGATGTTGTTGACAG	CGACTTGTGAAGTGGTATA	TGGTATCCTCTGTGAAGTCTCCTCT
PGC1β	CACCACACCTCCATATAAG	TGAGCTGAAGAGTCTCAG	CAAGCAGGACACCAAGCACAG
SHP	GTCCTAGGCAAGACTGTA	GGTTCCTCTAGCAAGATC	AACCTGCCGTCCTTCTGCCT
SREBP1c	CAGCCACACTTCATCAAG	GTCCACAACCAGTGGTAC	AGACTCGCTGCTGCTGACAG
TNFα	CTCAGCCTCTTCACATTC	CATGGAACTGATGAGAGG	CACCACGCTCTTCTGTCTACTGA

Each 40 μL qPCR reaction mix contained: 4 μL of 10X PCR buffer (minus Mg^{2+}), 3.6 μL of 50 mM $MgCl_2$, 2.4 μL of 2.5 mM dNTP mixture, 1 μL of 20 μM Forward primer, 1 μL of 20 μM Reverse primer, 0.25 μL of 20 μM 5'FAM- 3'TAM labeled Probe, 0.25 μL of 5 U/μL Taq DNA polymerase, 100 ng of

cDNA per sample, and autoclaved milliQ water up to the total volume of 40 μL. The cycling conditions were as follows:

Table 7: qPCR profiles

Step	Temperature	Time	Total number of cycles
Initial denaturation	95ºC	60 sec	1
Denaturation	95ºC	15 sec	40
Annealing/Extension	60ºC	60 sec	

A "*no template control*" with sterile water was performed for each master mix. DNA standards were created by pooling 1mg of cDNA from each sample. Serial dilutions were made from the pooled samples to obtain DNA standards at 0.1, 1, 10, 100 and 1000 ng/μL, and were used as the template for qPCR to generate a standard curve. Each sample was performed in duplicate or triplicate in a 96-well clear qPCR plate. Relative gene expression quantification was normalized to endogenous housekeeping genes, namely β-actin, glyceraldehyde 3-phosphate dehydrogenase (GAPDH) and/or cyclophilin.

2.7 Animal feeding studies

All studies were approved by the Institutional Animal Care and Use Committee (IACUC) at the University of Nevada Reno.

The animal studies were a treatment-control comparison to evaluate the effect of GSPE on plasma triglyceride (TG) levels either in a normolipidemic or in a hyperlipidemic state and to understand the mechanism of action of GSPE at the molecular level. They were conducted at the University of Nevada Reno.

2.7.1 *In vivo* assessment of the triglyceride lowering ability of GSPE in normolipidemic wild type mice

Two studies were performed in male C57BL/6 mice purchased from Charles River Laboratories (Wilmington, MA, USA). The animals were housed under standard conditions with free access to food and water, and were allowed to acclimatize for one week in the laboratory of animal medicine (LAM) at the University of Nevada Reno, prior to commencement of experiments.

Twelve male C57BL/6 mice, aged 8 weeks of age were used to assess the effects of GSPE treatment after 14 hours of administration. Six mice were allocated to either the vehicle or GSPE administration group.

Subsequently, 36 male C57BL/6 mice, aged 8 weeks of age at the beginning of the study, were used to assess the effects of GSPE treatment after mice were fed a bile acid sequestrant diet (2% cholestyramine-supplemented diet). Eighteen mice were fed a control diet (Harlan Tekland rodent diet 2019) for 4 weeks and 18 mice were fed the 2% cholestyramine-supplemented diet for 4 weeks. After 4 weeks, the mice were then divided as follows (n=9 per treatment, per group):

1. Control diet + 14 hours treatment with vehicle
2. Control diet + 14 hours treatment with GSPE
3. 2% cholestyramine-supplemented diet + 14 hours treatment with vehicle
4. 2% cholestyramine-supplemented diet + 14 hours treatment with GSPE

The number of mice used in the described studies was based on previously determined power analysis to achieve statistically significant results, as used in previous studies utilizing GSPE (34, 99).

2.7.1.1 Diets and treatments

Mice were fed a standard rodent chow (Harlan Tekland rodent diet 2019) and water *ad libitum*. On experimental day 1, mice were treated with either vehicle (water), or GSPE (250 mg/kg) via oral gavage.

GSPE powder was dissolved in autoclaved milli-Q water the night before to obtain a solution that was administered via oral gavage using a metallic 20 gauge gavage needle. A first dose was administered at 9:00 pm and a second dose 12 hours later at 9 am. The mice were then fasted for 2 hours until 11 am when they were terminated.

In the cholestyramine experiment, mice were fed the standard rodent chow (Harlan Tekland rodent diet 2019) alone or supplemented with 2% cholestyramine during 4 weeks. Following 4 weeks on the diets, mice were treated with either vehicle (water), or GSPE (250 mg/kg) via oral gavage, using the same protocol described above.

2.7.2 *In vivo* assessment of the triglyceride lowering ability of GSPE in a hypertriglyceridemic state using the fructose fed rat model

Twenty male Wistar rats, aged 8 weeks of age were purchased from Charles River Laboratories (Wilmington, MA, USA). The animals were housed under standard conditions and were allowed to acclimatize for one week in the LAM at the University of Nevada Reno, prior to commencement of the experiment.

2.7.2.1 Experimental Diets

The control and fructose chow diets were obtained from Harlan Laboratories (Indianapolis, IN, USA). The high fructose diet comprised approximately 65% fructose, while the starch control diet had the fructose replaced by cornstarch and maltodextrin, keeping the other components in the formula constant. The specific components and proportions of the both diets are listed in Table 8.

Table 8: Composition of the control and high-fructose diets used in the fructose-fed rat model

Formula	65% Fructose Diet (g/Kg)	Starch Control Diet (g/Kg)
Casein	200.0	200.0
L-Cystine	3.0	3.0
Fructose	647.0	0
Corn Starch	0	515.0
Maltodextrin	0	132.0
Soybean Oil	70.0	70.0
Cellulose	32.486	32.486
Mineral Mix, AIN-93G-MX w/cellulose	35.0	35.0
Vitamin Mix, AIN-93-VX w/cellulose	10	10
Choline Bitartrate	2.5	2.5
TBHQ, antioxidant	0.014	0.014

2.7.2.2 GSPE treatment

Following 8 weeks on the diets, the rats were fed either vehicle (water) or GSPE 250 mg/kg via oral gavage for 7 days. The GSPE dose used is one-fifth of the no-observed-adverse-effect level (NOAEL) described for GSPE and male rats (35). GSPE was dissolved in autoclaved milli-Q water the night before to obtain a solution that was administered via oral gavage using a metallic 16 gauge gavage needle. A first dose was administered at 9:00 pm and a second dose 12 hours later at 9 am on the first day. The following 6 days, only one dose of GSPE 250 mg/kg was administered at 9 am. After 5 hours following the last treatment (2 pm), the rats were terminated.

2.7.3 Serum collection

Blood was collected in amber CAPIJECT® capillary micro-collection tubes obtained from Terumo Medical Products (Somerset, NJ, USA). The amber tubes have a gel barrier with clot activator (silica particles and inert gel) that makes them suitable to determine light-sensitive serum analytes.

2.7.3.1 Serum collection from mice

Blood was drawn from mice utilizing the retro-orbital bleeding technique. Standard micro-hematocrit capillary tubes were used for blood collection. Mice were anesthetized with isoflurane in a chamber. The anesthetized animal was held by the back of the neck and the loose skin of the head was tightened with the thumb and middle finger. The tip of the capillary tube was placed and pressed against the medial canthus of the eye under the nictitating membrane. As soon as the sinus was punctured, blood entered the tubing by capillary action. When 100 µL of blood was collected, the tube was withdrawn and slight pressure with a piece of gauze on the eyeball was used in order to prevent further bleeding. The eyeball itself remained uninjured during the procedure.

2.7.3.2 Serum collection from rats

Blood was drawn from the saphenous vein. The rats were anesthetized with isoflurane in a chamber and anesthesia was maintained via a nasal cone throughout the procedure. The back of the left leg was shaved with an electric trimmer, in order to reveal the saphenous vein and to clear the puncture site. The base of the leg was then compressed above the saphenous vein, in order to dilate and bulge out the vein. The vein was then punctured using a 5 mm lancet and approximately 100-200 µL of blood was collected. A clean compress was held on the puncture site to stop any further bleeding. The rats were then brought out of anesthesia and returned to their home cage.

2.7.3.3 Serum isolation

The blood samples once collected were centrifuged at 12,000 rpm for 10 minutes, to obtain the serum, which was then stored at -20˚C until subsequent analysis.

2.7.4 Biochemical analysis

Serum triglycerides and fecal bile acids were determined and each sample was analyzed in triplicate.

2.7.4.1 Serum triglyceride (TG) measurement

Serum TG levels were determined by an enzymatic procedure using the commercially available Infinity™ kit from Fisher Scientific, and performed according to the manufacturers' instructions. Each sample was analyzed in triplicate. Briefly, 2 µL of sample and 198 µL of reagent were added in a 96 well plate. The plate was then incubated at 37ºC for 5 min, and absorbance was measured at 520 nm using a Finstruments™ Microplate Reader from MTX Lab Systems (Vienna, VA, USA). A standard curve using standards from Matrix Plus™ Chemistry Reference Kit (Verichem Laboratories, Providence, RI, USA) was constructed to allow determination of the TG content in each sample.

2.7.4.2 Fecal bile acid (BA) measurement

To determine fecal bile acid excretion, the feces from mice participating in the cholestyramine diet experiment were manually collected and dried. Then 0.5 g of dried feces was minced using a morter and extracted in 10 ml of 75% ethanol at about 50ºC for 2 hours. The extract was then centrifuged at 10,000 rpm for 5 minutes, and 1 ml samples of supernatant were diluted down for assay up to 4 ml with a 25% PBS solution. The bile acid concentration was measured enzymatically using the Total Bile Acid Assay from Diazyme Laboratories (Poway, CA, USA). Each sample was analyzed in triplicate. Briefly, 5 µL of sample, 135 µL of reagent 1 and 45 µL of reagent 2 were added to a 96 well plate. The plate was then incubated at 37ºC for 10 min, and absorbance was measured at 405 nm using a Finstruments™ Microplate Reader from MTX Lab Systems (Vienna, VA, USA). A standard curve using the standard provided with the Diazyme kit was constructed to allow determination of the BA content in each sample.

2.8 Statistical Analysis

One-way analysis of variance (ANOVA) was employed as the statistical tool to detect significant differences between groups. Treatment differences were considered statistically significant at $p<0.05$. All statistical analyses were performed using the statistical software Minitab 15 from Quality Analysis Results ® (State College, PA, USA).

Chapter 3

Assessing the effects of GSPE on FXR target genes in a human colonic cell model

3 Assessing the effects of GSPE on FXR target genes in a human colonic cell model

3.1 Introduction

As previously mentioned, the main function of FXR is to control hepatic and intestinal gene expression involved in the enterohepatic recycling, and detoxification of bile acids, as well as the regulation of genes involved in metabolic homeostasis, including glucose and lipid regulation.

Using a transgenic FXR luciferase reporter mouse model, it has previously been shown that the ileum is the primary bile acid signaling tissue in the basal state (115). FXR signaling in the liver is only induced under pathological conditions characterized by a slowed or blocked flow of bile from the liver into the intestine, which would occur in conditions such as cholestasis (115). Consequently, the terminal ileum may be an important mediator of FXR effects since it is the tissue with the highest level of FXR signaling under physiological conditions.

In the intestine, FXR activation by bile acids decreases luminal reabsorption of BAs by reducing ileal bile acid transporter (IBAT) expression, also known as apical sodium dependent bile acid transporter (ASBT) (88); facilitates transport of BA through the enterocyte via induction of intestinal bile acid-binding protein (IBABP) (97); facilitates the efflux of BA into the portal circulation via induction of organic solute transporters (OST) α/β (89); and induces the expression and secretion of fibroblast growth factor (FGF) 15/19 (FGF15 in mice and FGF19 in humans) from the enterocyte into the portal circulation (93). FGF15/19 has been shown to act as a hormone signaling to the liver and plays a key role in bile acid metabolism (93, 94), as well as metabolic homeostasis (123).

GSPE has been demonstrated to decrease serum triglyceride levels via activation of FXR in the liver (34, 35, 99). As previously mentioned, when CV-1 cells are transiently transfected with a FXR plasmid construct, GSPE has been shown to act as a ligand-dependent co-agonist, enhancing the activity of CDCA

bound FXR in a dose-dependent manner (34, 99). FXR activation in the liver by GSPE induces the expression of small heterodimer partner (SHP) (34, 35, 99). SHP then acts as a repressor to decrease hepatic expression of sterol response element binding protein 1c (SREBP1c), a key transcription factor regulating lipogenic gene expression, thereby lowering serum TG levels (34, 35, 99).

Whether or not GSPE exerts an effect on FXR intestinal target genes has not yet been determined.

The main aim of this chapter is to investigate the *in vitro* effects of GSPE on the regulation of FXR and its intestinal target-genes, namely, ASBT, IBABP, OST α/β, FGF19, and SHP. For this purpose the human colonic adenocarcinoma cell line Caco2 was used. Caco2 cells represent a good model to study the effects of GSPE on enterohepatic circulation via activation of FXR due to the following reasons:

- Although Caco2 cells are derived from colonic cells, they have been shown to possess the same morphological and biochemical characteristics as small intestine mature enterocytes when cultured, which starts at 7 days and is completed within 20 days after confluence is reached (119).

- Caco2 cells have been shown to express FXR (124, 125), which is the key NHR in the regulation of bile acids homeostasis.

3.2 Materials and methods

Caco2 cells were obtained from the American Type Culture Collection (ATCC) and they were routinely cultured as described in section 2.2.1.1.

Caco2 cells were first cultured to evaluate the expression of FXR and related NHRs. After 10 days post-confluence, mRNA was extracted using TRI Reagent (as described in section 2.3.1), cDNA was made using Superscript III Reverse transcriptase (as described in section 2.4), and PCR was conducted to evaluate NHR expression (as detailed in section 2.5).

Subsequently, Caco2 cells were sub-cultured into 6 well plates in order to evaluate the effects of GSPE and CDCA on intestinal FXR target gene expression. After 10 days post-confluence, the media was completely removed and replaced with DMEM supplemented with 1% glutamine and 0.5% charcoal-stripped FBS (instead of 20% FBS previously used in routine culture), for a further 24 hours. The goals of replacing the DMEM + 20% FBS with DMEM + 0.5% charcoal-stripped FBS were:

- to minimize the effect of non-polar material such as certain growth factors, hormones and cytokines which are removed by activated charcoal, and

- to reduce the effects of bile salts found in FBS by decreasing the concentration of FBS added to DMEM (120).

After 24 hours the media was replaced, cells were treated in duplicate for time points ranging from 1 to 72 hours with DMEM + 0.5% charcoal-stripped FBS supplemented with the following treatments:

1. Water
2. 50 or 100μM CDCA
3. 20 mg/L GSPE
4. 50 mg/L GSPE
5. 100 mg/L GSPE
6. 50 or 100μM CDCA + 20 mg/L GSPE
7. 50 or 100μM CDCA + 50 mg/L GSPE
8. 50 or 100μM CDCA + 100 mg/L GSPE

After 1-72 hours treatment, mRNA was extracted using TRI Reagent (as described in 2.3.1), cDNA was made using Superscript III Reverse transcriptase (as described in 2.4), and real time qPCR was used to determine gene expression changes (as detailed in 2.6). Gene expression changes assessed in the Caco2

cell model included ASBT, IBABP, OSTα/β, FGF19 and FXR. Additionally, β-actin expression was used as the endogenous control gene. All the results for the target genes were standardized to β-actin levels, and the data shown represents the fold change for each target gene relative to β-actin expression.

The Vybrant® MTT Cell Proliferation Assay Kit (V-13154) from Life Technologies (Grand Island, NY, USA) was used to assess Caco2 cell viability and proliferation following treatment with GSPE, since lower levels of β-actin (endogenous control gene) were observed after Caco2 cells were treated with GSPE for longer than 24 hours. The detailed protocol is described in 2.2.1.5.

3.3 Results

3.3.1 Evaluation of FXR and related NHR expression in Caco2 cells

Caco2 cells express FXR (Figure 10) and SHP (Figure 11) upon differentiation; therefore they represent an appropriate model to investigate the effects of GSPE on known FXR target genes in the intestine.

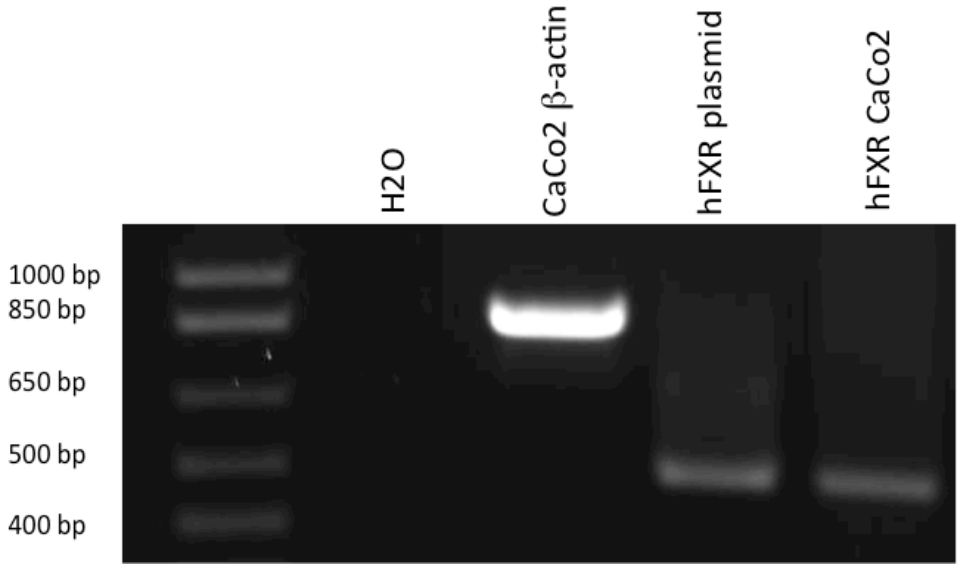

Figure 10: Caco2 cells express FXR
Caco2 cells were cultured to 10 days post-confluence, RNA was isolated and cDNA reverse transcribed. PCR was then performed on the cDNA obtained from Caco2 cells. β-actin was used as internal control. The FXR product size is 478bp and the β-actin product size is 866bp. Water and a human farnesoid X receptor (hFXR) plasmid were used as a negative and positive control, respectively.

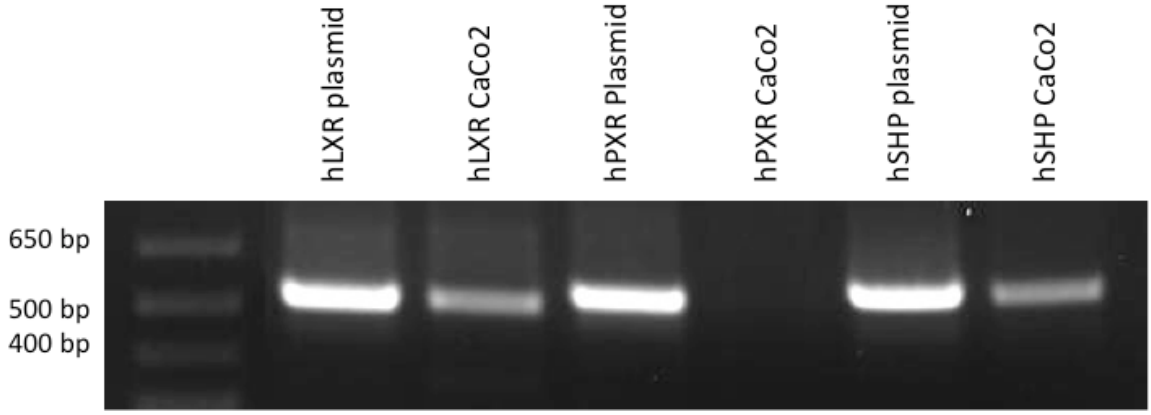

Figure 11: Caco2 cells express LXR and SHP, but not PXR
Caco2 cells were cultured to 10 days post-confluence, RNA was isolated and cDNA reverse transcribed. PCR was then performed on the cDNA obtained from Caco2 cells. The product sizes are 573bp for liver X receptor (LXR), 598bp for pregnane X receptor (PXR) and 621bp for small heterodimer partner (SHP).

3.3.2 Determination of the effect of GSPE on Caco2 cell proliferation

Grape seed extracts have been demonstrated to exert numerous and different biological effects in several cancer types, such as skin, colorectal, prostate and breast cancer cells (126). Anti-cancer effects exerted by grape seed extract are generally attributed to the epigallocatechin and procyanidin compounds, which possess relevant pro-apoptotic, as well as growth inhibitory properties (126).

Grape seed extracts have been demonstrated to induce strong biological effects on Caco2 cells, which include growth inhibition, stimulation of markers of apoptotic signaling pathways, and the induction of programmed cell death (127, 128). Growth inhibition has been shown to be evident after the first 24 hours of treatment and progressively increases thereafter (127, 128).

Since we are using the Caco2 cell model for the studies outlined in this thesis, it is important to address the effects of GSPE on cell growth in these cells. Therefore, the anti-proliferation effects of GSPE were assessed using the MTT assay, described in detail in section 2.2.1.5. The MTT assay developed by Mosmann (121) allows measurement of proliferation rate, and conversely, the reduction in cell viability when metabolic events have led to apoptosis or necrosis.

When Caco2 cells were treated with GSPE (20-100 mg/L) for 4 to 48 hours, a time and dose-dependent reduction in the percentage of viable Caco2 cells was observed. 20 mg/L GSPE only affected Caco2 cell growth after 48 hours of treatment, causing a 30% reduction in viable cell number ($p=0.007$). However, higher doses of GSPE (50-100 mg/L) induced a significant inhibition in Caco2 cell growth, an effect that progressively increased over time, reaching a 95% reduction in Caco2 cell viability after 48 hours following 100 mg/L GSPE treatment ($p=0.007$).

3.3.3 Evaluation of FXR target gene expression in Caco2 cells following treatment with chenodeoxycholic acid alone or in combination with GSPE

3.3.3.1 Apical sodium dependent bile acid transporter (ASBT)

The intestinal absorption of BAs is largely an active process where ASBT, also known as ileal bile acid transporter (IBAT), is of major importance (88). ASBT disruption increases the fecal loss of BAs that in turn strongly induces BA synthesis (88). FXR is a negative regulator of intestinal ASBT expression. In mice, ASBT protein and mRNA were decreased when the male C57BL/6 mice were fed a diet supplemented with FXR ligands either 0.5% cholic acid or 0.5% taurocholic acid for a period of 7 days (129).

In Caco2 cells, as was expected, 100μM CDCA repressed ASBT mRNA expression after 24 hours treatment ($P=0.004$) by 16% compared to water, while co-administration of GSPE (50-100 mg/L) with 100 μM CDCA further enhanced repression in a dose-dependent manner (as shown in Figure 12). Interestingly, GSPE alone (20-100mg/L) also decreased ASBT mRNA expression dose dependently (Figure 12).

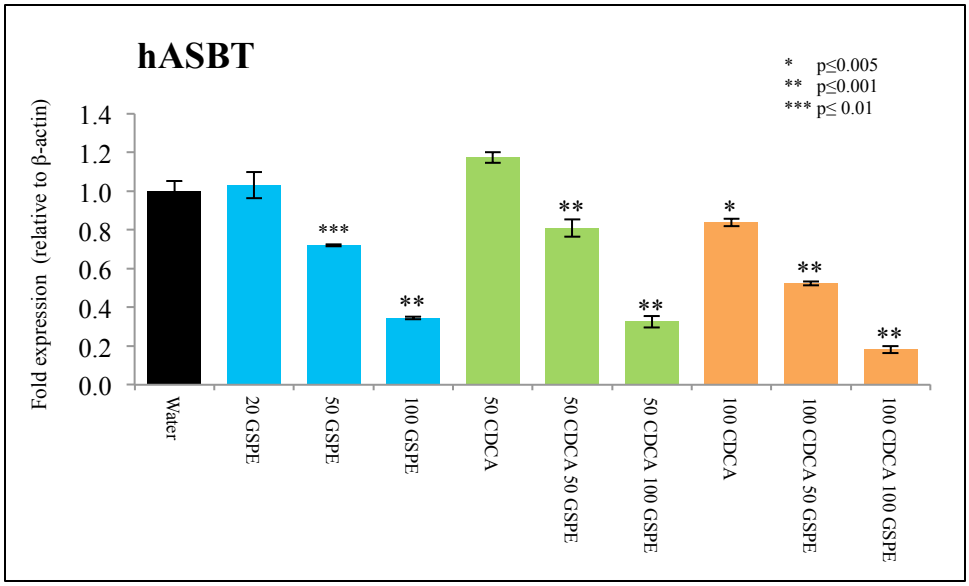

Figure 12: ASBT mRNA expression in Caco2 cells 24 hours after treatment with either CDCA or GSPE alone or in combination

Caco2 cells were treated for 24 hours with either CDCA (50-100 μM), GSPE (50-100 mg/L) or in combination, as indicated. 100 μM CDCA significantly decreased ABST mRNA levels by 16% (p=0.004), while the addition of GSPE further decreased ABST expression in a dose-dependent manner (n=3, in triplicate). hASBT: human apical sodium dependent bile acid transporter, CDCA: chenodeoxycholic acid, GSPE: grape seed procyanidin extract.

As indicated in the figure overleaf, 100 μM CDCA and 100 μM CDCA + GSPE repressed ASBT expression after 4 hours of treatment, an effect which was persistent during all time points evaluated (Figure 13). Additionally, GSPE treatment alone started to repress ASBT gene expression after 2 hours in Caco2 cells and after 12 hours, a statistically significant dose-dependent inhibition in ASBT mRNA levels was observed (Figure 14).

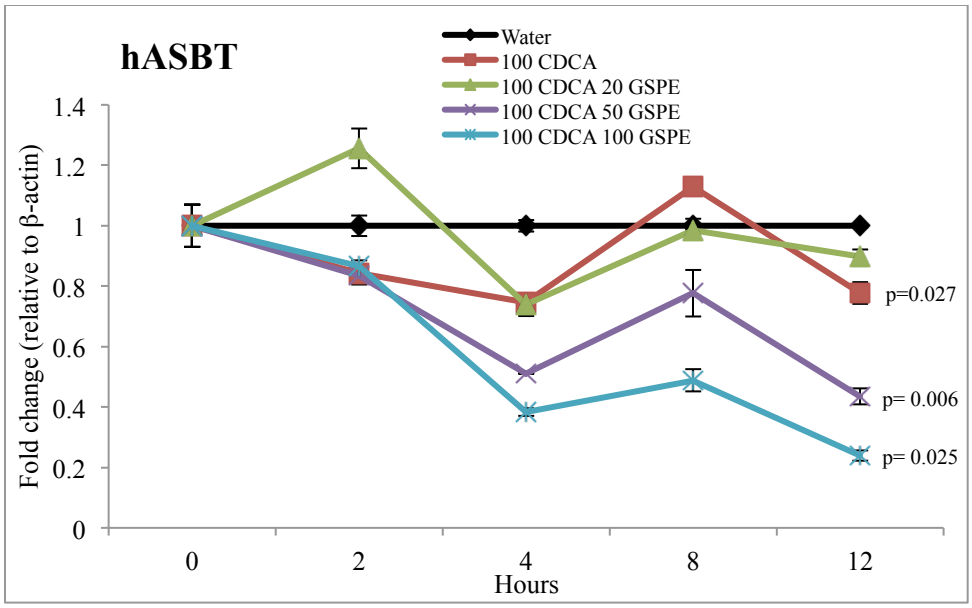

Figure 13: The effects of CDCA and CDCA+GSPE on ASBT expression in Caco2 cells
100 μM CDCA slightly decreased ASBT expression, while co-administration of GSPE and CDCA further increased the repression on ABST expression induced by CDCA, in a dose-dependent manner (n=2, in duplicate). hASBT: human apical sodium dependent bile acid transporter, CDCA: chenodeoxycholic acid, GSPE: grape seed procyanidin extract.

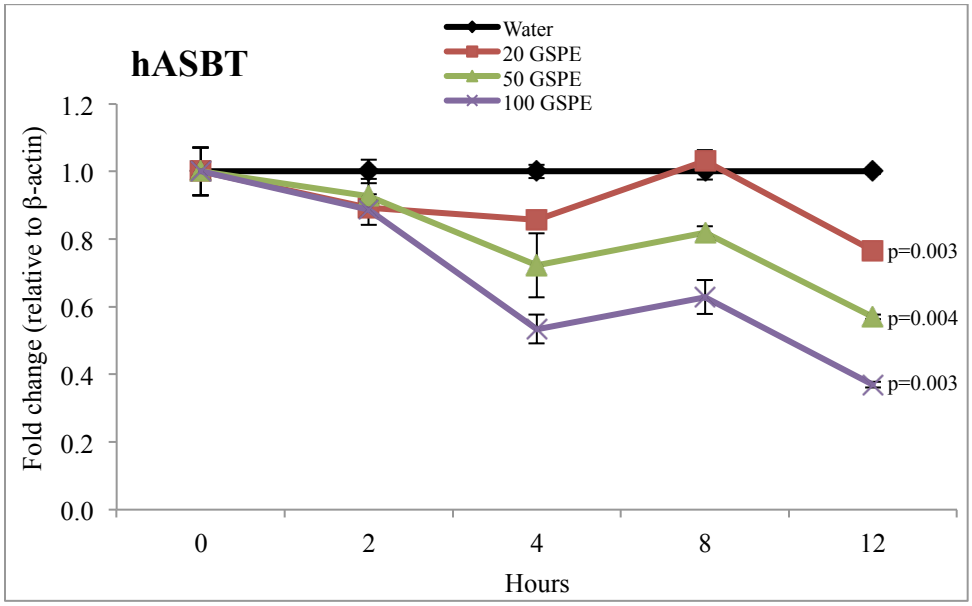

Figure 14: The effects of GSPE alone on ASBT expression in Caco2 cells
A decreased in ABST mRNA levels was observed in response to GSPE (20-100 mg/L) treatments. This effect was dose-dependent and statistically significant after 12 hours (n=2, in duplicate). hASBT: human apical sodium dependent bile acid transporter, GSPE: grape seed procyanidin extract.

In summary, GSPE alone or in combination with CDCA caused a significant repression in ASBT expression, as is expected when FXR is activated.

3.3.3.2 Intestinal bile acid-binding protein (IBABP)

IBABP is expressed in the ileum, and is responsible for shuttling BAs from the apical to basolateral membrane inside the enterocyte (97). It has been suggested that IBABP plays an important role in enterohepatic circulation through the regulation of bile acid trafficking (97). Bile acid-activated FXR strongly induces IBABP gene expression, while IBABP mRNA levels are significantly decreased in FXR knockout mice (97).

As shown in Figure 15, after 24 hours treatment in Caco2 cells, 100 μM CDCA resulted in a 400-fold increase in IBABP mRNA expression ($p<0.001$). However, the combination of GSPE with 100 μM CDCA dose dependently inhibited the CDCA-induced expression of IBABP ($p<0.001$). GSPE alone did not cause any change in IBABP mRNA expression compared to water (data not shown).

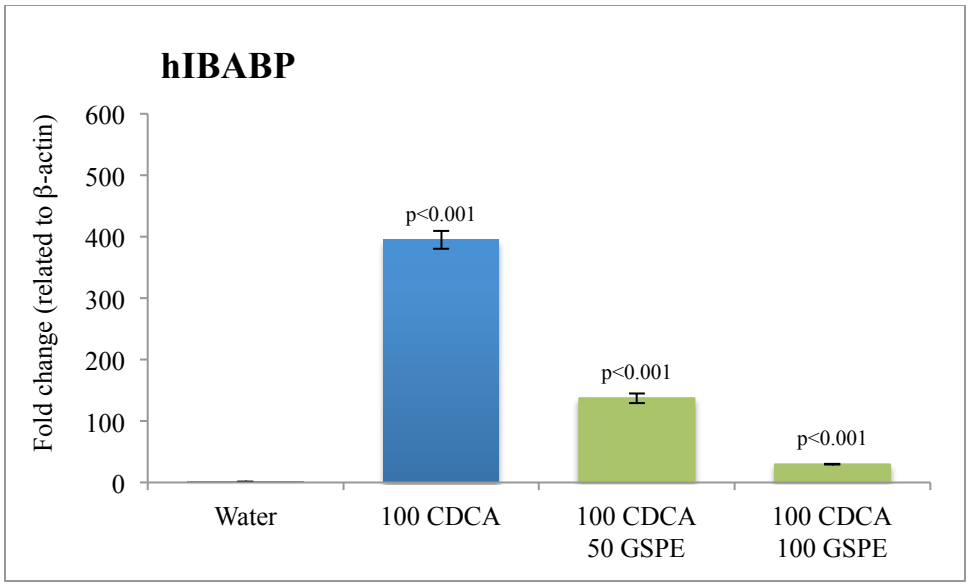

Figure 15: IBABP mRNA expression in Caco2 cells after 24 hours treatment
100 μM CDCA significantly induced IBABP mRNA by 400-fold. However, co-administration of CDCA and GSPE dose-dependently reduced the CDCA-induced IBABP expression (n=3, in triplicate). hIBABP: human intestinal bile acid-binding protein , CDCA: chenodeoxycholic acid, GSPE: grape seed procyanidin extract.

A further detailed analysis revealed that IBABP mRNA levels in Caco2 cells start rising as early as 1 hour after administration with 100 μM CDCA. IBABP expression exponentially increased over time, as shown in Figure 16, reaching a statistically significant 50-fold induction after 12 hours ($p<0.001$, compared to water). The addition of GSPE (20-100 mg/L) caused a dose-dependent repression in CDCA-induced IBABP expression. At 12 hours, the differences observed between 100 μM CDCA and 100 μM CDCA plus 50 mg/L and 100 mg/L GSPE were statistically significant ($p=0.021$ and 0.005 respectively).

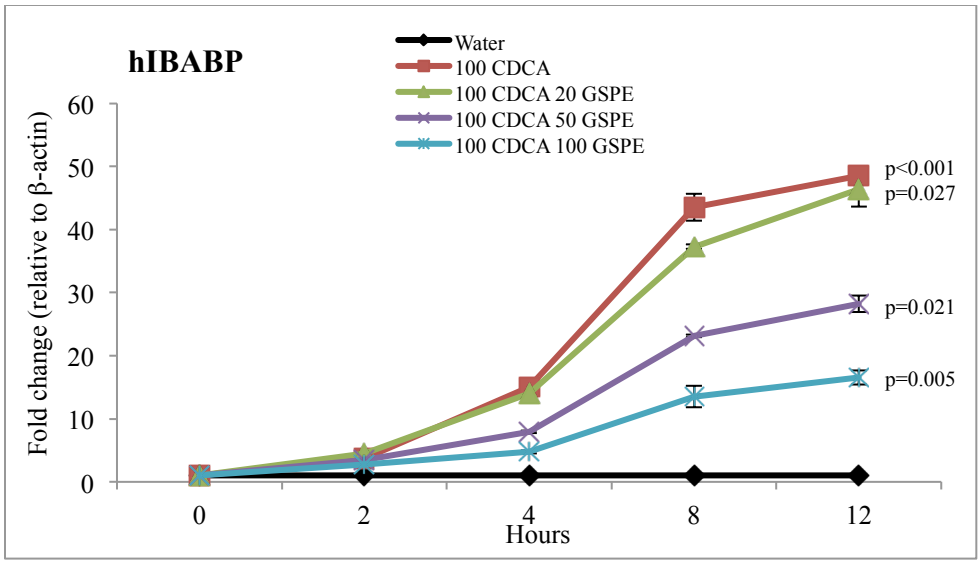

Figure 16: Time course for IBABP expression in Caco2 cells following treatments
IBABP expression exponentially increased following incubation with 100 μM CDCA. The addition of GSPE (20-50 mg/L) repressed the CDCA-induced expression in a dose-response manner (n=2, in duplicate). hIBABP: human intestinal bile acid-binding protein , CDCA: chenodeoxycholic acid, GSPE: grape seed procyanidin extract.

In conclusion, GSPE alone does not alter IBABP mRNA expression. Additionally, following co-administration of CDCA with GSPE, instead of inducing IBABP expression, as would be expected if GSPE is acting as a co-agonist ligand for FXR, the opposite result was obtained, whereby co-incubation resulted in a dose-dependent inhibition in CDCA-induced IBABP mRNA expression.

3.3.3.3 Organic solute transporters (OST) α/β

The heteromeric organic solute transporters OSTα and OSTβ contribute to enterohepatic BA circulation by moving bile salts from the enterocytes into the blood, in accordance with their location at the basolateral membrane (89). This heteromeric transporter requires both subunits (α and β) for the transport of various BAs. Ileal expression of both genes is induced in wild-type mice following cholic acid

treatment, while induction is not observed in FXR knockout mice (130). Treatment with GW4064, a synthetic FXR ligand, also has been shown to induce OSTα and OSTβ mRNAs in the ileum (131).

As expected, treatment with 100 μM CDCA increasingly induced OSTα and β expression over time up to 2.8 fold for OSTα (p=0.006) at 8 hours, and up to 1.8 fold for OSTβ at 12 hours (p=0.028). However, when GSPE was added to CDCA, a dose-dependent inhibition in the CDCA-induced expression of both OSTα and β was observed (Figure 17). Moreover, GSPE treatment alone repressed OSTα and β expression in a dose-dependent manner, as compared to water (Figure 18).

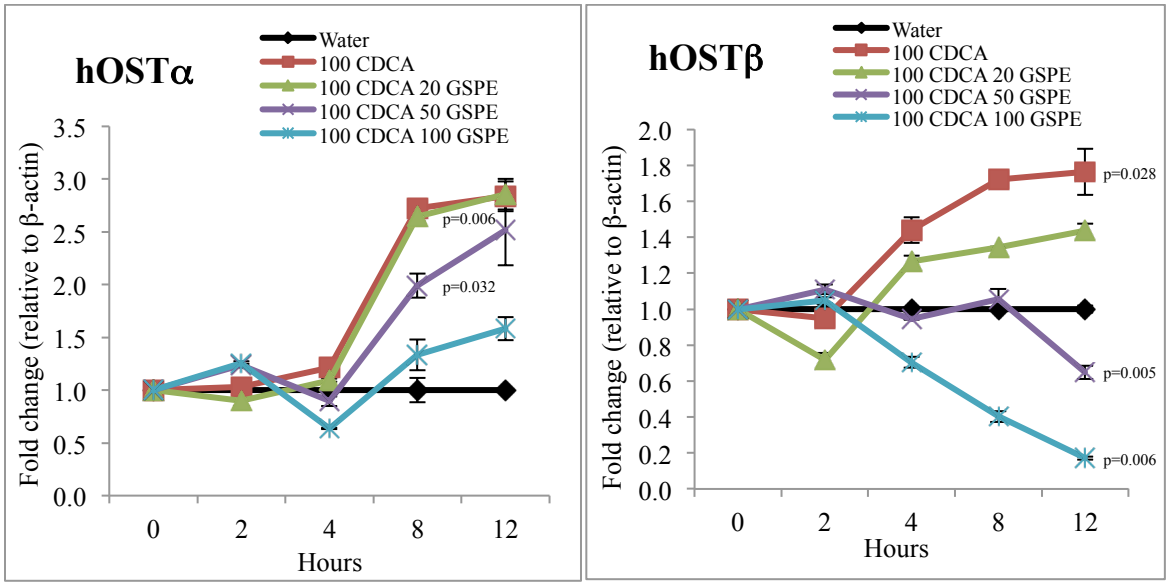

Figure 17: The effects of CDCA and CDCA+GSPE on OSTα/β expression in Caco2 cells
100 μM CDCA began to induce OSTα/β expression after 4h of treatment. Co-administration of GSPE and CDCA resulted in a dose-dependent repression in the CDCA-induction of OSTα/β levels (n=2, in duplicate). hOSTα/β: human organic solute transporter alpha/beta, CDCA: chenodeoxycholic acid, GSPE: grape seed procyanidin extract.

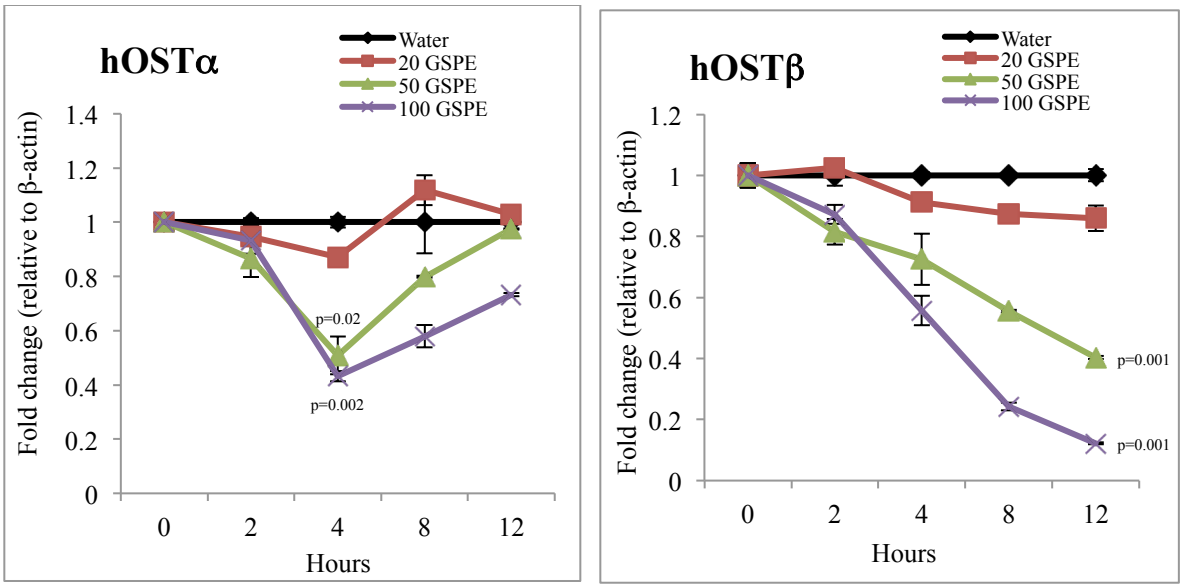

Figure 18: The effects of GSPE treatment alone on OSTα/β expression in Caco2 cells
GSPE alone decreased OSTα/β mRNA levels in a dose-dependent manner, compared to water (n=2, in duplicate). hOSTα/β: human organic solute transporter alpha/beta, GSPE: grape seed procyanidin extract.

In summary, CDCA enhanced the expression of OSTα and β as was expected, which is probably mediated via FXR activation. The simultaneous administration of CDCA with GSPE did not induce the expression of OSTα and β as was originally expected, but rather it appears to repress the positive effect of CDCA treatment on the expression of these transporters. Furthermore, treatment with GSPE alone also significantly dose-dependently reduced OSTα/β mRNA expression.

3.3.3.4 Fibroblast growth factor 19 (FGF19)

FGF19 is expressed in the ileum when FXR is activated by BAs (132). FGF19 acts as an enterohepatic hormone, signaling to the liver when it binds to its receptor FGFR4 present in hepatocytes (132). FGF19 mediates the inhibitory effects of intestinal BAs on the expression of hepatic cholesterol 7α-hydroxylase

(CYP7A1), a key regulatory step in the classical pathway for BA synthesis (94, 132). FGF-19 also has been shown to regulate carbohydrate and lipid metabolism (123, 133).

In Caco2 cells, treatment with 100 μM CDCA transiently induced the expression of FGF19. The maximal effect was observed at 4 hours (8 fold increase relative to control; p=0.0019). At 8 hours, FGF19 mRNA levels returned to basal levels.

Additionally, FGF19 expression was induced in Caco2 cells treated with GSPE alone (Figure 19). 100 mg/L GSPE enhanced FGF19 expression in a transient manner (4 fold after 4 hours; p=0.01), and again mRNA levels returned to basal after 8 hours.

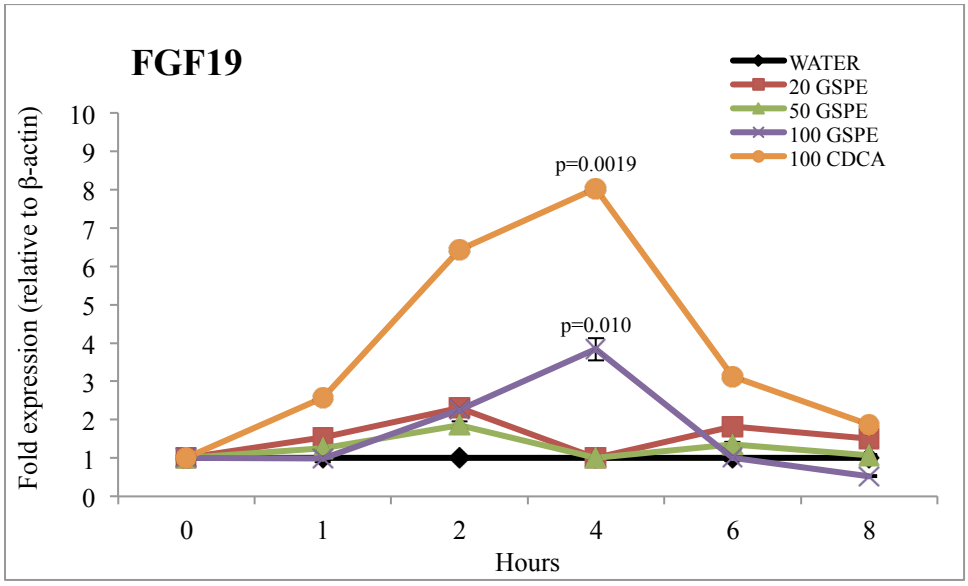

Figure 19: Time course for FGF19 mRNA expression in Caco2 cells following treatments with GSPE or CDCA
100 mg/L GSPE maximally increased FGF19 mRNA levels after 4 hours treatment (n=2, in duplicate). FGF19: fibroblast growth factor 19, CDCA: chenodeoxycholic acid, GSPE: grape seed procyanidin extract

When Caco2 cells were treated for 24 hours with either 50 or 100 μM CDCA alone or 50 or 100 μM CDCA + GSPE, FGF19 mRNA levels were not induced compared to the control (Figure 20).

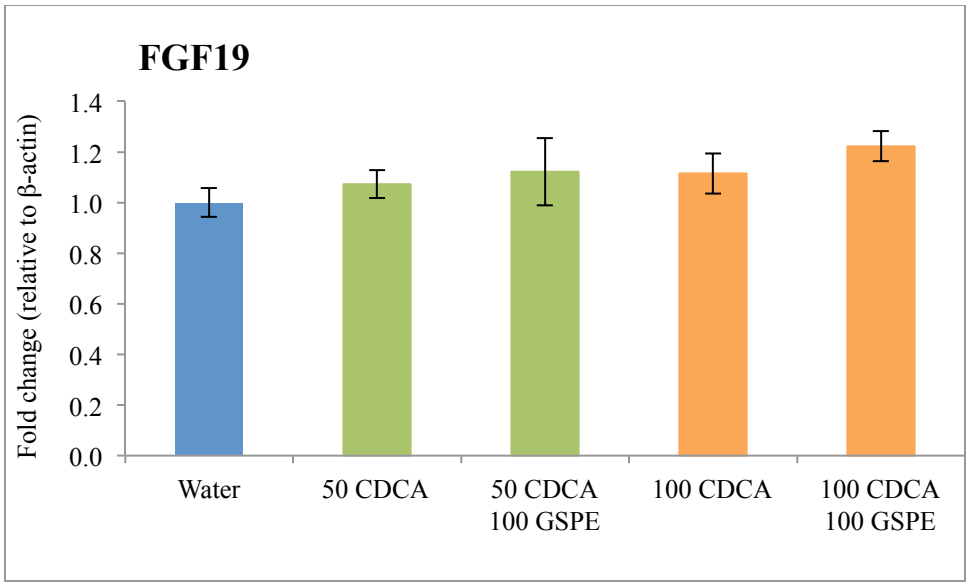

Figure 20: The effects of CDCA and CDCA+GSPE treatment on FGF19 expression in Caco2 cells after 24 hours
FGF19 expression was not induced after 24 hours of treatments in Caco2 cells (n=3, in triplicate). FGF19: fibroblast growth factor 19, CDCA: chenodeoxycholic acid, GSPE: grape seed procyanidin extract.

In summary, as was expected CDCA induced FGF19 expression, which is probably mediated via FXR activation in the Caco2 cells. However, the changes in FGF19 mRNA levels were fast and transient. This was also confirmed by the fact that FGF19 mRNA levels were not induced after 24 hours treatment. In addition, GSPE treatment alone also transiently induces FGF19 mRNA expression.

3.3.3.5 Farnesoid X receptor (FXR)

As previously mentioned, in the intestine FXR controls the absorption of bile acids via the regulation of expression of three important transporters: ASBT, IBABP and OSTα/β.

In Caco2 cells, 100 μM CDCA treatment did not cause a statistically significant change in FXR mRNA levels, following 12 hours treatment (Figure 21). When GSPE was either administered alone or in

combination with 100 μM CDCA, a dose-dependent reduction in FXR mRNA levels was observed (as shown in Figure 21 and Figure 22).

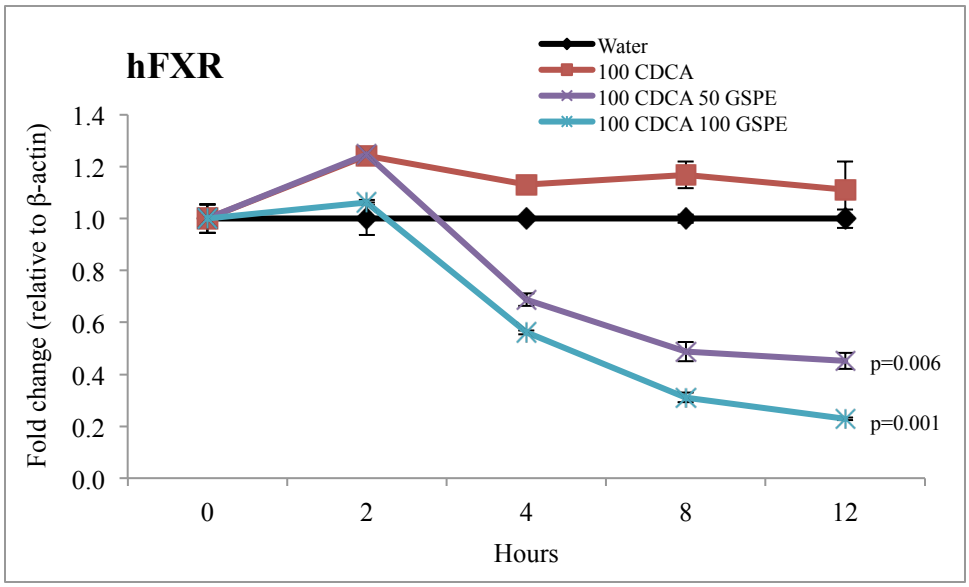

Figure 21: The effects of CDCA and CDCA+GSPE on FXR expression in Caco2 cells
CDCA alone slightly increased FXR expression without reaching statistical significance. When GSPE and CDCA were co-administered, a dose-dependent decrease in FXR mRNA levels was observed (n=2, in duplicate). hFXR: human farnesoid X receptor, CDCA: chenodeoxycholic acid, GSPE: grape seed procyanidin extract.

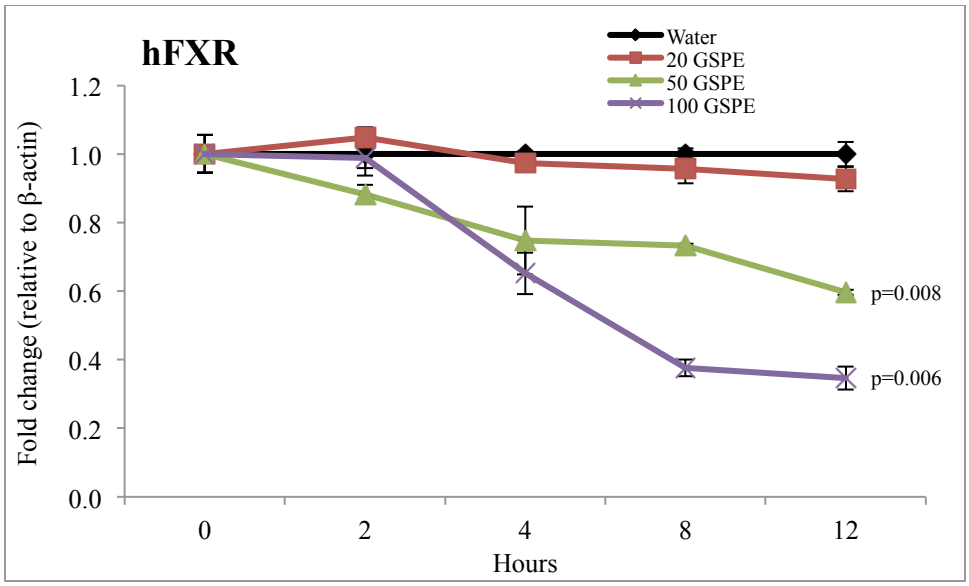

Figure 22: The effects of GSPE treatment on FXR expression in Caco2 cells
GSPE treatment alone induced a dose-dependent reduction in FXR mRNA levels when compared to water (n=2, in duplicate). hFXR: human farnesoid X receptor, GSPE: grape seed procyanidin extract.

In summary, GSPE treatment alone or in combination with CDCA resulted in reduced FXR mRNA expression in Caco2 cells. However, CDCA treatment alone did not induce a statistically significant change in FXR mRNA levels.

3.4 Discussion

Our results from these *in vitro* studies strongly suggest that GSPE treatment may selectively alter intestinal FXR-target gene expression, thereby potentially altering enterohepatic recirculation. GSPE treatment inhibited ASBT expression and induced a rapid and transient increase in FGF19 mRNA levels, which is consistent with FXR activation. In contrast, GSPE inhibited OSTα/β, and co-administration of CDCA with GSPE resulted in repression in IBABP expression, indicating that GSPE may be acting as an FXR antagonist. These results indicate that the actions of GSPE are intriguing, and that it does not simply act as a co-agonist ligand for FXR, as previously proposed, but instead the results strongly suggest that

GSPE alters the expression of FXR-target genes in the intestine, including ASBT, IBABP and FGF19, in a gene-selective manner, acting therefore as a gene-selective FXR modulator.

These *in vitro* findings strongly suggest that GSPE has the potential, *in vivo,* to alter the enterohepatic recirculation of bile acids, by decreasing BA absorption in the ileum, and subsequently increasing BA output in the feces. When intestinal cells (Caco2) were treated with GSPE, either alone or in combination with CDCA, a reduction in both the enterocyte luminal and basal bile acid transporters, namely ASBT and OSTα/β respectively, was observed. Furthermore, after GSPE/CDCA treatment a decrease in the expression of IBABP, the bile acid binding protein that regulates BAs trafficking inside the enterocyte, was also observed. If enterocyte luminal BA uptake is impaired, and BA transport through the enterocyte and across the basolateral membrane is also compromised, a decrease in BA absorption and consequently an increase in excretion of BAs in the feces would be expected. These findings are consistent with the enhanced BA excretion seen in hamsters following treatment with a grape seed extract (134) described by Jiao et al. When Golden Syrian hamsters were treated with a diet containing 1% grape seed procyanidins for 6 weeks, a 15% reduction in plasma total cholesterol and a 30% reduction in plasma triglyceride levels was observed, while intestinal excretion of bile acids showed a 3-4 fold increase ($p<0.05$) (134). Interestingly, another recent study also described an association between decreased intestinal absorption of BAs and improved triglyceride metabolism in mice (135). A decrease in plasma TG levels was observed in ASBT knockout mice, which demonstrated increased BA fecal loss, as well as induced BA synthesis, resulting from increased CYP7A1 mRNA and protein expression (135). The observed 35% reduction in plasma TG levels was associated with reduced SREBP1c expression (both mRNA and protein), and reduced expression of several enzymes involved in fatty acid synthesis (135). The authors propose a possible mechanism stating that the metabolic demand for acetyl-CoA, utilized in cholesterol synthesis to replenish BAs, may have resulted in reduced amounts of acetyl-CoA, which is also a substrate for fatty acid synthesis (135). Bile acid-binding resins, which bind BAs in the intestinal lumen

reducing their absorption, are currently used as treatment strategies for hypercholesterolemia, due to the fact that they elicit a compensatory increase in BA synthesis, thereby enhancing the hepatic demand for cholesterol. However, the possible effects of an interruption in BA recirculation and its' subsequent beneficial effects on plasma TG levels represents a previously unrecognized metabolic response. Further studies are therefore needed in order to elucidate the detailed mechanisms in regard to the relationship between impaired enterohepatic recirculation and plasma TGs, and the differences among species.

Interestingly, GSPE treatment, either alone or in combination with CDCA, caused a dose-dependent decrease in FXR mRNA expression after 4 hours. Our gene expression studies are consistent with fast and early FXR activation, since it has been shown that several FXR target genes are either induced or modulated after only a few hours of treatment with GSPE. Therefore, we propose that a possible explanation for the observed decrease in FXR mRNA expression could be that after GSPE exerts its effects on FXR, the resulting decrease in availability of BAs inside the enterocyte elicits a negative effect on FXR expression. Consequently, the decreased ileal uptake of bile acids, which represent the natural ligands for FXR, may serve as a stimulus to repress FXR expression.

Additionally, our results show that FGF19 mRNA expression was rapidly and transiently induced after 4 hours by GSPE treatment alone in Caco2 cells. FGF19 is secreted from enterocytes into the portal circulation, signaling to the liver primarily to repress BA synthesis (136). Interestingly, FGF19 has additionally been linked to TG metabolism, since it may act by inhibiting hepatic fatty acid synthesis (123). Incubation of primary hepatocyte cultures with recombinant FGF19 resulted in the repression of SREBP1c, via a decreased expression in peroxisome proliferator-activated receptor γ co-activator 1β (PGC1β), an activator of SREBP1c activity, as well as an increased activity of signal transducer and activator of transcription 3 (STAT3), an inhibitor of SREBP1c expression (123). FGF19 was also found to increase the hepatic expression of SHP, which is an established inhibitor of SREBP1c (123). Consequently, FGF19 may be contributing to the previously described FXR-mediated serum TG lowering

effect of GSPE. Based on these *in vitro* observations, the next chapters will assess the effects of GSPE *in vivo*, to further elucidate how alterations in FXR-target gene expression in the intestine may contribute to GSPE-mediated effects in the liver, and thereby contribute to whole body triglyceride regulation.

A possible limitation of these *in vitro* studies is that the effects of GSPE exerted on intestinal cells were conducted using a cancer-derived cell line, and therefore any GSPE anti-cancer related effects may affect the viability of the Caco2 cells, and therefore, the observed results. The highest reductions in cell viability were seen with longer treatment times and with higher doses of GSPE. The highest reduction was seen after 48 hours of 100 mg/L GSPE, where a 95% decrease in Caco2 cell viability was observed. Additionally we observed a marked reduction in gene expression of β-actin, the internal control gene, with GSPE treatments longer than 24 hours. These two reasons therefore led us to only consider the GSPE-induced changes in gene-expression up to and including 24 hours of GSPE treatment. Previous studies have measured the effects grape seed extracts have on apoptosis and cell growth in Caco2 cells (127, 128), and showed that growth inhibition becomes evident following the first 24 hours of treatment and progressively increases thereafter. Three grape seed extracts tested at a concentration of 100 mg/L induced apoptosis by 15-20% in Caco2 cells after 24 hours treatment (127). Our results using the MTT assay showed a greater reduction in Caco2 cell growth at all time points assessed. As the MTT assay measures the reduction in cell viability, and not only apoptosis, this may account for some of the differences observed between our results and previous studies. Additionally, the cell culture conditions were not exactly the same during the course of the MTT assays, as compared to GSPE-gene expression studies, due to specific requirements of the MTT assay. For example, gene-expression experiments were performed after Caco2 cells reached 10 days post-confluence. In the MTT assay, Caco2 cells were only cultured for 48 hours in total, and thus, the observed effect of GSPE on cell growth may be magnified in the MTT experiments, since there was a lower number of cells at the time of the assay, as compared to the number of cells when conducting the gene expression studies.

In conclusion, these *in vitro* studies strongly suggest that GSPE may represent a novel naturally occurring gene-selective bile acid receptor modulator, therefore potentially altering bile acid enterohepatic recirculation. GSPE may act as an intestinal FXR co-agonist for FXR in the regulation of certain genes such as ASBT and FGF19, as well as acting as a gene selective modulator for other intestinal FXR-target genes, namely OSTα/β and IBABP. Consequently, further studies assessing the effects of GSPE on intestinal FXR target genes *in vivo* is warranted.

Chapter 4

Determination of the molecular effects of GSPE in the intestine *in vivo* in a normolipidemic state

4 Determination of the molecular effects of GSPE in the intestine *in vivo* in a normolipidemic state

4.1 Introduction

The studies described in chapter 3, showed that the *in vitro* effects of GSPE treatment in the intestine are complex and intriguing. The results indicate that GSPE may be acting as a gene-selective bile acid receptor modulator in human Caco2 cells, instead of acting as a simple FXR co-agonist ligand, as may have been expected based on the effects of GSPE previously observed in the liver and *in vitro* in transient transfection studies (34, 99). Based on the observations from the *in vitro* studies conducted in Chapter 3, we propose that GSPE administration may be altering bile acid enterohepatic circulation, resulting in increased BA loss in the feces, and thereby, decreasing the amount of BA is returned to the liver. As discussed in chapter 3, the *in vitro* gene-expression changes induced by GSPE administration to intestinal cells may represent an additional mechanism contributing to the hypotriglyceridemic effect of GSPE, however further studies are needed to confirm whether or not this occurs *in vivo*.

GSPE has previously been shown to decrease serum TGs by activating a FXR-dependent pathway in the liver (99). FXR co-activation by GSPE and CDCA induces SHP transcription, leading subsequently to a reduced hepatic expression of SREBP1c, which is translated into a diminished hepatic fatty acid synthesis and an increased plasma TG catabolism (34, 35, 99). Our *in vitro* results shown in chapter 3, indicate that certain intestinal effects of GSPE treatment may also contribute to the hypotriglyceridemic effects of this compound, since there is an intimate metabolic inter-relationship between the intestine and liver, due to the unique anatomical position of both tissues using the portal vein as the communicating channel (137). Consequently, the TG lowering effect attributed to GSPE may be additionally mediated via effects exerted in the intestine, which is then related to effects mediated as a consequence of the inter-relationship with the liver, as follows:

- GSPE administration may alter enterohepatic circulation by decreasing BA absorption in the ileum, and subsequently increasing BA output in the feces. The lower amount of BAs that then reach the liver results in an increase in BA synthesis from cholesterol in the liver, in order to replenish the amount that is not recirculated (35, 135), increasing the metabolic demand for acetyl-CoA. This may result in reduced amounts of acetyl-CoA, which is also a substrate for fatty acid synthesis, subsequently decreasing fatty acid synthesis and therefore lowering plasma TGs (135).
- GSPE treatment induced FGF19 expression in Caco2 cells. As previously discussed, FGF19 has been shown to be a novel factor that inhibits hepatic fatty acid synthesis, lowering plasma TGs. FGF19 decreased SREBP1c expression, by increasing STAT3 activity, an inhibitor of SREBP1c expression, and by decreasing the expression of PGC1β, which activates SREBP1c activity. Therefore, GSPE effects on intestinal FGF19 expression may also contribute to the reduced expression of SREBP1c induced by GSPE.

The aim of this chapter therefore is to assess the effects of GSPE administration in an *in vivo* model, in order to determine the changes in both intestinal and liver gene-expression. Therefore, this will allow a more detailed determination of the possible interactions between the intestine and the liver in decreasing plasma TGs following GSPE administration. An animal model utilizing male C57BL/6 mice, previously used to determine GSPE treatment effects (34, 99), was used.

4.2 Materials and methods

Male C57BL/6 mice were purchased from Charles River Laboratories. Twelve mice aged 8 weeks of age were used to assess the effects of GSPE treatment after 14 hours administration. After 1 week of acclimatization, six mice were randomly allocated to either control or treatment group. Mice were fed a

standard rodent chow (see section 2.7.1.1) and water *ad libitum*. On experimental day 1, mice were fed either vehicle (water) or GSPE (250 mg/kg) via oral gavage. A first dose was administered at 9 pm and a second dose 12 h later at 9 am on experimental day 2. Food was then removed and 2 h later mice were anesthetized with isoflurane to obtain blood samples using the retro-orbital bleeding technique (described in section 2.7.3.1). Mice were then euthanized under anesthesia by cervical dislocation, performed according to IACUC approval. Intestines and livers were harvested and kept in liquid nitrogen until they were stored at –80ºC. RNA was extracted from the tissues as described in section 2.3.2, cDNA was made using Superscript III Reverse transcriptase (as described in section 2.4), and real time qPCR was used to determine gene expression changes (as detailed in section 2.6). Gene expression changes assessed in the intestine included ASBT, IBABP, OSTα/β, FGF15 and FXR. In the liver, SREBP1c, PGC1β, CYP7A1 and down-stream target genes of SREBP1c, namely Apolipoprotein A5 (ApoA5), and 3-hydroxy-3-methylglutaryl-CoA synthase 1 (HMGCS1) were also assessed. Additionally, β-actin and cyclophilin expression were used as endogenous controls. All the results for the target gene expression analysis were standardized to β-actin and cyclophilin levels, and the data shown represents the fold change for each target gene relative to β-actin and/or cyclophilin expression (n=6 per treatment).

Triglyceride levels were measured in plasma that was isolated from blood drawn following treatments, as indicated (as detailed in sections 2.7.3.3 and 2.7.4.1).

Additionally, a second animal study was performed to evaluate the effect of cholestyramine, a bile acid binding resin, on changes in gene-expression in the intestine and in the liver following GSPE administration compared to the control. Thirty six male C57BL/6 mice were allocated to either a control diet (Harlan Tekland rodent diet 2019) or a 2% (wt/wt) cholestyramine-supplemented diet. Following 4 weeks of diet administration, mice were fed either vehicle (water) or GSPE (250 mg/kg) via oral gavage. A first dose was administered at 9 pm and a second dose 12 h later at 9 am on the next day. Food was then removed and 2 h later mice were anesthetized with isoflurane to obtain blood samples using the

retro-orbital bleeding technique (described in section 2.7.3.1). Mice were then euthanized under anesthesia by cervical dislocation. Intestines and livers were harvested and placed in liquid nitrogen and then stored at –80ºC until analysis. Gene expression analysis was performed utilizing the same procedures described above. Cholestyramine absorbs BAs in the intestine, thereby preventing their uptake in the ileum and interrupting their enterohepatic circulation (138). For this reason, cholestyramine is currently used as an effective drug in the treatment of hypercholesterolemia, since it lowers LDL cholesterol (138). *In vitro* studies have previously shown that GSPE enhances the activity of CDCA-bound FXR, while GSPE alone does not cause any transactivation of FXR (99), highly suggesting that the presence of BAs is essential for GSPE function. Therefore, in this study where mice received a cholestyramine-supplemented diet prior to GSPE treatment may represent a good model to understand the *in vivo* effects of GSPE treatment when there are reduced levels of bile acids present in the circulation.

4.3 Results

4.3.1 Effects of GSPE treatment on intestinal gene expression

4.3.1.1 Apical sodium dependent bile acid transporter (ASBT)

Comparable to what was observed in Caco2 cells, oral gavage with GSPE (250 mg/Kg/body weight) significantly reduced ASBT mRNA expression by 24% ($p=0.05$), as shown in Figure 23. This effect is consistent with FXR activation, which acts as a negative regulator of intestinal ASBT expression.

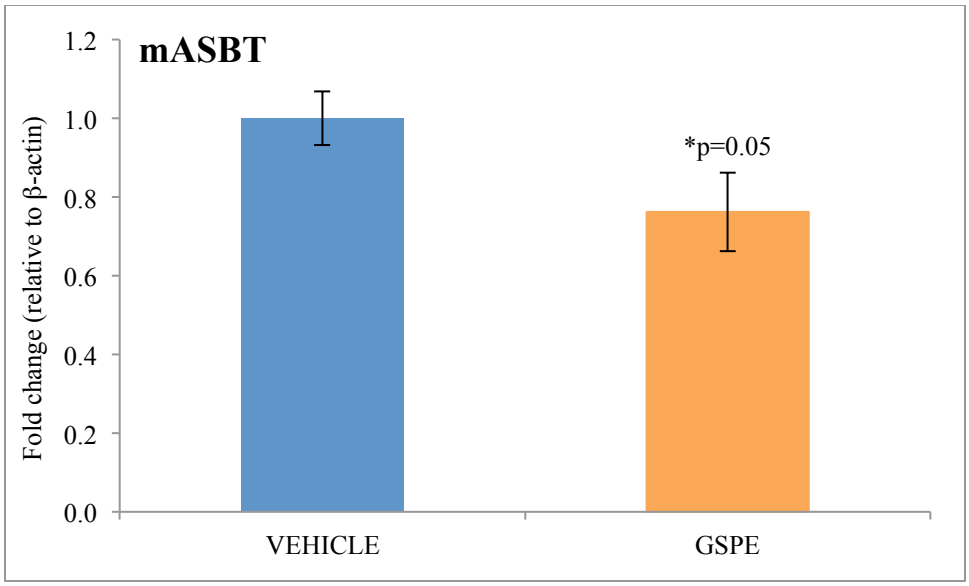

Figure 23: GSPE treatment reduces mASBT expression *in vivo*
Oral gavage with GSPE 250 mg/Kg/body weight (14 hours treatment) reduced ASBT mRNA expression by 24% (p=0.05), (n=6 per treatment, per group, in triplicate). mASBT: mice apical sodium dependent bile acid transporter, GSPE: grape seed procyanidin extract.

4.3.1.2 Intestinal bile acid-binding protein (IBABP)

GSPE treatment alone after 14 hours resulted in a 25% reduction in IBABP mRNA expression, although it was not found to be statistically significant, p=0.09 (Figure 24). In Caco2 cells, the co-administration of GSPE and CDCA dose-dependently reduced IBABP expression (as shown in section 3.3.3.2).

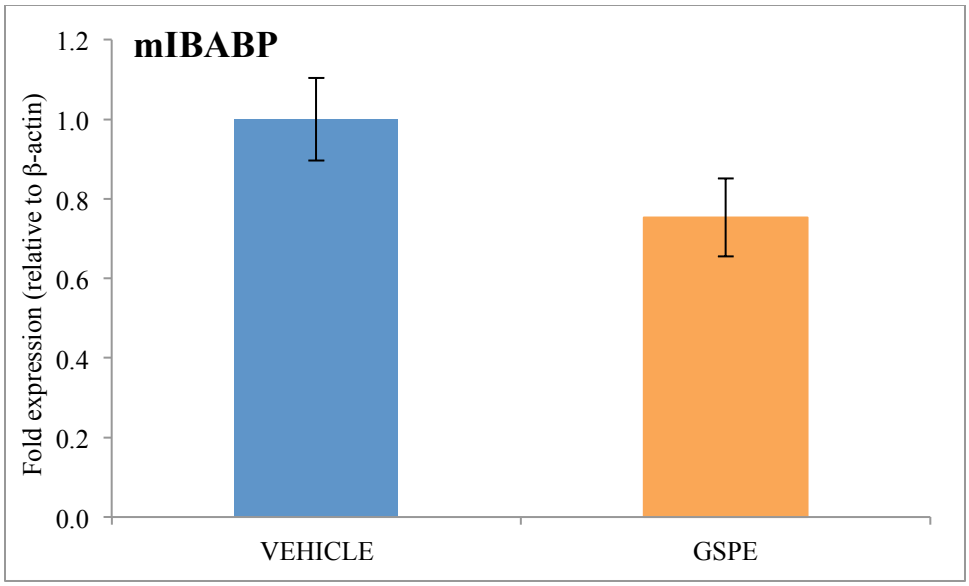

Figure 24: The effect of GSPE treatment on mIBABP expression *in vivo*
Oral gavage with GSPE 250 mg/Kg/body weight (14 hours treatment) non-significantly reduced IBABP expression by 25%, (n=6 per treatment, per group, in triplicate). mIBABP: mice intestinal bile acid-binding protein , GSPE: grape seed procyanidin extract.

4.3.1.3 Organic solute transporters (OST) α/β

Oral gavage with GSPE 250 mg/Kg/body weight did not change OSTα/β mRNA expression *in vivo* after 14 hours (as shown in Figure 25). In Caco2 cells, GSPE either alone or in combination with CDCA reduced OSTα/β expression. However, this inhibitory effect was not observed *in vivo*. Ileal expression of both genes should be induced by FXR activation (130), therefore from these results it appears that GSPE does not exert any effects on these genes, at least after 14 hours treatment.

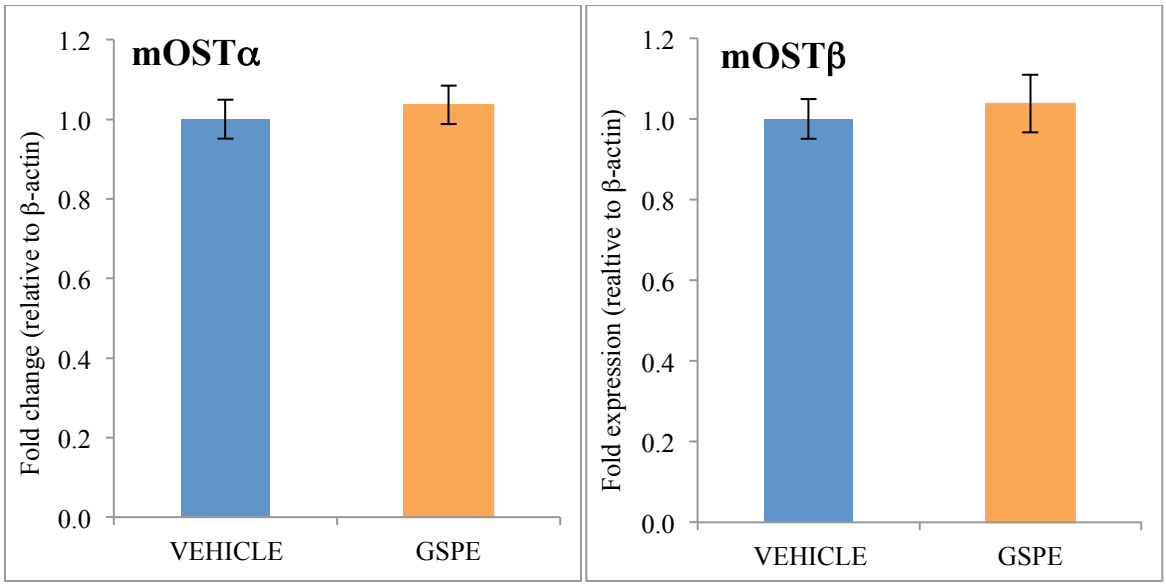

Figure 25: The effect of GSPE treatment on mOSTα/β expression *in vivo*
Oral gavage with GSPE 250 mg/Kg/body weight (14 hours treatment) did not change mRNA OSTα/β levels, (n=6 per treatment, per group, in triplicate). mOSTα/β: mice organic solute transporter alpha/beta, GSPE: grape seed procyanidin extract.

4.3.1.4 Fibroblast growth factor 15 (FGF15)

As previously mentioned, FGF15 represents the mouse homologue of human FGF19 (92-94). Ileal FXR activation by cholic acid has been shown to induce the expression of FGF15 in mice (93).

Oral gavage with GSPE 250 mg/Kg/body weight (14 hours treatment) significantly decreased FGF15 mRNA expression by 38%, $p<0.001$ (as shown in Figure 26).

When mice were fed a 2% cholestyramine-supplemented diet, to reduce the absorption of BAs by the enterocytes, and therefore reduce the circulating pool of BAs, FGF15 mRNA expression was significantly suppressed ($p<0.001$) compared to control diet group. Oral gavage with GSPE 250 mg/Kg/body weight in the cholestyramine-fed mice did not further reduce or increase FGF15 expression (Figure 27).

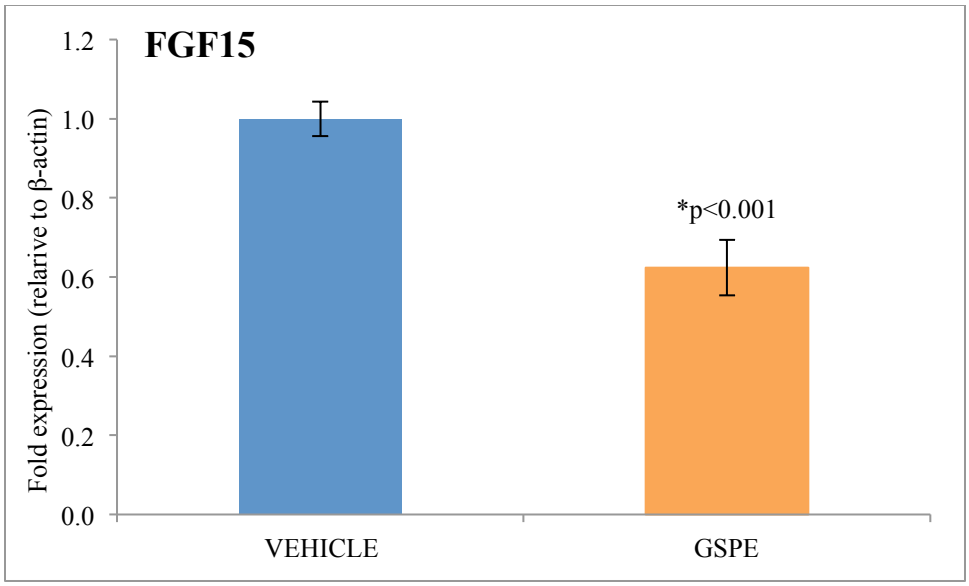

Figure 26: GSPE treatment reduces intestinal FGF15 expression *in vivo* after 14 hours treatment
Oral gavage with GSPE 250 mg/Kg/body weight (14 hours treatment) significantly reduced FGF15 mRNA expression in mouse intestine, (n=6 per treatment, per group, in triplicate). FGF15: fibroblast growth factor 15, GSPE: grape seed procyanidin extract.

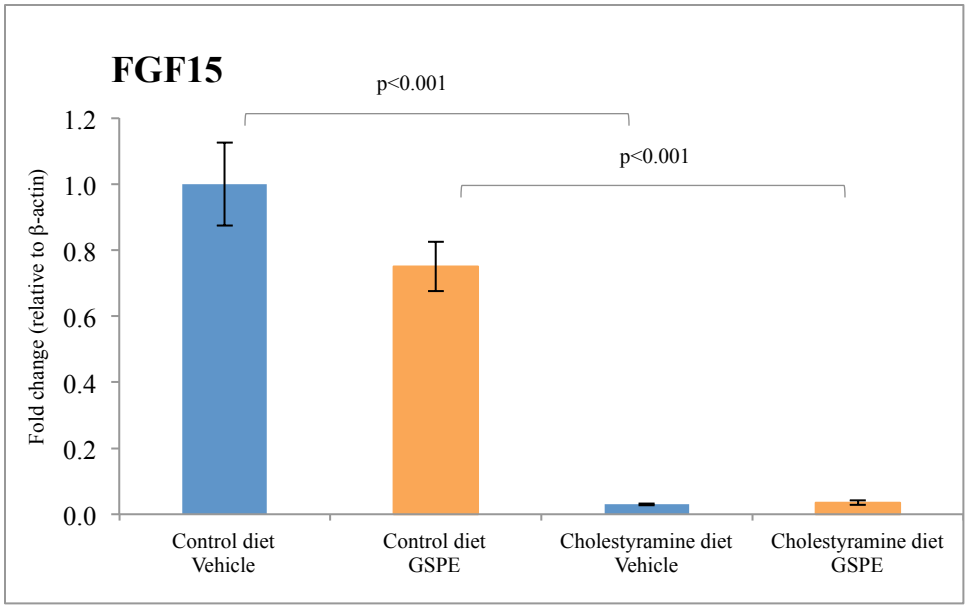

Figure 27: The effects of GSPE treatment on intestinal FGF15 mRNA expression in mice fed a 2% cholestyramine-supplemented diet
Following either a control diet or a 2% cholestyramine-supplemented diet for 4 weeks, mice were treated with either vehicle or 250 mg/Kg/body weight GSPE (14 hours treatment). In the cholestyramine group, FGF15 mRNA expression was significantly suppressed, compared to control group. FGF15 mRNA expression in the cholestyramine-treated group was not affected by GSPE treatment, (n=9 per treatment, per group, in duplicate). FGF15: fibroblast growth factor 15, GSPE: grape seed procyanidin extract.

4.3.1.5 Farnesoid X receptor (FXR)

GSPE treatment did not significantly change FXR mRNA expression in the intestine after 14 hours treatment (p=0.063). Although GSPE treatment activated FXR, since it modulated FXR-target gene expression, FXR mRNA levels *per se* did not change.

4.3.2 Effects of GSPE treatment on hepatic gene expression

4.3.2.1 Sterol regulatory element binding protein 1c (SREBP1c)

Bile acids, by activating FXR, have been shown to induce the expression of SHP, which then inhibits SREBP1c expression (114). SREBP1c is a key lipogenic transcription factor that has been recognized as an important downstream effector of the TG lowering response triggered by GSPE (34)

However, in this study oral gavage with GSPE (250 mg/Kg/body weight) did not change SREBP1c mRNA expression *in vivo* after 14 hours treatment, as is expected when FXR is activated (data not shown).

4.3.2.2 Peroxisome proliferator-activated receptor γ coactivator 1β (PGC1β)

PGC1β is a transcriptional co-activator that induces hypertriglyceridemia in response to dietary fats, via activation of hepatic lipogenesis and lipoprotein secretion (139). PGC1β has been demonstrated to interact and activate several transcription factors involved in hepatic lipogenesis, such as SREBP1c (140).

As shown in Figure 28, GSPE treatment significantly decreased mPGC1β mRNA expression, $p=0.007$.

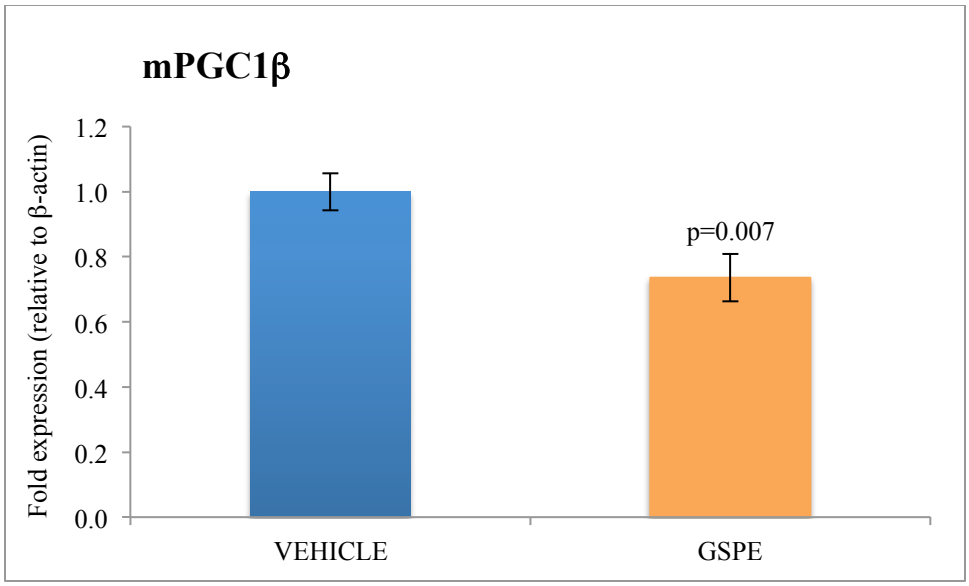

Figure 28: GSPE treatment decreases hepatic PGC1β expression *in vivo* after 14 hours
GSPE administration (14 hours treatment) significantly reduced PGC1β expression, which acts as a SREBP1c co-activator (n=6 per treatment, per group, in triplicate). mPGC1β: mice peroxisome proliferator-activated receptor γ coactivator 1β, GSPE: grape seed procyanidin extract.

4.3.2.3 3-hydroxy-3-methylglutaryl-Coenzyme A synthase 1 (HMGCS1)

HMGCS1 catalyzes the first physiologically irreversible step in the biosynthesis of isoprenoids and sterols from acetyl-CoA (141) and its' expression is regulated by SREBP1c (35).

GSPE treatment significantly reduced HMGCS1 mRNA expression in mice after 14 hours, p=0.032 (as shown in Figure 29). Therefore, although we did not see a direct effect on SREBP1c mRNA expression *per se* (shown in section 4.3.2.1), GSPE did reduce the expression of a SREBP1c target-gene, namely HMGCS1, after 14 hours treatment.

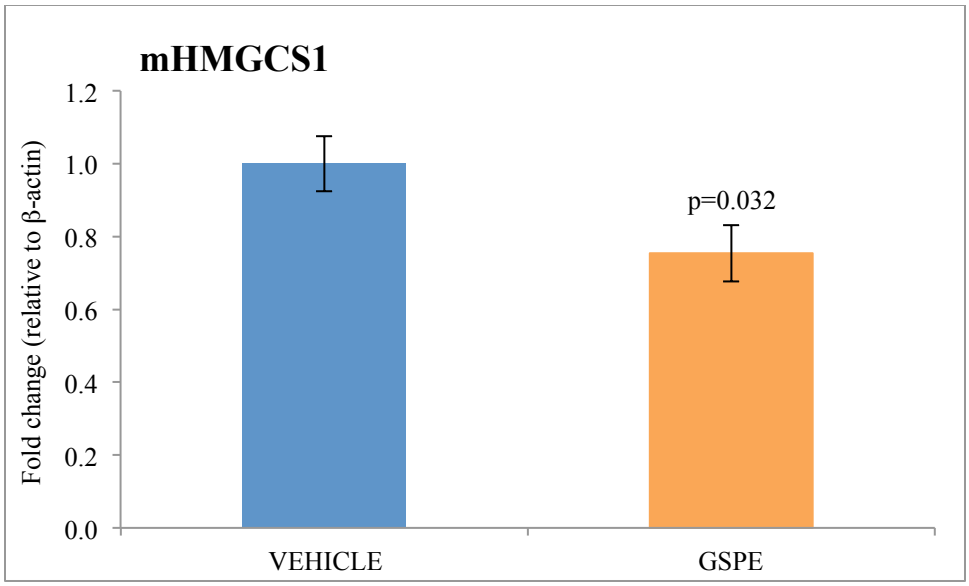

Figure 29: GSPE treatment decreases hepatic HMGCS1 expression *in vivo*
GSPE administration significantly decreased HMGCS1 mRNA expression in mice by 25%, (n=6 per treatment, per group, in triplicate). mHMGCS1: mice 3-hydroxy-3-methylglutaryl-Coenzyme A synthase 1, GSPE: grape seed procyanidin extract.

4.3.2.4 Apolipoprotein A-V (ApoA5)

ApoA5 has been documented to play a major role in TG metabolism by enhancement of VLDL lipolysis and clearance (142). ApoA5 concentrations are inversely associated with plasma TG levels: transgenic mice overexpressing human ApoA5 revealed a 60‑70% decline in plasma TG levels (143), whereas ApoA5 knockout mice manifested a 4-fold higher plasma TG level compared to control animals (143). Therefore, ApoA5 plays an important role in regulating plasma TG levels (142, 143). Interestingly, ApoA5 gene expression is negatively regulated by SREBP1c (144). Consistent with this, as shown in Figure 30, as would be expected if SREBP1c expression is reduced, GSPE administration resulted in a significant induction in ApoA5 expression after 14 hours treatment, p=0.003

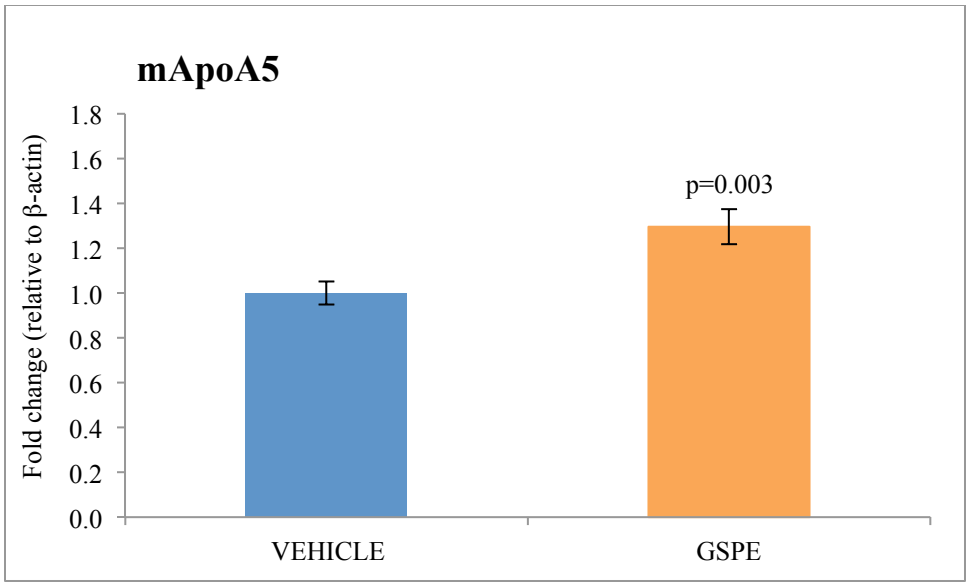

Figure 30: GSPE treatment increases ApoA5 expression *in vivo* after 14 hours treatment
GSPE (250 mg/Kg/body weight) increased hepatic mApoA5 mRNA expression in mice, (n=6 per treatment, per group, in triplicate). mApoA5: mice apolipoprotein A-V, GSPE: grape seed procyanidin extract.

4.3.2.5 Cytochrome P450, family 7, subfamily A, polypeptide 1 (CYP7A1)

The CYP7A1 gene encodes a member of the cytochrome P450 superfamily of enzymes, specifically cholesterol 7α-hydroxylase, which catalyzes the rate-limiting step in the classical pathway for bile acid synthesis (145). Expansion of the bile acid pool by administration of bile acids suppresses CYP7A1 expression, reducing BA synthesis (145). Conversely, interruption of the enterohepatic circulation of BAs increases CYP7A1 expression and activity (146).

Treatment with GSPE for 14 hours caused a 2-fold increase in CYP7A1 mRNA expression, $p=0.026$ (as shown in Figure 31). When mice were fed a 2% cholestyramine-supplemented diet, which reduces ileal BA uptake and therefore decreases BA enterohepatic circulation, a 8-fold increase in CYP7A1 expression was observed, compared to the control group ($p<0.001$). GSPE treatment for 14 hours following the 2% cholestyramine diet further induced CYP7A1 mRNA expression (13-fold compared to control group; $p=0.017$), as shown in Figure 31.

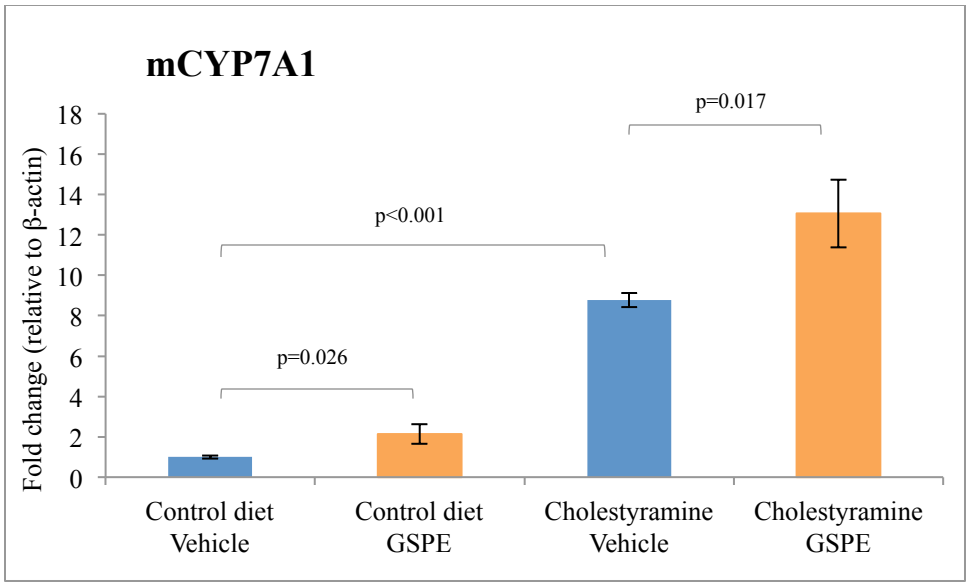

Figure 31: The effects of 14 hours GSPE treatment on hepatic Cyp7A1 expression in mice fed a 2% cholestyramine-supplemented diet compared to the control diet
GSPE significantly increased mCyp7A1 mRNA expression in mice fed either a control diet or a 2% cholestyramine diet. Additionally, the cholestyramine diet alone highly induced Cyp7A1 expression, (n=9 per treatment, per group, in duplicate). mCYP7A1: mice cytochrome P450, family 7, subfamily A, polypeptide 1, GSPE: grape seed procyanidin extract.

4.3.3 Effects of GSPE on serum triglyceride levels in a normolipidemic state

4.3.3.1 Effect of GSPE after 14 hours treatment (250 mg/Kg/body weight) on serum triglyceride levels in normolipidemic C57BL/6 mice

Serum TG levels were significantly reduced from 98 mg/dL in the control group to 68 mg/dL in the GSPE-treated group, p=0.001 (as shown in Figure 32). Therefore, GSPE administration triggered a 30% reduction in plasma TG levels in normolipidemic C57BL/6 mice (p=0.001).

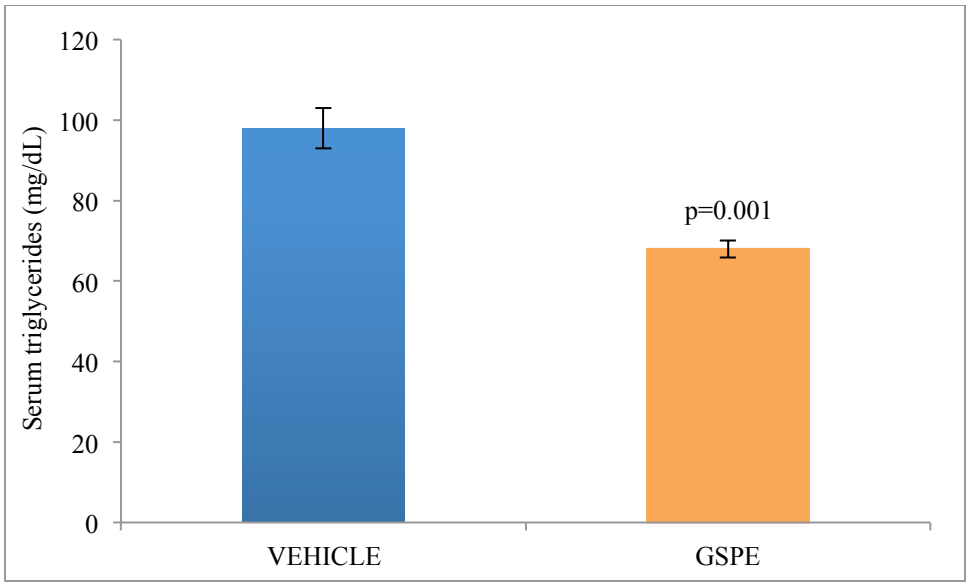

Figure 32: The effect of GSPE treatment on serum triglyceride levels in normolipidemic mice after 14 hours
GSPE (250 mg/Kg/body weight) significantly reduced serum TGs by 30%, from 98 mg/dL to 68 mg/dL (p=0.001), (n=6 per treatment, per group, in triplicate). GSPE: grape seed procyanidin extract.

4.3.3.2 Effect of GSPE after 14 hours treatment on serum triglyceride levels in C57BL/6 mice following a 2% cholestyramine-supplemented diet

Serum TG levels significantly decreased from 77 mg/dL in the control group to 59 mg/dL in the cholestyramine group ($p<0.001$), after 4 weeks of treatment (as shown in Figure 33). Therefore, the cholestyramine diet triggered a 24% reduction in serum TGs as compared to the control diet. GSPE treatment after the cholestyramine-supplemented diet further decreased serum TGs by 15% ($p=0.007$). Additionally, GSPE treatment in the control diet group caused a statistically significant 15% reduction in serum TG levels, $p=0.03$ (Figure 33).

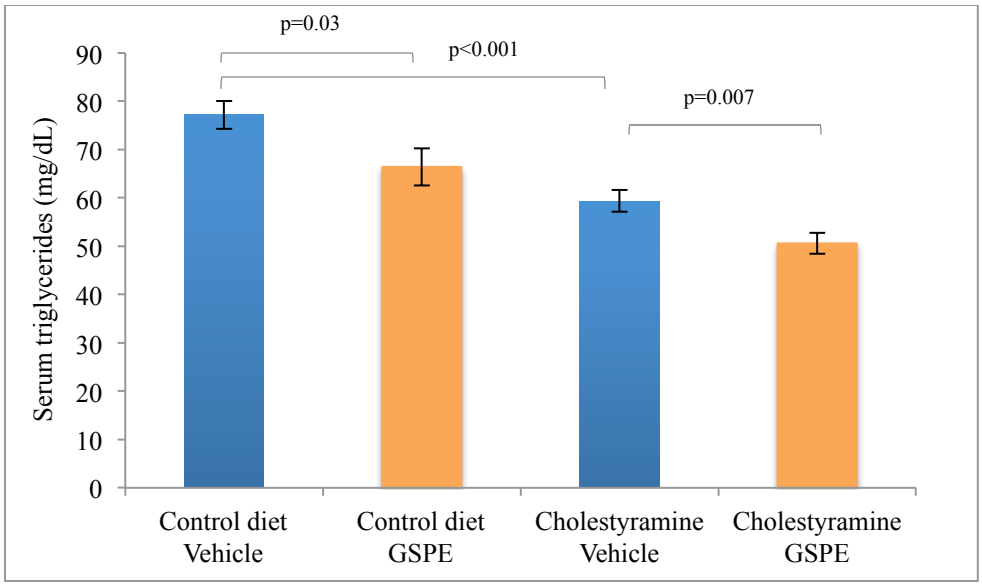

Figure 33: The effect of GSPE treatment on serum triglyceride levels in normolipidemic mice receiving a 2% cholestyramine-supplemented diet
Treatment with a 2% cholestyramine diet decreased serum TG levels by 24% compared to control diet group. GSPE treatment of the cholestyramine-supplemented group further reduced the serum TGs by an additional 15%, (n=9 per treatment, per group, in duplicate). GSPE: grape seed procyanidin extract.

4.3.4 Effects of GSPE and 2% cholestyramine-supplemented diet on fecal bile acid content

As was expected, following 4 weeks of a 2% cholestyramine-supplemented diet, the bile acid content of the feces significantly increased by 26% compared to control diet, $p<0.001$ (as shown in Figure 34). Although 14 hours treatment with GSPE did not significantly increase fecal bile acid excretion, a slight increase of 2 μmole/L in fecal bile acid content was seen in both the control diet and cholestyramine diet groups.

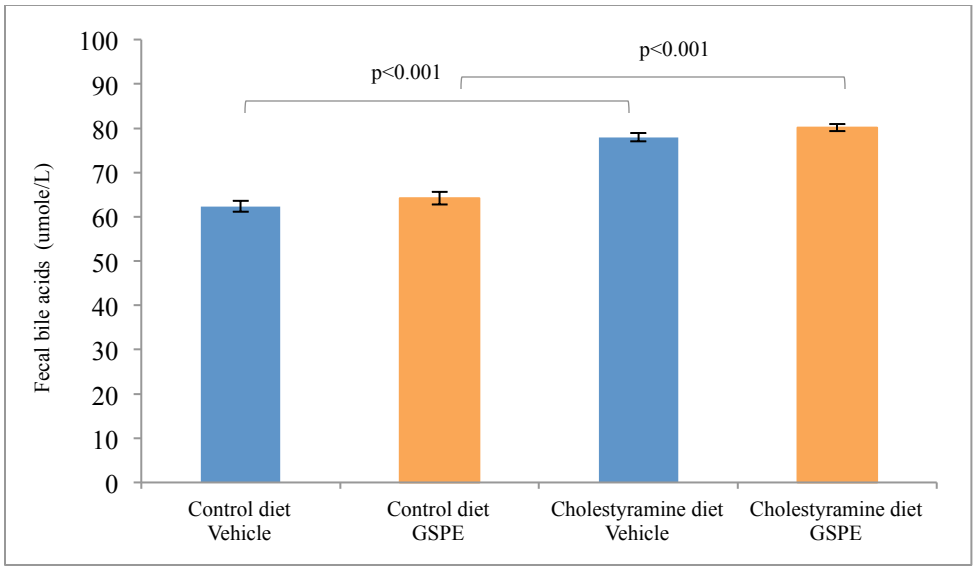

Figure 34: The effect of GSPE treatment on fecal bile acid content in mice receiving a 2% cholestyramine-supplemented diet
Treatment with a 2% cholestyramine diet significantly increased fecal bile acid excretion by 26% compared to control diet, (n=9 per treatment, per group, in duplicate). GSPE: grape seed procyanidin extract.

4.4 Discussion

The effects of GSPE treatment in the intestine *in vivo* were consistent with the effects exerted by GSPE *in vitro* in Caco2 cells (described in chapter 3). GSPE administration via oral gavage decreased ASBT and IBABP mRNA expression, indicating a possible reduction in BA uptake in the apical membrane of enterocytes, as well as BA transport through ileal enterocytes. Therefore, GSPE administration *in vivo* may reduce enterohepatic recirculation of BAs due to a decreased uptake of BAs in the ileum. Although a statistically significant increase in fecal BA content was not demonstrated after 14 hours of GSPE administration in this study, it is possible that a longer period of time of continued GSPE administration may be needed in order to reveal an effect on bile acid excretion. In fact, in the study by Jiao *et al* (134), a 3-4 fold increase in bile acid excretion was observed after 6 weeks administration of a diet containing 1% grape seed procyanidins (134). Therefore, it may be possible that longer term administartion of GSPE would show a significant effect on bile acid excretion.

FGF15, the mouse homolog of human FGF19, was reduced in C57BL/6 mice after 14 hours following GSPE administration. In Caco2 cells, GSPE treatment alone rapidly and transiently induced FGF19 expression after 4 hours. Consequently, since FGF15 mRNA expression was measured *in vivo* 14 hours after GSPE administration, an induction in FGF15 mRNA may have been missed due to the time point at which gene expression was measured. Based on the observation that PGC1β mRNA is decreased 14 hours after GSPE administration, and since it is proposed that this effect is mediated via FGF15/19 (123), it is possible that FGF15 mRNA expression was induced earlier than 14 hours.

GSPE administration did not change FXR mRNA expression after 14 hours. However, FXR activity was modulated by GSPE since the expression of several of its' intestinal target genes, e.g. ASBT expression was reduced.

Consequently, our *in vivo* results in the intestine support our previous hypothesis that GSPE acts as gene-selective FXR modulator that may result in the alteration in bile acid enterohepatic circulation.

In regards to hepatic gene-expression, GSPE treatment changed the expression of certain targets down-stream of SREBP1c, such as ApoA5 and HMGCS1. When SREBP1c is activated, a reduction in ApoA5 expression and an induction in HMGCS1 expression are expected. In contrast, GSPE treatment increased expression of ApoA5 and decreased expression of HMGCS1, indicating that SREBP1c activity was indeed modulated by GSPE.

Additionally, PGC1β mRNA expression, which acts as a SREBP1c co-activator, was repressed by GSPE administration. This result is consistent with the described effect of GSPE treatment on SREBP1c downstream target-genes, namely ApoA5 and HMGCS1, although SREBP1c mRNA expression was not changed. As previously discussed, FGF19, synthesized by ileal enterocytes, has been shown to decrease mRNA levels of SREBP1c via a decreased expression in PGC1β, as well as via increased activity of STAT3, an inhibitor of SREBP1c expression (123). Therefore, if FGF15/19 is increased by GSPE

treatment (as shown in Caco2 cells), a reduction in SREBP1c-target genes may be caused by low levels of the SREBP1c co-activator, PGC1β. PGC1β enhances the ability of SREBP1c to activate gene transcription of certain SREBP1c target-genes involved in lipid synthesis, such as fatty acid synthase (FAS), Stearoyl-CoA desaturase-1 (SCD1), and HMG-CoAR (140). Previous studies have shown that the expression of PGC1β is regulated by hormonal and nutritional status and that alterations in PGC1β expression play a role in mediating the induction of lipogenic enzyme expression by high-fat feeding (140). Therefore, the possible link between the observed induction in FGF19 mRNA expression by GSPE *in vitro*, and the decreased expression of PGC1β observed *in vivo* , highly indicates an important relationship exists between the intestine and the liver in mediating the hypotriglyceridemic effects of GSPE.

Additionally, our results show that GSPE administration significantly increases CYP7A1 mRNA expression, which encodes the rate-limiting enzyme in the synthesis of bile acids from cholesterol. This is consistent with previous studies that have also shown that grape seed procyanidins induced the expression of CYP7A1 in the liver of Wistar rats (35), and hamsters (134). Our *in vivo* and *in vitro* results suggest that GSPE treatment impairs BA enterohepatic circulation, decreasing BA uptake by the ileum, which may subsequently increase CYP7A1 expression, in order to restore BA homeostasis. The same effect on CYP7A1 expression was seen after administration with a cholestyramine-supplemented diet, which likewise alters enterohepatic circulation by preventing intestinal BA uptake. Additionally, when mice fed the cholestyramine diet were treated with GSPE, a further increase in CYP7A1 expression was observed, which is consistent with the proposed intestinal effect of GSPE.

Finally, GSPE treatment caused a 30% reduction in serum TGs, confirming previously published observations regarding the effect of GSPE on serum triglyceride levels in a normolipidemic state (34, 35, 99). Interestingly, serum TG levels were inversely proportional to CYP7A1 mRNA levels in mice fed either a control or a cholestyramine-supplemented diet and then subsequently treated with GSPE (as

shown in Figure 31 and Figure 33). These findings are consistent with the observations made by Jiao et al (134) and Lundasen et al (135), discussed in section 3.4. These studies demonstrated a relationship between a TG-lowering effect and an increased CYP7A1 expression, due to altered enterohepatic circulation. Our results also support this conclusion; GSPE appears to impair ileal BA uptake and therefore we propose that this results in alterations in BA enterohepatic circulation, similar to the effects exerted by the cholestyramine resin, albeit to a lesser extent. Although our results did not demonstrate a statistically significant increase in fecal BA content after 14hours of GSPE administration, it is possible that a longer period of time of continued GSPE administration may be needed in order to reveal an effect on bile acid excretion. This unique intestinal effect exerted by GSPE could represent a novel mechanism involved in the ability of GSPE to lower serum TG levels.

In conclusion, the hypotriglyceridemic effect of GSPE has previously been demonstrated to be mediated by hepatic changes in gene-expression (34, 35, 99). Additionally, based on the studies conducted herein we propose that GSPE exerts effects on intestinal gene expression which then results in alterations in bile acid enterohepatic circulation, highlighting the complex inter-relationship between the intestine and liver, which may represent a novel mechanism underlying in the TG-lowering ability of GSPE.

Chapter 5

Determination of the molecular effects of GSPE *in vivo* in a hyperlipidemic state

5 Determination of the *in vivo* molecular effects of GSPE in a hyperlipidemic state

5.1 Introduction

Hypertriglyceridemia is a prevalent condition in the US, affecting 36.2% of the population (147). Hypertriglyceridemia has been identified as an independent risk factor for cardiovascular heart disease (148), therefore efforts to lower serum TG levels are particularly important. There is compelling evidence that a hypercaloric, high fructose diet can induce, not only in animal models, but also in humans, a whole range of metabolic alterations, including hypertriglyceridemia (149). This, together with the observation that total sugar and fructose intakes have increased significantly over the past three decades (150, 151), has led to the speculation that a high fructose intake may bear a direct, causal effect in the current obesity epidemic and its' related metabolic disorders. In fact, the average fructose consumption in the US has increased from about 37 g/day in the late 1970s (151) to 49 g/day in the period between 1999–2004 (150).

A high fructose diet disturbs lipid homeostasis via several mechanisms:

- Increased *de novo* lipogenesis: Fructose is nearly completely metabolized in the liver through metabolic pathways distinct from those utilized for glucose. Dietary fructose is largely metabolized via *fructokinase*, which is not inhibited by adenosine triphosphate (ATP) and citrate when energy status is high (152). This results in greater fructose uptake by the liver, although there is a high cellular energy state. In the liver, virtually all the fructose ingested in a meal is rapidly converted into lipogenic substrates, namely glyceraldehyde 3-phosphate and acetyl CoA (153). These compounds generate fatty acids for production of hepatic TGs, therefore increasing *de novo* lipogenesis (153). Additionally, fructose up-regulates SREBP1c independently from insulin levels, activating genes involved in lipogenesis, and therefore inducing hypertriglyceridemia (154).

- Impairment of TG-rich lipoprotein catabolism: The rate-limiting step in the removal of TGs from TG-rich lipoproteins is catalyzed by the insulin-sensitive enzyme *lipoprotein lipase* (LPL) (155). LPL hydrolyzes the TG core of lipoproteins, liberating free fatty acids that are absorbed by diffusion into adjacent tissues (155). Insulin increases lipoprotein lipase (LPL) mRNA expression and its' activity, especially LPL in subcutaneous adipose tissue, which has been shown to be more responsive to the effects of insulin than LPL in visceral adipose tissue (152). Conversely to glucose, fructose metabolism does not require insulin secretion. Thus, decreased insulin responses to fructose consumption lead to decreased insulin-mediated LPL activity in subcutaneous adipose tissue, allowing for an overall impaired TG removal (156), as well as a greater TG uptake by visceral adipose tissue (152). Consequently, a high fructose diet leads to a reduced clearance of TGs from the circulation and a greater visceral adipose deposition of TG, which is more closely associated with metabolic diseases, such as cardiovascular disease and type 2 diabetes, compared with subcutaneous adipose tissue (157).

GSPE has previously been demonstrated to lower triglycerides levels by 50% in a normolipidemic state (34, 35, 99), while studies conducted during the course of this thesis, and discussed in chapter 4, showed a 30% decrease in serum TGs following GSPE administration in normolipidemic C57BL/6 mice. However, the hypotriglyceridemic effect of GSPE when serum TGs are elevated has not yet been investigated.

Therefore the aim of this chapter is to investigate the ability of GSPE to lower serum triglyceride levels in a hyperlipidemic state and to understand the underlying molecular mechanisms. To generate a hypertriglyceridemic state, rats were fed a 65% fructose diet for 8 weeks and then GSPE was administered via oral gavage for 7 days. As was previously discussed, a high fructose diet is commonly involved in the development of hypertriglyceridemia, by increasing TG synthesis, as well as decreasing TG clearance. It was decided to administer the GSPE following treatment with a high fructose diet, to first induce hypertriglyceridemia, rather than co-administration of the fructose and GSPE, since it is a

better representation of a model that could then be utilized in future human research studies. In the clinical setting, usually hypertriglyceridemia has already manifested in a patient before a drug treatment or diet modification is prescribed or recommended. It is important to note that hypertriglyceridemia was first induced by the high fructose diet for 8 weeks and the rats were then maintained on the high fructose diet during the following 7 days treatment with either vehicle or GSPE as indicated.

5.2 Materials and methods

Twenty male Wistar rats aged 8 weeks of age were purchased from Charles River Laboratories. Male rats were used since female rats are protected against fructose-induced changes in lipid and insulin homeostasis (158). After one week of acclimatization, rats were randomly allocated (n=10 in each group) to either control diet or 65% fructose diet for 8 weeks (as described in section 2.7.2.1, page 46). Blood samples were collected at 0, 4 and 8 weeks to assess the effect of the high fructose diet on serum TG levels. Following 8 weeks on the diets, the rats were randomized to receive either vehicle (water) or GSPE 250 mg/kg/body weight via oral gavage for 7 days (as detailed in section 2.7.2.2). After 5 hours following the last treatment (2 pm), blood was collected from the saphenous vein as described in section 2.7.3.2. Rats were then euthanized under carbon dioxide, performed according to IACUC approval. The livers were harvested and weighed and then kept in liquid nitrogen until they were stored at –80ºC. RNA was extracted from the tissues as described in section 2.3.2, cDNA was made using Superscript III Reverse transcriptase (as described in section 2.4), and qPCR was used to determine gene expression changes (as detailed in section 2.6). Gene expression changes assessed in the liver included SREBP1c, PGC1β, and down-stream target genes of SREBP1c, namely Apolipoprotein A5 (ApoA5), and 3-hydroxy-3-methylglutaryl-CoA synthase 1 (HMGCS1). Additionally, β-actin and glyceraldehyde 3-phosphate dehydrogenase (GAPDH) expression were used as endogenous control genes. All the results

for the target genes were standardized to β-actin and GAPDH levels, and the data shown represents the fold change for each target gene relative to β-actin and/or GAPDH expression.

Triglyceride levels were measured in plasma that was isolated from blood drawn following treatments, as indicated (in sections 2.7.3.3 and 2.7.4.1).

Sections of the excised liver were immersed in 10% buffered formalin, and processed for hematoxylin and eosin (H&E) staining, which was performed by the Pathology Laboratory at University of Nevada, Reno.

Wistar rats were used to determine the effects of GSPE in a hypertriglyceridemic state, instead of C57BL/6 mice, due to the fact that C57BL6 mice do not respond by increasing triglyceride levels when exposed to a high fructose diet (159). Additionally, Wistar rats have previously been used to assess the effect of GSPE on triglyceride levels (35) and this strain of rats have also been shown to increase plasma TGs when fed a high fructose diet (160-162).

5.3 Results

5.3.1 Effects of fructose on triglyceride homeostasis

The high fructose diet triggered a 58% increase in serum TG levels after 8 weeks, $p<0.001$ (as shown in Figure 35), while the control diet group maintained constant serum TG levels during the course of the 8 weeks. Therefore, the 65% fructose diet induced a hypertriglyceridemic state in which the effects of GSPE can be determined.

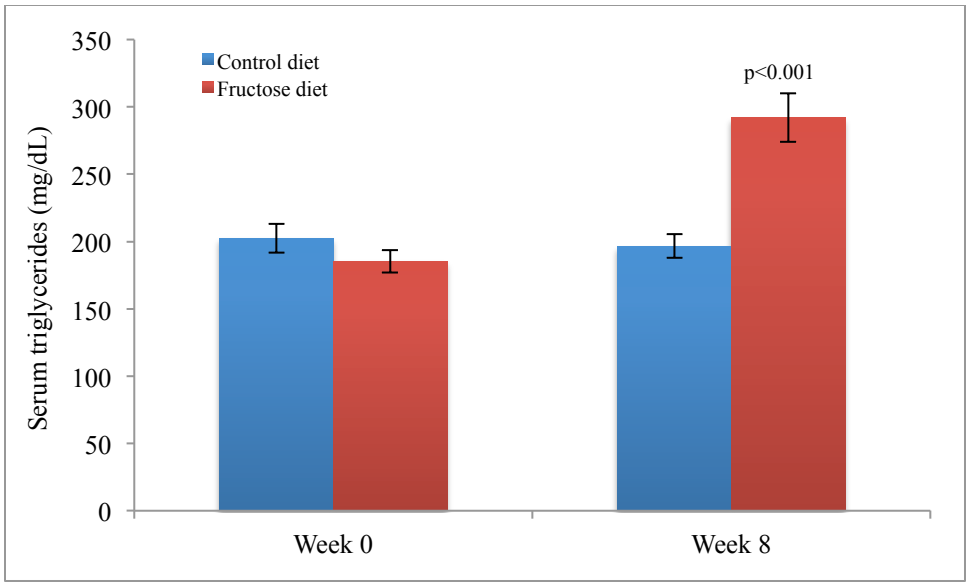

Figure 35: The effect of a high fructose diet on serum triglyceride levels
Wistar rats were fed a 65% fructose diet for 8 weeks. The high fructose diet increased serum TGs from 185 mg/dL to 292 mg/dL (58% increment, $p<0.001$ compared to fructose diet group at week 0), (n=5 per treatment, per group, in triplicate).

As previously mentioned, a high fructose diet has additionally been shown to increase visceral adipose tissue, such as hepatic adipose tissue. When the livers were harvested, the liver size in the fructose-fed group visually seemed greater than in the control group. This observation was confirmed by a significant increase in the percentage of liver weight relative to body weight in the fructose-fed group (3.38%) compared to the control group (2.97%), $p<0.001$. The increase in the liver weight was correlated to an increase in the amount and size of lipid droplets in the liver, as shown in the H&E stained sections below in Figure 36.

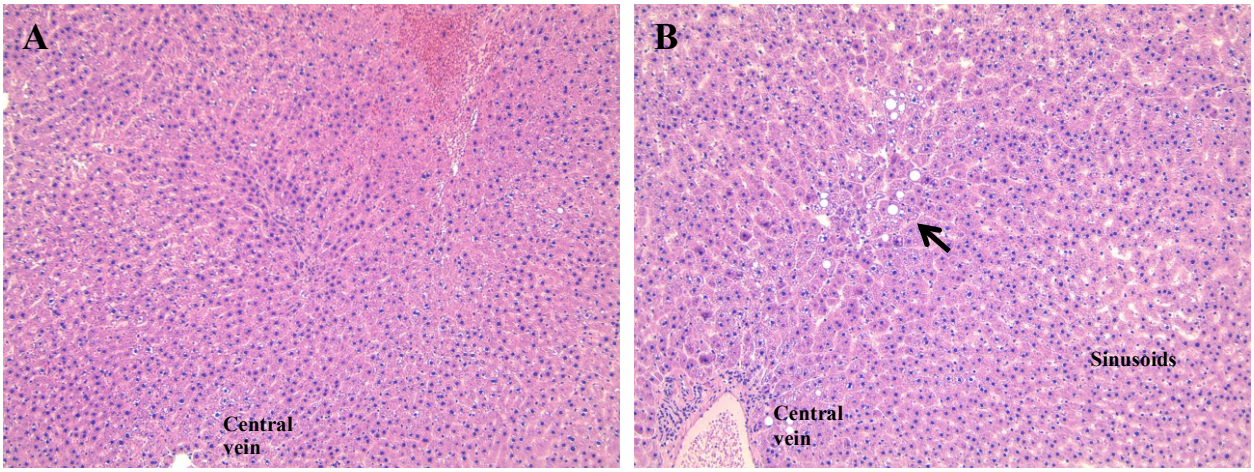

Figure 36: Hematoxylin and eosin (H&E) staining in rat liver sections from (A) a control diet group and (B) fructose diet group
Liver tissue from rats fed a high fructose diet showed more and bigger lipid droplet infiltration (indicated by the black arrow) compared to rats fed a control diet (10x magnification).

5.3.2 Effects of GSPE administration on serum triglyceride levels in rats with fructose-induced hypertriglyceridemia

As previously described, a high fructose diet for 8 weeks induced a hypertriglyceridemic state in Wistar rats. In this group of animals, a 27% reduction in serum TG levels was observed following treatment with 250 mg/kg/body weight GSPE for 5 days. Serum TGs significantly decreased from 310 mg/dL to 227 mg/dL, p=0.009 (as shown in Figure 37).

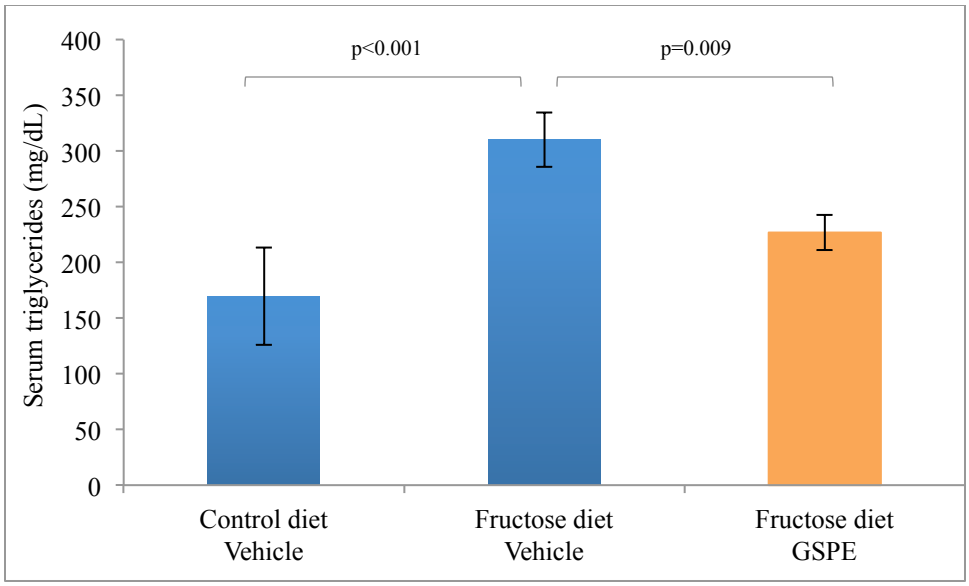

Figure 37: The effects of GSPE on serum triglyceride levels in a hypertriglyceridemic state
GSPE (5 days treatment) significantly decreased serum TGs by 27%, p=0.009, (n=5 per treatment, per group, in triplicate). GSPE: grape seed procyanidin extract.

5.3.3 Effects of GSPE treatment on hepatic gene expression

5.3.3.1 Sterol regulatory element binding protein 1c (SREBP1c)

As previously mentioned, it has been shown that fructose increases lipogenesis, in part via SREBP1c activation (154).

Although our results did not show an increase in SREBP1c expression after 8 weeks following a high fructose diet, SREBP1c mRNA levels were significantly decreased by 19% following GSPE treatment for 7 days in rats fed a 65% fructose diet, p=0.021 (as shown in Figure 38).

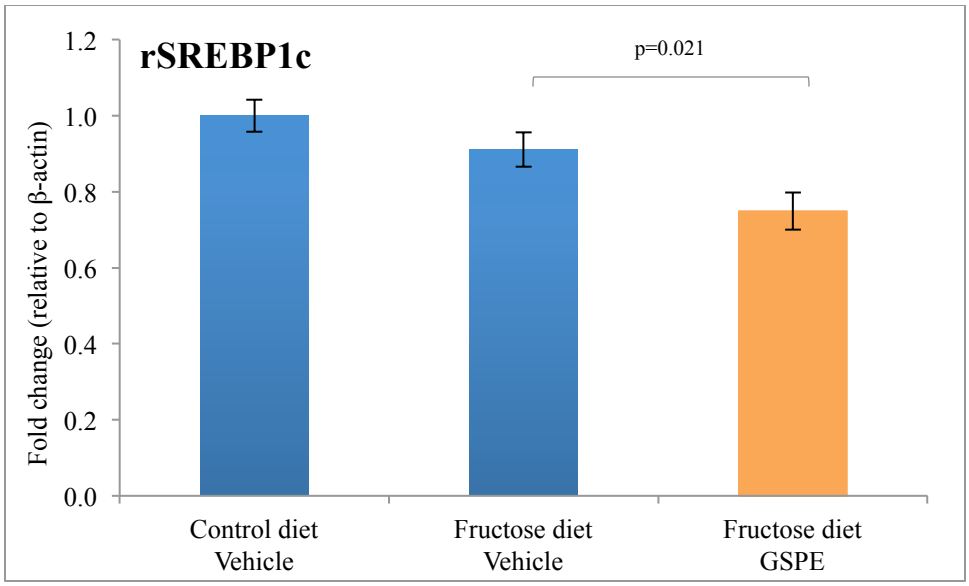

Figure 38: The effects of a high fructose diet and GSPE treatment on SREBP1c expression *in vivo*
GSPE treatment decreased SREBP1c expression after a high fructose diet, although the fructose diet did not increase SREBP1c mRNA expression, (n=5 per treatment, per group, in triplicate). rSREBP1c: rat sterol regulatory element binding protein 1c, GSPE: grape seed procyanidin extract.

5.3.3.2 Peroxisome proliferator-activated receptor γ coactivator 1β (PGC1β)

Rats fed a high fructose diet did not show an increased expression in PGC1β, a transcriptional co-activator that induces hypertriglyceridemia via activation of hepatic lipogenesis and lipoprotein secretion. Additionally, PGC1β mRNA levels did not change following GSPE treatment (data not shown).

5.3.3.3 Apolipoprotein A-V (ApoA5)

ApoA5 expression is inversely associated with plasma TG levels and is negatively regulated by SREBP1c (142). The high fructose diet significantly reduced ApoA5 mRNA expression, $p<0.001$ (as shown in Figure 39), which may be consistent with SREBP1c activation. Treatment with GSPE for 7 days increased ApoA5 mRNA expression ($p=0.004$), thereby increasing the ApoA5 mRNA levels close to the normal levels seen in the control vehicle group (Figure 39).

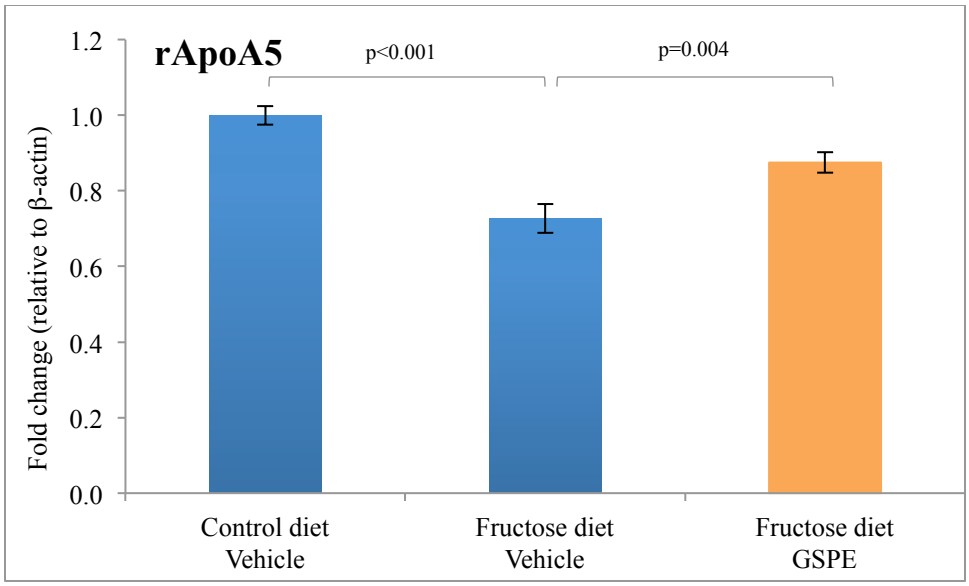

Figure 39: The effects of a fructose diet and GSPE treatment on ApoA5 expression *in vivo*
Rats fed a 65% fructose diet showed a decreased expression in ApoA5 mRNA ($p<0.001$), while GSPE treatment significantly returned ApoA5 mRNA levels close to those seen in the control diet vehicle treated group ($p=0.004$), ($n=5$ per treatment, per group, in triplicate). rApoA5: rat apolipoprotein A-V, GSPE: grape seed procyanidin extract.

5.3.3.4 3-hydroxy-3-methylglutaryl-Coenzyme A synthase 1 (HMGCS1)

As previously described, HMGCS1 is involved in cholesterol synthesis and its' transcription is increased when SREBP1c is activated (141).

The fructose diet did not cause any significant changes in HMGCS1 mRNA expression. However, GSPE treatment following the high fructose diet, significantly increased HMGCS mRNA expression by 2-fold compared to the fructose diet vehicle treated group, $p<0.001$ (as shown in Figure 40).

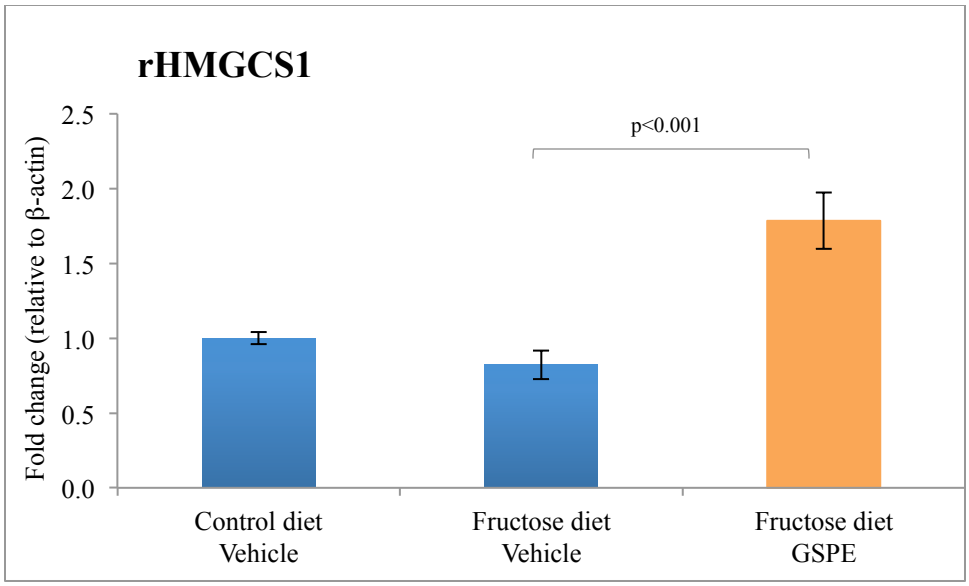

Figure 40: The effects of a high fructose diet and GSPE treatment on HMGCS1 expression *in vivo*
GSPE treatment significantly increased HMGCS1 expression ($p<0.001$) in rats fed a 65% fructose diet, (n=5 per treatment, per group, in triplicate). rHMGCS1: rat 3-hydroxy-3-methylglutaryl-Coenzyme A synthase 1, GSPE: grape seed procyanidin extract.

5.4 Discussion

These studies clearly demonstrate that GSPE treatment lowered serum TG levels by 27% in diet-induced hypertriglyceridemic rats when continuing to consume a high fructose diet. Previous studies have demonstrated the ability of GSPE to decrease serum TGs in a normolipidemic state in several animal models (34, 35, 99, 134). Therefore, this study demonstrates the hypotriglyceridemic effect of GSPE administration *in vivo* when serum TGs are highly elevated, as would be common in an individual seeking amelioration of hypertriglyceridemia. The TG lowering ability of GSPE in this animal study is comparable to the effect of fenofibrate, one of the most commonly prescribed lipid-lowering agents in the world (163), which has been shown to reduce serum TGs by 36% (164), as well as the reduction in TGs seen in normolipidemic mice using this particular batch of GSPE extract in this thesis (chapter 4). Moreover, the positive effect of GSPE treatment on serum TGs was achieved only after 5 days of GSPE administration and when the hypertriglyceridemia was already installed, and while the rats were

continuing to consume the fructose diet, making the effect of GSPE more applicable to a possible clinical setting, since co-administration of GSPE while the rats were fed the fructose diet was not necessary to exert its' hypotriglyceridemic effects.

Although our results did not show an increase in SREBP1c mRNA levels following consumption of the fructose diet, GSPE administration was shown to significantly decrease SREBP1c levels. An increase in SREBP1c levels has previously been shown to partly explain the hypertriglyceridemic effect of fructose, although it is not the only mechanism involved (149, 152, 153, 156, 158). As previously discussed, fructose administration additionally alters lipid homeostasis via the generation of lipogenic substrates, as well as leading to a reduced clearance of TGs from circulation, due to decreased activation of LPL. Additionally, GSPE treatment increased ApoA5 expression, which is also consistent with the observed SREBP1c decreased expression caused by GSPE. Therefore, the GSPE-induced hypotriglyceridemic effect seems to be mediated, at least in part, by inhibiting SREBP1c and its' down-stream target-gene activation.

In contrast to what is expected when SREBP1c activity is decreased, the expression of HMGCS1, another down-stream target of SREBP1c, was increased following GSPE administration. HMGCS1 expression was also induced when GSPE was administered to normolipidemic rats by Del Bas *et al* (35). HMGCS1 is involved in cholesterol biosynthesis in the liver, although an increase in HMGCS1 expression was not accompanied by an increase in cellular cholesterol levels *(35)*. Our results described in chapters 3 and 4 show that GSPE treatment may reduce enterohepatic recirculation of BAs due to a decreased uptake of BAs in the ileum. This could represent an alternative explanation for the observed increased expression in HMGCS1. Therefore, the cholesterol synthesized *de novo* by the liver may be channeled to maintain the normal flux of bile acids following GSPE administration.

In conclusion, our results are innovative since they confirm the positive triglyceride lowering effect of GSPE in a hypertriglyceridemic state *in vivo*. Moreover, our results are relevant since the TG lowering

ability of GSPE was demonstrated when the diet-induced hypertriglyceridemia had already been established, and while the rats were maintained on a high fructose diet. Therefore, the hypotriglyceridemic effect of GSPE treatment demonstrated in the studies conducted herein may be valuable for future human research studies, since the model utilized in these studies represents a more realistic situation observed in a clinical setting, where patients with hypertriglyceridemia require a pharmaceutical drug or dietary treatment in order to ameliorate their condition. However, the precise molecular mechanisms by which GSPE exerts its TG-lowering effect in this model warrant further investigation.

Chapter 6

Discussion

6 Discussion and conclusions

Our results provide further insight and understanding regarding the hypotriglyceridemic effect of GSPE and its' mechanism of action. In particular, in regards to the effect of GSPE in a hypertriglyceridemic state and the role of the intestine and its inter-relationship with the liver, in mediating GSPE-induced molecular alterations.

GSPE had previously been shown to exert a hypotriglyceridemic effect in a normolipidemic state via a FXR and SHP-mediated mechanism of action in the liver (34, 35, 99). The SHP-dependent hepatic down-regulation in the expression of SREBP1c and SREBP1c down-stream target genes, leads to repression of hepatic fatty acid synthesis, increased hepatic fatty acid oxidation and increased catabolism of TG-rich lipoproteins (34, 35, 99). Using FXR-responsive luciferase reporter assays, GSPE was shown not to enhance the transcriptional activity of the FXR/RXR heterodimer by itself, but instead to behave as a ligand-dependent co-agonist, enhancing the transactivation of CDCA-activated FXR (99). Consequently, GSPE lowers serum TGs by acting as a bile acid-dependent co-agonist ligand of FXR in the liver (99).

FXR is highly expressed in the liver and intestine (69). For several years it was thought that the liver was the main bile acid signaling tissue, however, following the recent development of an FXRE-luciferase reporter mouse model it was established that the main bile acid signaling tissue under normal physiological circumstances is in fact the intestine (115). Activation of FXR in the liver occurs primarily under conditions of excess bile acids, such as that found in cholestasis (115). Consequently, it was interesting to assess the effects of GSPE administration on the intestine and to determine how these effects may contribute to the hypotriglyceridemic action of GSPE. Interestingly, our *in vitro* and *in vivo* results show that GSPE may act as a gene-selective bile acid receptor modulator (BARM) in the intestine, instead of simply a bile acid-dependent co-agonist of FXR, as previously proposed in the liver. GSPE treatment was shown to affect the expression of ileal FXR-target genes in different ways, acting as a FXR co-agonist-ligand by suppressing ASBT gene expression, while acting as a FXR modulator for select

genes e.g. by decreasing IBABP and OSTα/β expression. Recently, another natural compound, namely tea catechin, has also been shown to act as as a FXR modulator, since it appears to activate FXR in a tissue-specific and a gene-specific manner (165). Therefore, the intriguing behavior of GSPE is not entirely unique and it has been described for other natural substances. Moreover, synthetic gene-selective bile acid receptor modulators (BARM) have also been identified, such as AGN34 (166). This compound antagonizes FXR in transient tranfection and *in vitro* co-activator recruitment assays, although it acts as a gene-selective modulator *in vivo,* acting as an agonist on CYP7A1, an antagonist on IBABP and neutral on SHP (166). This divergent pattern of regulation is evocative of the activity of selective estrogen receptor (ER) modulators or SERMs, such as tamoxifen and raloxifen, which are either estrogenic or anti-estrogenic depending on the tissue (167). The precise molecular mechanisms underlying the actions of previously reported BARMs have not yet been clearly elucidated.

After analyzing the effect of GSPE treatment on intestinal FXR-target gene expression, it appears that GSPE may impair bile acid enterohepatic recirculation, by decreasing the expression of ASBT, IBABP and OSTα/β. Consequently, the intestinal up-take of bile acids, as well as the transport throughout and outside the enterocyte into the blood, should be impaired, therefore decreasing the amount of BA that return to the liver via the portal circulation. These findings are additionally supported by the GSPE-induced hepatic expression of CYP7A1 seen in our experiments utilizing C57BL/6 mice and previously described studies utilizing rats and hamsters (35, 134). It would make sense that CYP7A1 expression is induced in order to replenish the bile acid pool in the liver, which may have been decreased by GSPE-mediated effects on BA enterohepatic circulation. Moreover, a greater fecal excretion of BAs has been reported following grape seed procyanidin administration (134), which is also consistent with the proposed decreased bile acid enterohepatic recirculation induced by GSPE treatment.

It has been described that decreased BA enterohepatic recirculation is associated with improved triglyceride metabolism in both mice and hamsters (134, 135). Therefore, we hypothesize that the

impairment in BA absorption caused by GSPE administration may represent another mechanism involved in its' hypotriglyceridemic effect. A plausible explanation may be that the metabolic demand for acetyl-CoA, utilized in cholesterol synthesis to replenish BAs, may result in reduced amounts of acetyl-CoA, which is also a substrate for fatty acid synthesis (135).

Another interesting finding resulting from these studies is that GSPE alone induced a transient expression in FGF19 mRNA expression in Caco2 cells, although we did not demonstrate the same effect *in vivo*, after 14 hours treatment. We hypothesize that this may be related to the time-point at which gene-expression was assessed, since gene expression in hepatic tissue was measured 14 hours after GSPE administration, and FGF19 mRNA expression was maximally induced *in vitro* after only 4 hours and then its' levels decreased. FGF19 has been identified as a novel factor that inhibits hepatic fatty acid synthesis via a SREBP1c-mediated mechanism (123). FGF19 treatment has been shown to result in repression of SREBP1c, via an increased activity in STAT3 (via increased tyrosine phosphorylation), an inhibitor of SREBP1c expression, as well as via a decreased expression in PGC1β mRNA, an activator of SREBP1c activity (123). Our results additionally show that GSPE treatment decreases PGC1β mRNA expression *in vivo*, which may have been secondary to any effect on FGF15 mRNA expression. SREBP1c repression caused by FGF15/19 may represent another possible mechanism contributing to the FXR-mediated serum TG lowering effect of GSPE.

Additionally, our results show that GSPE treatment effectively reduces serum TGs when a hypertriglyceridemic state is induced by a high fructose diet. Interestingly, after only five days of oral gavage with GSPE (250 mg/kg/body weight), serum TGs were decreased by 27%, from 310 mg/dL to 227 mg/dL ($p=0.009$). Although the rats did not return to their normal serum TG levels after GSPE treatment, these results seem promising since GSPE was administered after the hypertriglyceridemia was induced and only for 5 days, and while the rats were also concomitantly still consuming the high fructose diet. The gene expression analysis in the liver showed that GSPE treatment reduced SREBP1c mRNA

expression while increasing ApoA5 expression, which is negatively regulated by SREBP1c. ApoA5 enhances VLDL lipolysis and clearance, and therefore its' concentration is inversely associated with plasma TG levels (143). Previous studies have mostly demonstrated the hypotriglyceridemic ability of GSPE in a normolipidemic state (34, 35, 99). Only one previous study has evaluated the capacity of GSPE to correct a dyslipidemic state induced by feeding a high-fat diet (108). Female Wistar rats were fed a high-fat diet composed of standard chow plus a cafeteria diet consisting of cookies with foie-grass and cheese triangles, sweets, bacon, biscuits, chocolate, croissants, carrots and sugary milk (108). After 13 weeks, one group was supplemented with GSPE at a concentration of 25 mg/kg body weight dissolved in condensed milk for 10 days. On the high fat diet the rats had increased their total cholesterol, LDL, HDL and TG levels; therefore a mixed dyslipidemic state was induced. Serum TGs increased only up to moderate levels in this model (204mg/dL), and GSPE was found to significantly decrease serum TG levels by 36%. The results of this study are consistent with our results. However, it is important to consider that in both cases GSPE was administered after the hyperlipidemic state was induced by changes in the diets. Our results assessed the effect of GSPE in a more severe hypertriglyceridemic state (311 mg/dL) induced by a high-fructose diet, and GSPE was shown to still be able to decrease serum TG levels.

In summary, as shown in the studies conducted herein, the effects of GSPE treatment in the intestine highly suggest that GSPE may represent a novel naturally occurring gene-selective bile acid receptor modulator. GSPE administration probably alters bile acid enterohepatic recirculation, by decreasing ASBT, IBABP and OST α/β expression, which are involved in the transport of BAs from the intestinal lumen into the portal circulation. Additionally, GSPE treatment may transiently induce FGF15/19 expression, which acts as a hormone signaling to the liver in order to exert its' effects on bile acid and lipid metabolism. These two novel intestinal effects shown following GSPE treatment may represent an additional explanation for the already recognized hypotriglyceridemic ability of GSPE. Additionally, our

results demonstrate the TG-lowering ability of GSPE when it is administered in a hypertriglyceridemic state, and while the rats are maintained on the high fructose diet, while concomitantly being administered with GSPE. Therefore, GSPE may represent an interesting natural compound warranting further investigation in human research studies.

Chapter 7

Future studies

7 Future studies

Our results represent an important starting point to understand the effects of GSPE on FXR-target gene expression in the intestine and how these gene-expression changes contribute to the hypotriglyceridemic actions of GSPE. Based on the results obtained during the course of these studies, we propose that GSPE may act as a gene-selective FXR modulator in the intestine, thereby affecting bile acid recirculation. Further studies are needed in order to corroborate these observations. GSPE treatments longer than 14 hours are probably needed in order to prove the effects of GSPE on fecal bile acid excretion. Following a longer period of GSPE treatment, fecal and serum BAs could be measured to confirm that GSPE decreases BA uptake by the enterocytes, increasing fecal BA output and decreasing the return of BA to the liver. Additionally, *in vitro* bile acid-binding assays using the procedure previously described by Hu *et al* (168) could be performed to identify the ability of GSPE to bind to BAs and determine its affinity for primary and secondary BAs. Interestingly, other natural products, such an extract derived from dried-young fruits of persimmon (*Diospyros kaki*) which are rich in procyanidins, have been demonstrated to bind BAs in the intestine, decreasing fecal bile acid excretion (169, 170). Therefore, this may help to clarify whether GSPE decreases BA uptake by the enterocytes due only to changes in gene expression, including ASBT, IBABP and OSTα/β, or whether GSPE is additionally able to chelate BAs in the intestinal lumen, analogous to the cholestyramine resin.

Additionally, it would be useful to determine whether or not the impaired enterohepatic circulation of BAs contributes to the hypotriglyceridemic effect of GSPE, as indicated from previous studies using mice and hamsters (134, 135). Interestingly, these studies have found an association between an increased fecal bile acid excretion resulting in increased BA synthesis and lower serum TG levels, however the exact molecular mechanism behind this association has not yet been elucidated. As previously mentioned, it has been suggested that the metabolic demand for acetyl-CoA, utilized in cholesterol synthesis to replenish BAs, may result in reduced amounts of acetyl-CoA, which is also a substrate for fatty acid synthesis

(135), therefore resulting in decreased serum TG levels. Further studies evaluating the amount of acetyl-CoA or other substrates necessary for TG synthesis while BA enterohepatic recirculation is impaired, as well as assessment of the enzymatic expression of enzymes involved in cholesterol synthesis could be important in order to confirm the above-mentioned hypothesis and the causal relationship between the hypotriglyceridemic effects when enterohepatic bile acid recirculation is impaired.

Our *in vitro* results showed that GSPE transiently increased FGF19 mRNA expression. As previously mentioned, FGF19 is a postprandial hormone released from the small intestine that signals to the liver via the portal circulation. The physiological relevance of the enterohepatic BA-FXR-FGF15/19 axis has been recently emphasized in that it may exert beneficial effects for the treatment of glucose and lipid-related metabolic disorders (123, 133). In fact, several metabolic effects of FGF15/19 have been described in addition to the TG-lowering effect, such as decreased gluconeogenesis and increased glycogen synthesis (133). Therefore, if GSPE increases FGF15/19 *in vivo*, it may also emerge as a possible therapeutic option for lipid and glucose-related disorders. We are currently assessing the effect of GSPE treatment on FGF15/19 mRNA expression at earlier time-points (2 hours, 4 hours and 8 hours post-administration) *in vivo*, in order to adequately determine whether or not our *in vitro* observations are replicable *in vivo*.

In regard to the TG-lowering ability of GSPE in a hyperlipidemic state, it is important to elucidate the lowest effective dose of GSPE *in vivo*, in order to minimize any potential adverse effects, although GSPE in animal studies has been demonstrated to be safe even at very high doses (111, 112). Additional studies are also needed to further delineate the complete mechanism of action involved in the ability of GSPE to lower serum TGs in a hyperlipidemic state, understanding that SREBP1c is not the only mechanism involved in high-fructose induced hypertriglyceridemia.

Additionally, it would be very interesting to elucidate the potential beneficial effects of GSPE in conditions usually associated with hypertriglyceridemia, such as the metabolic syndrome and non-alcoholic fatty liver disease. Hypertriglyceridemia is one of the cardinal signs of the metabolic syndrome,

which also includes, increased visceral fat deposition, hypertension and hyperglycemia (109). Additionally, elevated TG and depressed HDL-C levels are the defining components of dyslipidemia in non-alcoholic fatty-liver disorder (171). There is a strong basis to support the notion that GSPE may be beneficial in the treatment of these diseases, since glucose and TG regulation are involved in their pathogenesis, which may be regulated by GSPE-mediated effects on FXR activation, modification of enterohepatic circulation, as well as FGF15/19 activity. Currently, there is some evidence showing the beneficial effects of GSPE on certain hypertriglyceridemic-related conditions mentioned above (110, 118, 172). A grape seed extract (GSE) has been shown to reduce plasma insulin levels and to improve the homeostasis model assessment-insulin resistance (HOMA) index in hyperinsulinemic-induced rats fed either a cafeteria diet or a high-fructose diet (110, 172). Moreover, a GSE was shown to reduce white adipose tissue depots and to induce lipoprotein lipase activity in the retroperitoneal and mesenteric white adipose tissue, while reducing plasma TGs, in hamsters (173). However, the complete understanding of the molecular mechanism involved in these GSPE-mediated effects is still lacking, and therefore further studies are needed in order to clarify the mechanism of action exerted by GSPE and its' effects on other conditions related to hypertriglyceridemia.

8 References

1. Aranda A, Pascual A. Nuclear hormone receptors and gene expression. Physiol Rev. 2001;81(3):1269-304.
2. Mangelsdorf DJ, Thummel C, Beato M, Herrlich P, Schutz G, Umesono K, et al. The nuclear receptor superfamily: the second decade. Cell. 1995;83(6):835-9.
3. Aagaard MM, Siersbaek R, Mandrup S. Molecular basis for gene-specific transactivation by nuclear receptors. Biochim Biophys Acta. 1812. Netherlands: 2010 Elsevier B.V; 2011. p. 824-35.
4. McEwan IJ. Nuclear hormone receptors: Allosteric switches. Mol Cell Endocrinol. 348. Ireland2012. p. 345-7.
5. Olefsky JM. Nuclear receptor minireview series. J Biol Chem. 276. United States2001. p. 36863-4.
6. Giguere V. Orphan nuclear receptors: from gene to function. Endocr Rev. 1999;20(5):689-725.
7. Helsen C, Kerkhofs S, Clinckemalie L, Spans L, Laurent M, Boonen S, et al. Structural basis for nuclear hormone receptor DNA binding. Mol Cell Endocrinol. 348. Ireland: 2011 Elsevier Ireland Ltd; 2012. p. 411-7.
8. Biddie SC, John S, Hager GL. Genome-wide mechanisms of nuclear receptor action. Trends Endocrinol Metab. 2010;21(1):3-9.
9. Mangelsdorf DJ, Evans RM. The RXR heterodimers and orphan receptors. Cell. 1995;83(6):841-50.
10. Mangelsdorf DJ, Ong ES, Dyck JA, Evans RM. Nuclear receptor that identifies a novel retinoic acid response pathway. Nature. 1990;345(6272):224-9.
11. McKenna NJ, Lanz RB, O'Malley BW. Nuclear receptor coregulators: cellular and molecular biology. Endocr Rev. 1999;20(3):321-44.
12. Lee JW, Lee YC, Na SY, Jung DJ, Lee SK. Transcriptional coregulators of the nuclear receptor superfamily: coactivators and corepressors. Cell Mol Life Sci. 2001;58(2):289-97.
13. Miesfeld R, Okret S, Wikstrom AC, Wrange O, Gustafsson JA, Yamamoto KR. Characterization of a steroid hormone receptor gene and mRNA in wild-type and mutant cells. Nature. 1984;312(5996):779-81.
14. Petkovich M, Brand NJ, Krust A, Chambon P. A human retinoic acid receptor which belongs to the family of nuclear receptors. Nature. 1987;330(6147):444-50.
15. Sap J, Munoz A, Damm K, Goldberg Y, Ghysdael J, Leutz A, et al. The c-erb-A protein is a high-affinity receptor for thyroid hormone. Nature. 1986;324(6098):635-40.
16. Weinberger C, Thompson CC, Ong ES, Lebo R, Gruol DJ, Evans RM. The c-erb-A gene encodes a thyroid hormone receptor. Nature. 1986;324(6098):641-6.
17. Giguere V, Ong ES, Segui P, Evans RM. Identification of a receptor for the morphogen retinoic acid. Nature. 1987;330(6149):624-9.
18. Maglich JM, Sluder A, Guan X, Shi Y, McKee DD, Carrick K, et al. Comparison of complete nuclear receptor sets from the human, Caenorhabditis elegans and Drosophila genomes. Genome Biol. 2001;2(8):RESEARCH0029.
19. Zhang Z, Burch PE, Cooney AJ, Lanz RB, Pereira FA, Wu J, et al. Genomic analysis of the nuclear receptor family: new insights into structure, regulation, and evolution from the rat genome. Genome Res. 14. United States2004. p. 580-90.
20. Umesono K, Evans RM. Determinants of target gene specificity for steroid/thyroid hormone receptors. Cell. 1989;57(7):1139-46.
21. Khorasanizadeh S, Rastinejad F. Nuclear-receptor interactions on DNA-response elements. Trends Biochem Sci. 2001;26(6):384-90.

22. Schoenmakers E, Alen P, Verrijdt G, Peeters B, Verhoeven G, Rombauts W, et al. Differential DNA binding by the androgen and glucocorticoid receptors involves the second Zn-finger and a C-terminal extension of the DNA-binding domains. Biochem J. 1999;341 (Pt 3):515-21.
23. Hittelman AB, Burakov D, Iniguez-Lluhi JA, Freedman LP, Garabedian MJ. Differential regulation of glucocorticoid receptor transcriptional activation via AF-1-associated proteins. EMBO J. 1999;18(19):5380-8.
24. Iwamoto F, Umemoto T, Motojima K, Fujiki Y. Nuclear transport of peroxisome-proliferator activated receptor &alpha. J Biochem. 149. England2011. p. 311-9.
25. Glass CK, Ogawa S. Combinatorial roles of nuclear receptors in inflammation and immunity. Nat Rev Immunol. 2006;6(1):44-55.
26. Okabe T, Takayanagi R, Imasaki K, Haji M, Nawata H, Watanabe T. cDNA cloning of a NGFI-B/nur77-related transcription factor from an apoptotic human T cell line. J Immunol. 1995;154(8):3871-9.
27. Chang C, Kokontis J, Liao SS, Chang Y. Isolation and characterization of human TR3 receptor: a member of steroid receptor superfamily. J Steroid Biochem. 1989;34(1-6):391-5.
28. Wong M, Ramayya MS, Chrousos GP, Driggers PH, Parker KL. Cloning and sequence analysis of the human gene encoding steroidogenic factor 1. J Mol Endocrinol. 1996;17(2):139-47.
29. Guo W, Lovell RS, Zhang YH, Huang BL, Burris TP, Craigen WJ, et al. Ahch, the mouse homologue of DAX1: cloning, characterization and synteny with GyK, the glycerol kinase locus. Gene. 1996;178(1-2):31-4.
30. Lazar MA, Jones KE, Chin WW. Isolation of a cDNA encoding human Rev-ErbA alpha: transcription from the noncoding DNA strand of a thyroid hormone receptor gene results in a related protein that does not bind thyroid hormone. DNA Cell Biol. 1990;9(2):77-83.
31. Lee HK, Lee YK, Park SH, Kim YS, Lee JW, Kwon HB, et al. Structure and expression of the orphan nuclear receptor SHP gene. J Biol Chem. 1998;273(23):14398-402.
32. Seol W, Choi HS, Moore DD. An orphan nuclear hormone receptor that lacks a DNA binding domain and heterodimerizes with other receptors. Science. 1996;272(5266):1336-9.
33. Zhang Y, Hagedorn CH, Wang L. Role of nuclear receptor SHP in metabolism and cancer. Biochim Biophys Acta. 2011;1812(8):893-908.
34. Del Bas JM, Ricketts ML, Baiges I, Quesada H, Ardevol A, Salvado MJ, et al. Dietary procyanidins lower triglyceride levels signaling through the nuclear receptor small heterodimer partner. Mol Nutr Food Res. 2008;52(10):1172-81.
35. Del Bas JM, Fernandez-Larrea J, Blay M, Ardevol A, Salvado MJ, Arola L, et al. Grape seed procyanidins improve atherosclerotic risk index and induce liver CYP7A1 and SHP expression in healthy rats. FASEB J. 2005;19(3):479-81.
36. Denson LA, Sturm E, Echevarria W, Zimmerman TL, Makishima M, Mangelsdorf DJ, et al. The orphan nuclear receptor, shp, mediates bile acid-induced inhibition of the rat bile acid transporter, ntcp. Gastroenterology. 2001;121(1):140-7.
37. Wang L, Han Y, Kim CS, Lee YK, Moore DD. Resistance of SHP-null mice to bile acid-induced liver damage. J Biol Chem. 2003;278(45):44475-81.
38. Baes M, Gulick T, Choi HS, Martinoli MG, Simha D, Moore DD. A new orphan member of the nuclear hormone receptor superfamily that interacts with a subset of retinoic acid response elements. Mol Cell Biol. 1994;14(3):1544-52.
39. Forman BM, Tzameli I, Choi HS, Chen J, Simha D, Seol W, et al. Androstane metabolites bind to and deactivate the nuclear receptor CAR-beta. Nature. 1998;395(6702):612-5.
40. Tolson AH, Wang H. Regulation of drug-metabolizing enzymes by xenobiotic receptors: PXR and CAR. Adv Drug Deliv Rev. 2010;62(13):1238-49.
41. Wada T, Gao J, Xie W. PXR and CAR in energy metabolism. Trends Endocrinol Metab. 2009;20(6):273-9.

42. Ueda A, Hamadeh HK, Webb HK, Yamamoto Y, Sueyoshi T, Afshari CA, et al. Diverse roles of the nuclear orphan receptor CAR in regulating hepatic genes in response to phenobarbital. Mol Pharmacol. 2002;61(1):1-6.
43. Scheer N, Ross J, Rode A, Zevnik B, Niehaves S, Faust N, et al. A novel panel of mouse models to evaluate the role of human pregnane X receptor and constitutive androstane receptor in drug response. J Clin Invest. 2008;118(9):3228-39.
44. Willy PJ, Umesono K, Ong ES, Evans RM, Heyman RA, Mangelsdorf DJ. LXR, a nuclear receptor that defines a distinct retinoid response pathway. Genes Dev. 1995;9(9):1033-45.
45. Redinger RN. The role of the enterohepatic circulation of bile salts and nuclear hormone receptors in the regulation of cholesterol homeostasis: Bile salts as ligands for nuclear hormone receptors. Can J Gastroenterol. 2003;17(4):265-71.
46. N AG, Castrillo A. Liver X receptors as regulators of macrophage inflammatory and metabolic pathways. Biochim Biophys Acta. 2011;1812(8):982-94.
47. Janowski BA, Willy PJ, Devi TR, Falck JR, Mangelsdorf DJ. An oxysterol signalling pathway mediated by the nuclear receptor LXR alpha. Nature. 1996;383(6602):728-31.
48. Lehmann JM, Kliewer SA, Moore LB, Smith-Oliver TA, Oliver BB, Su JL, et al. Activation of the nuclear receptor LXR by oxysterols defines a new hormone response pathway. J Biol Chem. 1997;272(6):3137-40.
49. Peet DJ, Turley SD, Ma W, Janowski BA, Lobaccaro JM, Hammer RE, et al. Cholesterol and bile acid metabolism are impaired in mice lacking the nuclear oxysterol receptor LXR alpha. Cell. 1998;93(5):693-704.
50. Chiang JY, Kimmel R, Stroup D. Regulation of cholesterol 7alpha-hydroxylase gene (CYP7A1) transcription by the liver orphan receptor (LXRalpha). Gene. 2001;262(1-2):257-65.
51. Repa JJ, Berge KE, Pomajzl C, Richardson JA, Hobbs H, Mangelsdorf DJ. Regulation of ATP-binding cassette sterol transporters ABCG5 and ABCG8 by the liver X receptors alpha and beta. J Biol Chem. 2002;277(21):18793-800.
52. Houck KA, Borchert KM, Hepler CD, Thomas JS, Bramlett KS, Michael LF, et al. T0901317 is a dual LXR/FXR agonist. Mol Genet Metab. 2004;83(1-2):184-7.
53. Mitro N, Vargas L, Romeo R, Koder A, Saez E. T0901317 is a potent PXR ligand: implications for the biology ascribed to LXR. FEBS Lett. 2007;581(9):1721-6.
54. Varga T, Czimmerer Z, Nagy L. PPARs are a unique set of fatty acid regulated transcription factors controlling both lipid metabolism and inflammation. Biochim Biophys Acta. 2011;1812(8):1007-22.
55. Wagner KD, Wagner N. Peroxisome proliferator-activated receptor beta/delta (PPARbeta/delta) acts as regulator of metabolism linked to multiple cellular functions. Pharmacol Ther. 2010;125(3):423-35.
56. Wang YX. PPARs: diverse regulators in energy metabolism and metabolic diseases. Cell Res. 2010;20(2):124-37.
57. Huang TH, Teoh AW, Lin BL, Lin DS, Roufogalis B. The role of herbal PPAR modulators in the treatment of cardiometabolic syndrome. Pharmacol Res. 2009;60(3):195-206.
58. Rousset S, Alves-Guerra MC, Mozo J, Miroux B, Cassard-Doulcier AM, Bouillaud F, et al. The biology of mitochondrial uncoupling proteins. Diabetes. 2004;53 Suppl 1:S130-5.
59. Gustafson B, Jack MM, Cushman SW, Smith U. Adiponectin gene activation by thiazolidinediones requires PPAR gamma 2, but not C/EBP alpha-evidence for differential regulation of the aP2 and adiponectin genes. Biochem Biophys Res Commun. 2003;308(4):933-9.
60. Hammarstedt A, Smith U. Thiazolidinediones (PPARgamma ligands) increase IRS-1, UCP-2 and C/EBPalpha expression, but not transdifferentiation, in L6 muscle cells. Diabetologia. 2003;46(1):48-52.

61. Ihunnah CA, Jiang M, Xie W. Nuclear receptor PXR, transcriptional circuits and metabolic relevance. Biochim Biophys Acta. 2011;1812(8):956-63.
62. Luo G, Guenthner T, Gan LS, Humphreys WG. CYP3A4 induction by xenobiotics: biochemistry, experimental methods and impact on drug discovery and development. Curr Drug Metab. 2004;5(6):483-505.
63. Anzenbacher P, Anzenbacherova E. Cytochromes P450 and metabolism of xenobiotics. Cell Mol Life Sci. 2001;58(5-6):737-47.
64. Xie W, Barwick JL, Downes M, Blumberg B, Simon CM, Nelson MC, et al. Humanized xenobiotic response in mice expressing nuclear receptor SXR. Nature. 2000;406(6794):435-9.
65. Ma X, Shah Y, Cheung C, Guo GL, Feigenbaum L, Krausz KW, et al. The PREgnane X receptor gene-humanized mouse: a model for investigating drug-drug interactions mediated by cytochromes P450 3A. Drug Metab Dispos. 35. United States2007. p. 194-200.
66. Xie W, Evans RM. Pharmaceutical use of mouse models humanized for the xenobiotic receptor. Drug Discov Today. 7. England2002. p. 509-15.
67. Kemper JK. Regulation of FXR transcriptional activity in health and disease: Emerging roles of FXR cofactors and post-translational modifications. Biochim Biophys Acta. 2011;1812(8):842-50.
68. Mencarelli A, Fiorucci S. FXR an emerging therapeutic target for the treatment of atherosclerosis. J Cell Mol Med. 2010;14(1-2):79-92.
69. Zhang Y, Edwards PA. FXR signaling in metabolic disease. FEBS Lett. 2008;582(1):10-8.
70. Modica S, Gadaleta RM, Moschetta A. Deciphering the nuclear bile acid receptor FXR paradigm. Nucl Recept Signal. 2010;8:e005.
71. Zhang Y, Kast-Woelbern HR, Edwards PA. Natural structural variants of the nuclear receptor farnesoid X receptor affect transcriptional activation. J Biol Chem. 2003;278(1):104-10.
72. Kast HR, Goodwin B, Tarr PT, Jones SA, Anisfeld AM, Stoltz CM, et al. Regulation of multidrug resistance-associated protein 2 (ABCC2) by the nuclear receptors pregnane X receptor, farnesoid X-activated receptor, and constitutive androstane receptor. J Biol Chem. 2002;277(4):2908-15.
73. Park SS, Choi H, Kim SJ, Kim OJ, Chae KS, Kim E. FXRalpha down-regulates LXRalpha signaling at the CETP promoter via a common element. Mol Cells. 2008;26(4):409-14.
74. Forman BM, Goode E, Chen J, Oro AE, Bradley DJ, Perlmann T, et al. Identification of a nuclear receptor that is activated by farnesol metabolites. Cell. 1995;81(5):687-93.
75. Makishima M, Okamoto AY, Repa JJ, Tu H, Learned RM, Luk A, et al. Identification of a nuclear receptor for bile acids. Science. 1999;284(5418):1362-5.
76. Parks DJ, Blanchard SG, Bledsoe RK, Chandra G, Consler TG, Kliewer SA, et al. Bile acids: natural ligands for an orphan nuclear receptor. Science. 1999;284(5418):1365-8.
77. Lefebvre P, Cariou B, Lien F, Kuipers F, Staels B. Role of bile acids and bile acid receptors in metabolic regulation. Physiol Rev. 2009;89(1):147-91.
78. Makishima M, Lu TT, Xie W, Whitfield GK, Domoto H, Evans RM, et al. Vitamin D receptor as an intestinal bile acid sensor. Science. 2002;296(5571):1313-6.
79. Owen RW, Thompson MH, Hill MJ, Wilpart M, Mainguet P, Roberfroid M. The importance of the ratio of lithocholic to deoxycholic acid in large bowel carcinogenesis. Nutr Cancer. 1987;9(2-3):67-71.
80. Fukumori S, Murata T, Taguchi M, Hashimoto Y. Rapid and drastic induction of CYP3A4 mRNA expression via vitamin D receptor in human intestinal LS180 cells. Drug Metab Pharmacokinet. 2007;22(5):377-81.
81. Richter HG, Benson GM, Blum D, Chaput E, Feng S, Gardes C, et al. Discovery of novel and orally active FXR agonists for the potential treatment of dyslipidemia & diabetes. Bioorg Med Chem Lett. 2011;21(1):191-4.

82. Flatt B, Martin R, Wang TL, Mahaney P, Murphy B, Gu XH, et al. Discovery of XL335 (WAY-362450), a highly potent, selective, and orally active agonist of the farnesoid X receptor (FXR). J Med Chem. 2009;52(4):904-7.
83. Ma K, Saha PK, Chan L, Moore DD. Farnesoid X receptor is essential for normal glucose homeostasis. J Clin Invest. 2006;116(4):1102-9.
84. Shen H, Zhang Y, Ding H, Wang X, Chen L, Jiang H, et al. Farnesoid X receptor induces GLUT4 expression through FXR response element in the GLUT4 promoter. Cell Physiol Biochem. 2008;22(1-4):1-14.
85. Love MW, Dawson PA. New insights into bile acid transport. Curr Opin Lipidol. 1998;9(3):225-9.
86. Russell DW. The enzymes, regulation, and genetics of bile acid synthesis. Annu Rev Biochem. 2003;72:137-74.
87. Lee YK, Schmidt DR, Cummins CL, Choi M, Peng L, Zhang Y, et al. Liver receptor homolog-1 regulates bile acid homeostasis but is not essential for feedback regulation of bile acid synthesis. Mol Endocrinol. 2008;22(6):1345-56.
88. Dawson PA, Haywood J, Craddock AL, Wilson M, Tietjen M, Kluckman K, et al. Targeted deletion of the ileal bile acid transporter eliminates enterohepatic cycling of bile acids in mice. J Biol Chem. 2003;278(36):33920-7.
89. Dawson PA, Hubbert M, Haywood J, Craddock AL, Zerangue N, Christian WV, et al. The heteromeric organic solute transporter alpha-beta, Ostalpha-Ostbeta, is an ileal basolateral bile acid transporter. J Biol Chem. 2005;280(8):6960-8.
90. Kalaany NY, Mangelsdorf DJ. LXRS and FXR: the yin and yang of cholesterol and fat metabolism. Annu Rev Physiol. 2006;68:159-91.
91. Chanda D, Xie YB, Choi HS. Transcriptional corepressor SHP recruits SIRT1 histone deacetylase to inhibit LRH-1 transactivation. Nucleic Acids Res. 38. England2010. p. 4607-19.
92. Gupta S, Stravitz RT, Dent P, Hylemon PB. Down-regulation of cholesterol 7alpha-hydroxylase (CYP7A1) gene expression by bile acids in primary rat hepatocytes is mediated by the c-Jun N-terminal kinase pathway. J Biol Chem. 2001;276(19):15816-22.
93. Inagaki T, Choi M, Moschetta A, Peng L, Cummins CL, McDonald JG, et al. Fibroblast growth factor 15 functions as an enterohepatic signal to regulate bile acid homeostasis. Cell Metab. 2005;2(4):217-25.
94. Song KH, Li T, Owsley E, Strom S, Chiang JY. Bile acids activate fibroblast growth factor 19 signaling in human hepatocytes to inhibit cholesterol 7alpha-hydroxylase gene expression. Hepatology. 2009;49(1):297-305.
95. Choi M, Moschetta A, Bookout AL, Peng L, Umetani M, Holmstrom SR, et al. Identification of a hormonal basis for gallbladder filling. Nat Med. 2006;12(11):1253-5.
96. Ananthanarayanan M, Balasubramanian N, Makishima M, Mangelsdorf DJ, Suchy FJ. Human bile salt export pump promoter is transactivated by the farnesoid X receptor/bile acid receptor. J Biol Chem. 2001;276(31):28857-65.
97. Grober J, Zaghini I, Fujii H, Jones SA, Kliewer SA, Willson TM, et al. Identification of a bile acid-responsive element in the human ileal bile acid-binding protein gene. Involvement of the farnesoid X receptor/9-cis-retinoic acid receptor heterodimer. J Biol Chem. 1999;274(42):29749-54.
98. Li D, Zimmerman TL, Thevananther S, Lee HY, Kurie JM, Karpen SJ. Interleukin-1 beta-mediated suppression of RXR:RAR transactivation of the Ntcp promoter is JNK-dependent. J Biol Chem. 2002;277(35):31416-22.
99. Del Bas JM, Ricketts ML, Vaque M, Sala E, Quesada H, Ardevol A, et al. Dietary procyanidins enhance transcriptional activity of bile acid-activated FXR in vitro and reduce triglyceridemia in vivo in a FXR-dependent manner. Mol Nutr Food Res. 2009;53(7):805-14.

100. Horton JD, Goldstein JL, Brown MS. SREBPs: activators of the complete program of cholesterol and fatty acid synthesis in the liver. J Clin Invest. 2002;109(9):1125-31.
101. Sinal CJ, Tohkin M, Miyata M, Ward JM, Lambert G, Gonzalez FJ. Targeted disruption of the nuclear receptor FXR/BAR impairs bile acid and lipid homeostasis. Cell. 2000;102(6):731-44.
102. Kim I, Ahn SH, Inagaki T, Choi M, Ito S, Guo GL, et al. Differential regulation of bile acid homeostasis by the farnesoid X receptor in liver and intestine. J Lipid Res. 48. United States2007. p. 2664-72.
103. Aron PM, Kennedy JA. Flavan-3-ols: nature, occurrence and biological activity. Mol Nutr Food Res. 2008;52(1):79-104.
104. Bagchi D, Bagchi M, Stohs SJ, Das DK, Ray SD, Kuszynski CA, et al. Free radicals and grape seed proanthocyanidin extract: importance in human health and disease prevention. Toxicology. 2000;148(2-3):187-97.
105. Fine AM. Oligomeric proanthocyanidin complexes: history, structure, and phytopharmaceutical applications. Altern Med Rev. 2000;5(2):144-51.
106. Gu L, Kelm MA, Hammerstone JF, Beecher G, Holden J, Haytowitz D, et al. Concentrations of proanthocyanidins in common foods and estimations of normal consumption. J Nutr. 2004;134(3):613-7.
107. Diagnosis and classification of diabetes mellitus. Diabetes Care. 34 Suppl 1. United States2011. p. S62-9.
108. Quesada H, del Bas JM, Pajuelo D, Diaz S, Fernandez-Larrea J, Pinent M, et al. Grape seed proanthocyanidins correct dyslipidemia associated with a high-fat diet in rats and repress genes controlling lipogenesis and VLDL assembling in liver. Int J Obes (Lond). 2009;33(9):1007-12.
109. Grundy SM, Brewer HB, Jr., Cleeman JI, Smith SC, Jr., Lenfant C, American Heart A, et al. Definition of metabolic syndrome: Report of the National Heart, Lung, and Blood Institute/American Heart Association conference on scientific issues related to definition. Circulation. 2004;109(3):433-8.
110. Montagut G, Blade C, Blay M, Fernandez-Larrea J, Pujadas G, Salvado MJ, et al. Effects of a grapeseed procyanidin extract (GSPE) on insulin resistance. J Nutr Biochem. 2010;21(10):961-7.
111. Ray S, Bagchi D, Lim PM, Bagchi M, Gross SM, Kothari SC, et al. Acute and long-term safety evaluation of a novel IH636 grape seed proanthocyanidin extract. Res Commun Mol Pathol Pharmacol. 2001;109(3-4):165-97.
112. Yamakoshi J, Saito M, Kataoka S, Kikuchi M. Safety evaluation of proanthocyanidin-rich extract from grape seeds. Food Chem Toxicol. 40. England2002. p. 599-607.
113. Inoue J, Tanaka M, Nanmoku M, Yashiro T, Sato R. Stabilization of small heterodimer partner mRNA by grape seed procyanidins extract in cultured hepatocytes. Mol Nutr Food Res. 2011;55(7):1052-8.
114. Watanabe M, Houten SM, Wang L, Moschetta A, Mangelsdorf DJ, Heyman RA, et al. Bile acids lower triglyceride levels via a pathway involving FXR, SHP, and SREBP-1c. J Clin Invest. 2004;113(10):1408-18.
115. Houten SM, Volle DH, Cummins CL, Mangelsdorf DJ, Auwerx J. In vivo imaging of farnesoid X receptor activity reveals the ileum as the primary bile acid signaling tissue. Mol Endocrinol. 2007;21(6):1312-23.
116. Kostogrys RB, Pisulewski PM. Effect of conjugated linoleic acid (CLA) on lipid profile and liver histology in laboratory rats fed high-fructose diet. Environ Toxicol Pharmacol. 2010;30(3):245-50.
117. Pasko P, Zagrodzki P, Barton H, Chlopicka J, Gorinstein S. Effect of quinoa seeds (Chenopodium quinoa) in diet on some biochemical parameters and essential elements in blood of high fructose-fed rats. Plant Foods Hum Nutr. 2010;65(4):333-8.

118. Meeprom A, Sompong W, Suwannaphet W, Yibchok-anun S, Adisakwattana S. Grape seed extract supplementation prevents high-fructose diet-induced insulin resistance in rats by improving insulin and adiponectin signalling pathways. Br J Nutr. 2011;106(8):1173-81.
119. Meunier V, Bourrie M, Berger Y, Fabre G. The human intestinal epithelial cell line Caco-2; pharmacological and pharmacokinetic applications. Cell Biol Toxicol. 1995;11(3-4):187-94.
120. Neimark E, Chen F, Li X, Shneider BL. Bile acid-induced negative feedback regulation of the human ileal bile acid transporter. Hepatology. 2004;40(1):149-56.
121. Mosmann T. Rapid colorimetric assay for cellular growth and survival: application to proliferation and cytotoxicity assays. J Immunol Methods. 65. Netherlands1983. p. 55-63.
122. Chomczynski P, Sacchi N. Single-step method of RNA isolation by acid guanidinium thiocyanate-phenol-chloroform extraction. Anal Biochem. 1987;162(1):156-9.
123. Bhatnagar S, Damron HA, Hillgartner FB. Fibroblast growth factor-19, a novel factor that inhibits hepatic fatty acid synthesis. J Biol Chem. 2009;284(15):10023-33.
124. Martin P, Riley R, Back DJ, Owen A. Comparison of the induction profile for drug disposition proteins by typical. Br J Pharmacol. 2008;153(4):805-19.
125. Urizar NL, Liverman AB, Dodds DT, Silva FV, Ordentlich P, Yan Y, et al. A natural product that lowers cholesterol as an antagonist ligand for FXR. Science. 296. United States2002. p. 1703-6.
126. Kaur M, Agarwal C, Agarwal R. Anticancer and cancer chemopreventive potential of grape seed extract and other grape-based products. J Nutr. 139. United States2009. p. 1806S-12S.
127. Dinicola S, Cucina A, Pasqualato A, Proietti S, D'Anselmi F, Pasqua G, et al. Apoptosis-inducing factor and caspase-dependent apoptotic pathways triggered by different grape seed extracts on human colon cancer cell line Caco-2. Br J Nutr. 104. England2010. p. 824-32.
128. Dinicola S, Cucina A, Pasqualato A, D'Anselmi F, Proietti S, Lisi E, et al. Antiproliferative and Apoptotic Effects Triggered by Grape Seed Extract (GSE) versus Epigallocatechin and Procyanidins on Colon Cancer Cell Lines. Int J Mol Sci. 13. Switzerland2012. p. 651-64.
129. Chen F, Ma L, Dawson PA, Sinal CJ, Sehayek E, Gonzalez FJ, et al. Liver receptor homologue-1 mediates species- and cell line-specific bile acid-dependent negative feedback regulation of the apical sodium-dependent bile acid transporter. J Biol Chem. 278. United States2003. p. 19909-16.
130. Zollner G, Wagner M, Moustafa T, Fickert P, Silbert D, Gumhold J, et al. Coordinated induction of bile acid detoxification and alternative elimination in mice: role of FXR-regulated organic solute transporter-alpha/beta in the adaptive response to bile acids. Am J Physiol Gastrointest Liver Physiol. 290. United States2006. p. G923-32.
131. Lee H, Zhang Y, Lee FY, Nelson SF, Gonzalez FJ, Edwards PA. FXR regulates organic solute transporters alpha and beta in the adrenal gland, kidney, and intestine. J Lipid Res. 47. United States2006. p. 201-14.
132. Holt JA, Luo G, Billin AN, Bisi J, McNeill YY, Kozarsky KF, et al. Definition of a novel growth factor-dependent signal cascade for the suppression of bile acid biosynthesis. Genes Dev. 2003;17(13):1581-91.
133. Kir S, Beddow SA, Samuel VT, Miller P, Previs SF, Suino-Powell K, et al. FGF19 as a postprandial, insulin-independent activator of hepatic protein and glycogen synthesis. Science. 2011;331(6024):1621-4.
134. Jiao R, Zhang Z, Yu H, Huang Y, Chen ZY. Hypocholesterolemic activity of grape seed proanthocyanidin is mediated by enhancement of bile acid excretion and up-regulation of CYP7A1. J Nutr Biochem. 2010;21(11):1134-9.
135. Lundasen T, Andersson EM, Snaith M, Lindmark H, Lundberg J, Ostlund-Lindqvist AM, et al. Inhibition of intestinal bile acid transporter Slc10a2 improves triglyceride metabolism and normalizes elevated plasma glucose levels in mice. PLoS One. 7. United States2012. p. e37787.

136. Song KH, Li T, Owsley E, Strom S, Chiang JY. Bile acids activate fibroblast growth factor 19 signaling in human hepatocytes to inhibit cholesterol 7 alpha-hydroxylase gene expression. Hepatology. 2009;49(1):297-305.
137. Plauth M, Raible A, Gregor M, Hartmann F. Inter-organ communication between intestine and liver in vivo and in vitro. Semin Cell Biol. 1993;4(3):231-7.
138. Out C, Groen AK, Brufau G. Bile acid sequestrants: more than simple resins. Curr Opin Lipidol. 2012;23(1):43-55.
139. Hernandez C, Molusky M, Li Y, Li S, Lin JD. Regulation of hepatic ApoC3 expression by PGC-1beta mediates hypolipidemic effect of nicotinic acid. Cell Metab. 12. United States: 2010 Elsevier Inc; 2010. p. 411-9.
140. Lin J, Yang R, Tarr PT, Wu PH, Handschin C, Li S, et al. Hyperlipidemic effects of dietary saturated fats mediated through PGC-1beta coactivation of SREBP. Cell. 120. United States2005. p. 261-73.
141. Andrew Skaff D, Miziorko HM. A visible wavelength spectrophotometric assay suitable for high-throughput screening of 3-hydroxy-3-methylglutaryl-CoA synthase. Anal Biochem. 396. United States2010. p. 96-102.
142. Sharma V, Ryan RO, Forte TM. Apolipoprotein A-V dependent modulation of plasma triacylglycerol: a puzzlement. Biochim Biophys Acta. 1821. Netherlands: 2011. Published by Elsevier B.V.; 2012. p. 795-9.
143. Pennacchio LA, Olivier M, Hubacek JA, Cohen JC, Cox DR, Fruchart JC, et al. An apolipoprotein influencing triglycerides in humans and mice revealed by comparative sequencing. Science. 294. United States2001. p. 169-73.
144. Jakel H, Nowak M, Moitrot E, Dehondt H, Hum DW, Pennacchio LA, et al. The liver X receptor ligand T0901317 down-regulates APOA5 gene expression through activation of SREBP-1c. J Biol Chem. 279. United States2004. p. 45462-9.
145. Li YC, Wang DP, Chiang JY. Regulation of cholesterol 7 alpha-hydroxylase in the liver. Cloning, sequencing, and regulation of cholesterol 7 alpha-hydroxylase mRNA. J Biol Chem. 1990;265(20):12012-9.
146. Pandak WM, Li YC, Chiang JY, Studer EJ, Gurley EC, Heuman DM, et al. Regulation of cholesterol 7 alpha-hydroxylase mRNA and transcriptional activity by taurocholate and cholesterol in the chronic biliary diverted rat. J Biol Chem. 1991;266(6):3416-21.
147. Miranda JJ, Herrera VM, Chirinos JA, Gomez LF, Perel P, Pichardo R, et al. Major cardiovascular risk factors in Latin America: a comparison with the United States. The Latin American Consortium of Studies in Obesity (LASO). PLoS One. 8. United States2013. p. e54056.
148. Grundy SM, Cleeman JI, Merz CN, Brewer HB, Jr., Clark LT, Hunninghake DB, et al. Implications of recent clinical trials for the National Cholesterol Education Program Adult Treatment Panel III guidelines. Circulation. 2004;110(2):227-39.
149. Johnson RJ, Segal MS, Sautin Y, Nakagawa T, Feig DI, Kang DH, et al. Potential role of sugar (fructose) in the epidemic of hypertension, obesity and the metabolic syndrome, diabetes, kidney disease, and cardiovascular disease. Am J Clin Nutr. 86. United States2007. p. 899-906.
150. Marriott BP, Cole N, Lee E. National estimates of dietary fructose intake increased from 1977 to 2004 in the United States. J Nutr. 139. United States2009. p. 1228S-35S.
151. Park YK, Yetley EA. Intakes and food sources of fructose in the United States. Am J Clin Nutr. 1993;58(5 Suppl):737S-47S.
152. Stanhope KL, Havel PJ. Fructose consumption: recent results and their potential implications. Ann N Y Acad Sci. 1190. United States2010. p. 15-24.
153. Mayes PA. Intermediary metabolism of fructose. Am J Clin Nutr. 1993;58(5 Suppl):754S-65S.

154. Matsuzaka T, Shimano H, Yahagi N, Amemiya-Kudo M, Okazaki H, Tamura Y, et al. Insulin-independent induction of sterol regulatory element-binding protein-1c expression in the livers of streptozotocin-treated mice. Diabetes. 2004;53(3):560-9.
155. Hara T, Cameron-Smith D, Cooney GJ, Kusunoki M, Tsutsumi K, Storlien LH. The actions of a novel lipoprotein lipase activator, NO-1886, in hypertriglyceridemic fructose-fed rats. Metabolism. 47. United States1998. p. 149-53.
156. Chong MF, Fielding BA, Frayn KN. Mechanisms for the acute effect of fructose on postprandial lipemia. Am J Clin Nutr. 85. United States2007. p. 1511-20.
157. Fox CS, Massaro JM, Hoffmann U, Pou KM, Maurovich-Horvat P, Liu CY, et al. Abdominal visceral and subcutaneous adipose tissue compartments: association with metabolic risk factors in the Framingham Heart Study. Circulation. 116. United States2007. p. 39-48.
158. Galipeau D, Verma S, McNeill JH. Female rats are protected against fructose-induced changes in metabolism and blood pressure. Am J Physiol Heart Circ Physiol. 283. United States2002. p. H2478-84.
159. Nagata R, Nishio Y, Sekine O, Nagai Y, Maeno Y, Ugi S, et al. Single nucleotide polymorphism (-468 Gly to A) at the promoter region of SREBP-1c associates with genetic defect of fructose-induced hepatic lipogenesis [corrected]. J Biol Chem. 279. United States2004. p. 29031-42.
160. Castro MC, Francini F, Schinella G, Caldiz CI, Zubiria MG, Gagliardino JJ, et al. Apocynin administration prevents the changes induced by a fructose-rich diet on rat liver metabolism and the antioxidant system. Clin Sci (Lond). 123. England2012. p. 681-92.
161. Karsenty J, Landrier JF, Rousseau-Ralliard D, Robbez-Masson V, Margotat A, Deprez P, et al. Beneficial effects of omega-3 fatty acids on the consequences of a fructose diet are not mediated by PPAR delta or PGC1 alpha. Eur J Nutr. 2012.
162. Panchal SK, Poudyal H, Brown L. Quercetin ameliorates cardiovascular, hepatic, and metabolic changes in diet-induced metabolic syndrome in rats. J Nutr. 142. United States2012. p. 1026-32.
163. Moutzouri E, Kei A, Elisaf MS, Milionis HJ. Management of dyslipidemias with fibrates, alone and in combination with statins: role of delayed-release fenofibric acid. Vasc Health Risk Manag. 2010;6:525-39.
164. Birjmohun RS, Hutten BA, Kastelein JJ, Stroes ES. Efficacy and safety of high-density lipoprotein cholesterol-increasing compounds: a meta-analysis of randomized controlled trials. J Am Coll Cardiol. 45. United States2005. p. 185-97.
165. Li G, Lin W, Araya JJ, Chen T, Timmermann BN, Guo GL. A tea catechin, epigallocatechin-3-gallate, is a unique modulator of the farnesoid X receptor. Toxicol Appl Pharmacol. 258. United States: 2011 Elsevier Inc; 2012. p. 268-74.
166. Dussault I, Beard R, Lin M, Hollister K, Chen J, Xiao JH, et al. Identification of gene-selective modulators of the bile acid receptor FXR. J Biol Chem. 278. United States2003. p. 7027-33.
167. McKenna NJ, O'Malley BW. An issue of tissues: divining the split personalities of selective estrogen receptor modulators. Nat Med. 2000;6(9):960-2.
168. Hu Y-B, Wang Z, Xu S-Y. Treatment of corn bran dietary fiber with xylanase increases its ability to bind bile salts, in vitro. Food Chemistry. 2008;106(1):113-21.
169. Matsumoto K, Kadowaki A, Ozaki N, Takenaka M, Ono H, Yokoyama S, et al. Bile acid-binding ability of kaki-tannin from young fruits of persimmon (Diospyros kaki) in vitro and in vivo. Phytother Res. 2011;25(4):624-8.
170. Trautwein EA, Kunath-Rau A, Erbersdobler HF. Increased fecal bile acid excretion and changes in the circulating bile acid pool are involved in the hypocholesterolemic and gallstone-preventive actions of psyllium in hamsters. J Nutr. 1999;129(4):896-902.
171. Basaranoglu M, Basaranoglu G, Sabuncu T, Senturk H. Fructose as a key player in the development of fatty liver disease. World J Gastroenterol. 2013;19(8):1166-72.

172. Suwannaphet W, Meeprom A, Yibchok-Anun S, Adisakwattana S. Preventive effect of grape seed extract against high-fructose diet-induced insulin resistance and oxidative stress in rats. Food Chem Toxicol. 48. England: 2010 Elsevier Ltd; 2010. p. 1853-7.
173. Caimari A, Del Bas JM, Crescenti A, Arola L. Low doses of grape seed procyanidins reduce adiposity and improve the plasma lipid profile in hamsters. Int J Obes (Lond)2012.

Chapter 9

Appendices

9 Appendices

9.1 Appendix 1: Abbreviations

6-ECDCA:	6α-ethyl-chenodeoxycholic acid
ABCG:	ATP-binding cassette sub-family G
ACC:	Acetyl-coA carboxylase
AceCS:	Acetyl-coA synthase
AF:	Activation function
ANOVA:	Analysis of variance
Apo:	Apolipoprotein
AR:	Androgen receptor
ASBT:	Apical sodium-dependent bile acid transporter
ASCOM:	Activating signal cointegrator-2 -containing complex
ATP:	Adenosine triphosphate
BA:	Bile acid
BARM:	Bile acid receptor modulator
Brg-1:	Brahma-related gene 1
BSEP:	Bile salt export pump
CA:	Cholic acid
CAR:	Constitutive androstane receptor
CARM1:	p300, coactivator-associated arginine methyltransferase 1
CDCA:	Chenodeoxycholic acid
cDNA:	Complementary DNA
CETP:	Cholesteryl ester transfer protein
CITCO:	6-(4-Chlorophenyl) imidazo[2,1-b][1,3] thiazole-5-carbaldehyde O-3,4-dichlorobenzyl) oxime
CPT1:	Carnitine palmitoyltransferase 1
CSS:	Charcoal-stripped serum
CTE:	C-terminal extension
CYP:	Cytochrome P450 enzyme
DAX1:	Dosage-sensitive sex reversal adrenal hypoplasia critical region on chromosome X gene 1
DBD:	DNA binding domain
DEPC:	Diethylpyrocarbonate
dNTP:	Deoxyribonucleotide triphosphate
DMEM:	Dulbecco's modified eagle medium
DNA:	Deoxyribonucleic acid
DTT:	Dithiothreitol
DR:	Direct repeat
DRIP150:	Vitamin D receptor-interacting protein 150
EDTA:	Ethylenediaminetetraacetic acid
ER:	Everted repeat
ERα:	Estrogen receptor alpha
FAS:	Fatty-acid synthase
FBS:	Fetal bovine serum
FGF15/19:	Fibroblast growth factor 15/19
FGFR4:	Fibroblast growth factor receptor 4
FXR:	Farnesoid X receptor

FXRE:	Farnesoid X receptor response element
GAPDH:	Glyceraldehyde 3-phosphate dehydrogenase
GITC:	Guanidinium thiocyanate
GPAT:	Glycerol-3-phosphate acyltransferase
GR:	Glucocorticoid receptor
GSE:	Grape seed extract
GSPE:	Grape seed procyanidin extract
GST:	Glutathione S-transferase
HAT:	Histone acetyl transferase
HDAC:	Histone deacetylase activity
HDL:	High-density lipoprotein
HMG-CoAR:	3-hydroxy-3-methylglutaryl CoA reductase
HMGCS1:	3-hydroxy-3-methylglutaryl-CoA synthase
HPLC:	High Performance Liquid Chromatography
IACUC:	Institutional Animal Care and Use Committee
IBABP:	Intestinal bile acid binding protein
IBAT:	Ileal bile acid transporter
IR:	Inverted repeat
IRS-1:	Insulin receptor substrate-1
JNK:	c-jun N-terminal kinase
LBD:	Ligand binding domain
LCA:	Lithocholic acid
LDL:	Low-density lipoprotein
LPL:	Lipoprotein lipase
LRH-1:	Liver receptor homolog-1
LXR:	Liver X receptors
LXRE:	LXR response element
MDR1:	Multidrug resistance protein 1
MR:	Mineralocorticoid receptor
MRP2:	Multidrug resistance-associated protein 2
NASH:	Non-alcoholic steatohepatitis
NHR:	Nuclear hormone receptors
NLS:	Nuclear localization signal
NOAEL:	No-observed-adverse-effect level
NTCP:	Sodium-dependent sodium taurocholate cotransporting polypeptide
NURR1:	Nuclear receptor related 1 protein
OATP:	Organic anion transporting polypeptides
OSTα/β:	Organic solute transporters alpha-beta
PBS:	Phosphate buffered saline
PCN:	Pregnenolone 16α-carbonitrile
PCR:	Polymerase chain reaction
PCSK9:	Proprotein convertase subtilisin/kexin 9
PEPCK:	Phosphoenolpyruvate carboxykinase
PGC1α/β:	Peroxisome proliferator-activated receptor gamma coactivator 1-alpha/beta
PPAR:	Peroxisome-proliferator-activated receptor
PR:	Progesterone receptor
PRMT1:	Protein arginine N-methyltransferase 1
qPCR:	Real-time quantitative polymerase chain reaction
PXR:	Pregnane X receptor

RAR:	Retinoic acid receptor
RE:	Response element
RIF:	Rifampicin
RNA:	Ribonucleic acid
RXR:	Retinoid X receptor
SCD1:	Stearoyl-CoA desaturase-1
SF1:	Steroidogenic factor 1
SHP:	Small heterodimer partner
SIRT1:	Sirtuin-1
SR-B1:	Scavenger receptor B1
SRC-1:	Steroid receptor coactivator-1
SREBP1c:	Sterol regulatory element-binding protein 1c
STAT3:	Signal transducer and activator of transcription 3
SULT:	Sulfotransferase
TCPOBOP:	1,4-bis[2-[3,5 dichloropyridyloxyl]] benzene
TC:	Total cholesterol
TG:	Triglyceride
TNFα:	Tumor necrosis factor alpha
UCP:	Uncoupling protein
UGT:	Uridine 5'-diphospho-glucuronosyl transferase
VDR:	Vitamin D receptor
VLDL:	Very low density lipoprotein

9.2 Appendix 2: Preparation of buffers and reagents

9.2.1 Tris/acetate/EDTA (TAE) electrophoresis buffer

For each liter of 50x stock solution, 242 g Tris Base, 57.1 mL Glacial Acetic Acid, and 100 mL 0.5M EDTA were needed. Tris Base was mixed using a stir bar to dissolve in about 600 mL of autoclaved milliQ water. Then the EDTA and the acetic acid were added. Lastly, the final volume was brought up to 1 L with milliQ water, and stored at room temperature. This stock solution was diluted down to 1x to get the working solution used to prepare a DNA agarose gel.

9.2.2 Tris/borate/EDTA (TBE) electrophoresis buffer

For each liter of 10x stock solution**,** 108 g of Tris base, 55 g of boric acid, and 40 mL of 0.5M EDTA pH 8.0 were needed. Tris Base was mixed using a stir bar to dissolve in about 600 mL of DEPC water. Then boric acid and EDTA were added. Lastly, the final volume was brought up to 1 L with DEPC water, and stored at room temperature. This stock solution was diluted down to 1x to get the working solution used to prepare a RNA agarose gel.

9.2.3 Preparation of a 1% agarose gel

For each 100 mL of 1% agarose gel, 1 g of agarose was added to either 100 mL of TAE or TBE buffer. The mix was heated in the microwave for about 2 minutes, until the agarose was completely dissolved in the buffer. 2 uL of ethidium bromide were added to the solution, and then it was poured into the electrophoresis tray for 45 min to let it dry.